Lobbe Technologies Ltd.
P.O. Box 3570
Regina, Saskatchewan
S4P 3L7

# MODELLING METHANE FLOW INTO UNDERGROUND LONGWALL COAL MINES

Prepared by

A. J. Szladow
R. K. Chan
T. Ertekin

Work on this project was conducted under the auspices of the Canada Centre for Mineral and Energy Technology, under the support of PERD, Department of Energy, Mines and Resources, Canada.

D.S.S. Serial No. 23440-7-9141/01-SQ
CANMET Scientific Authority Dr. B. W. Konda

228 pp

MICROMEDIA

**DISCLAIMER**

The material in this Report is intended for general information only. Any use of this material in relation to any specific application should be based on independent examination and verification of its unrestricted applicability for such use and/or a determination of its suitability for the application. No license under any Lobbe Technology Ltd. patents or other proprietary interest is implied by the publication of this Report. Those making use of or relying upon the material assume all risks and liability arising from such use or reliance.

## SUMMARY

The overall objective of this project has been to develop a computer-based numerical model to simulate the time-dependent release of methane gas into longwall coal mine workings. The specific objective of this project has been to conduct an in-depth review of the reported models and background information on methane flow in coal seam, and to identify applicable elements of these models for the eventual development of a multi-seam methane flow model for longwall coal mines.

The background materials reviewed included technical and scientific information on: 1) the porosity of coal, 2) adsorption-desorption of gases, 3) diffusion, 4) laminar and non-laminar flow, 4) permeability, 6) flow through porous media, 7) effects of stress on porosity, permeability and gas flow, 8) effects of water saturation on gas flow, and 9) approximate or numerical methods. Based on the background materials, recommendations were made regarding the coal structure representation, and the physical phenomena and fundamental equations useful for modelling of methane flow into mine workings.

The models reviewed included the Pennsylvania State University model, the U.S. Bureau of Mines model, the METGEN model, the University of Nottingham model, and the Airey's model. None of these models have all the essential model elements for prediction

of methane flow into longwall mine workings (Table 1). However, a number of model parts can be adapted from the existing computer models.

The PSU computer model was selected for a parametric study to test the feasibility of the model for Canadian mines. The predicted total methane emission was in agreement with the reported field emission data; however, the predicted methane emission from drainage holes was somewhat lower than the reported methane emission for the Lingan mine, Sydney, N.S. Considering the uncertainties in the input seam data, the results of the simulation indicate that with additional development work, the model will satisfactorily predict the flow of methane into longwall mine workings.

The proposed research and development plan lists a number of research objectives required to develop a computer-based methane emission model for longwall mines. The program envisages three developmental phases, with Phase I resulting in implementation of the model at the CANMET Sydney Coal Laboratory, Phase II developing computational improvements and transferring the technology into the mines, and Phase III including future R&D developments such as research on in-situ coal seam characterization techniques and optimization and error analysis of mine data.

**Table 1. SUMMARY OF THE COMPUTER MODELS REVIEWED**

| MODEL CAPABILITIES | PSU[1] | BOM[2] | UON[3] | METGEN | AIREY |
|---|---|---|---|---|---|
| Essential Physical Modules | | | | | |
| 1. Dual-porosity to represent coal | √ | √ | NO | NO | NO |
| 2. Two-phase flow | √ | √ | NO | NO | NO |
| 3. Three-dimensional flow | √ | NO | NO | NO | NO |
| 4. Unsteady-state flow | √ | √ | √ | NO | NO |
| 5. Darcy's Law for water transport | √ | √ | NO | NO | NO |
| 6. Real gas law for gas state | √ | √ | √ | √ | √ |
| 7. Dual-mechanism for gas flow | √ | √ | NO | NO | √ |
| 8. Effects of slippage on gas transport | √ | √ | NO | NO | √ |
| 9. Pseudo-steady-state sorption phenomenon | √ | √ | NO | NO | POOR |
| Essential Application Modules | | | | | |
| 10. Interactions between multiple seams | NO | NO | NO | NO | POOR |
| 11. Mine layout | NO | Limited | NO | NO | Limited |
| 12. Emission from mine face | √ | √ | √ | √ | √ |
| 13. Emission from gob | NO | NO | NO | NO | √ |
| 14. Coal face advance rate | √ | √ | √ | NO | √ |
| 15. Atmospheric pressure in mine workings | Limited | Limited | Limited | Limited | Limited |
| 16. Executable in IBM PC | NO | NO | NO | NO | NO |

**Table 1. SUMMARY OF THE COMPUTER MODELS REVIEWED** (Continued)

| MODEL CAPABILITIES | PSU[1] | BOM[2] | UON[3] | METGEN | AIREY |
|---|---|---|---|---|---|
| Important Modules | | | | | |
| 17. Stress-dependent porosity | NO | √ | NO | NO | NO |
| 18. Stress-dependent permeability | NO | √ | √ | NO | √ |
| 19. Vertical boreholes | √ | √ | √ | NO | NO |
| 20. Horizontal boreholes | √ | √ | √ | Limited | √ |
| 21. Slanted boreholes | NO | NO | √ | NO | Limited |
| 22. Effects of stimulation | √ | √ | √ | Limited | √ |
| 23. Fast computational speed | NO | NO | NO | NO | √ |
| 24. User friendly | Limited | NO | NO | NO | NO |
| 25. Ease of future improvements | Limited | NO | NO | NO | NO |
| Useful Modules | | | | | |
| 26. Effects of turbulence on water flow | NO | √ | NO | NO | NO |
| 27. Effects of turbulence on gas transport | NO | √ | NO | NO | √ |
| 28. Unsteady-state sorption phenomenon | NO | NO | NO | NO | NO |

[1] PSU - Pennsylvania State University Model
[2] BOM - United States Bureau of Mines Model
[3] UON - University of Nottingham Model

√ - YES

## RÉSUMÉ

Ce projet a permis le développement d'un modèle numérique informatisé simulant l'écoulement à l'état non-permanent du méthane dans les longs murs des chantiers d'exploitation des mines de charbon. Pour ce faire, nous avons examiné les modèles et les renseignements disponibles sur l'écoulement du méthane dans les couches de charbon. Nous avons ensuite identifié les éléments de ces modèles qui pourraient servir au développement d'un modèle d'écoulement du méthane sur plusieurs couches pour les longs murs des mines de charbon.

Les ouvrages examinés, contenant des renseignements de nature technique et scientifique, portaient sur: 1) la porosité du charbon, 2) l'adsorption-désorption des gaz, 3) la diffusion, 4) l'écoulement laminaire et non-laminaire, 5) la perméabilité 6) l'écoulement à travers des matériaux poreux, 7) l'effet du stress sur la porosité, 8) les effets de la saturation d'eau sur l'écoulement du gaz, et 9) les méthodes approximatives ou numériques. D'après ces renseignements, nous avons proposé des recommendations sur la représentation de la structure du charbon ainsi que sur le phénomène physique et les équations fondamentales utiles à la création d'un modèle l'écoulement du méthane dans les chantiers d'exploitation des mines.

Les modèles examinés incluent celui de l'Université de Pennsylvanie, celui du Bureau américain des mines, celui de

METGEN, celui de l'Université de Nottingham et celui d'Airey. Aucun de ces modèles ne comporte tous les éléments essentiels nécessaires pour qu'un modèle puisse prédire l'écoulement du méthane dans les longs murs des chantiers d'exploitation des mines (Table 1). Cependant, plusieurs éléments du modèle pourront être adaptés des modèles informatisés actuels.

La praticabilité du modèle pour les mines canadiennes a été évaluée lors d'une étude paramétrique qui utilisait le modèle de l'Université de la Pennsylvanie. L'écoulement total de méthane prévu fut identique à celui des données prélevées sur le terrain, cependant l'écoulement du méthane prévu pour les trous d'écoulement a été légèrement inférieur à celui relevé à la mine de Sydney, Nouvelle Écosse. Si l'on tient compte de l'incertitude des données d'entrée concernant les couches, les résultats de la simulation indiquent, qu'en améliorant le modèle, l'on pourra prédire de façon satisfaisante l'écoulement du méthane dans les longs murs des chantiers d'exploitation des mines.

Le plan de recherche et de développement proposé enumère plusieurs objectifs nécessaires à l'élaboration d'un modèle informatisé sur l'écoulement du méthane dans les long murs des chantiers d'exploitation des mines. Le programme propose trois phases de développement: 1) implantation du modèle au laboratoire CANMET de Sydney, 2) amélioration du système informatisé et transfert de la technologie aux mines,

3) poursuite des programmes de recherche et de développement sur la caractérisation des couches de charbon sur les lieux ainsi que sur l'optimisation et l'analyse des erreurs des données relatives aux mines.

Table 1. RÉSUMÉ DES MODÈLES INFORMATISÉS ANALYSÉS

| CAPACITÉ DES MODÈLES | UP[1] | BAM[2] | UN[3] | METGEN | AIREY |
|---|---|---|---|---|---|
| Modules physiques essentiels | | | | | |
| 1. Double porosité pour la représentation du charbon | * | * | non | non | non |
| 2. Écoulement biphasé | * | * | non | non | non |
| 3. Écoulement tridimentionnel | * | non | non | non | non |
| 4. Écoulement d'un état non-permanent | * | * | * | non | non |
| 5. Loi de Darcy pour le transport de l'eau | * | * | non | non | non |
| 6. Loi du gaz réel pour l'état du gaz | * | * | * | * | * |
| 7. Double mécanisme pour l'écoulement du gaz | * | * | non | non | * |
| 8. Effets des glissements sur le transport du gaz | * | * | non | non | * |
| 9. Phénomène de sorption d'un état pseudo-permanent | * | * | non | non | faible |
| Modules utiles | | | | | |
| 10. Intéractions entre couches multiples | non | non | non | non | faible |
| 11. Tracé de la mine | non | limité | non | non | limité |
| 12. Écoulement du front de la mine | * | * | * | * | * |
| 13. Écoulement des remblais | non | non | non | non | * |
| 14. Taux d'avance du front de taille | * | * | * | non | * |
| 15. Pression atmosphérique dans les chantiers d'exploitation des mines | limité | limité | limité | limité | limité |
| 16. Réalisable sur IMB PC | non | non | non | non | non |

Table 1. RÉSUMÉ DES MODÈLES INFORMATISÉS ANALYSÉS (Suite)

| CAPACITÉ DES MODÈLES | UP[1] | BAM[2] | UN[3] | METGEN | AIREY |
|---|---|---|---|---|---|
| Modules importants | | | | | |
| 17. Porosité dépendante du Stress | non | * | non | non | non |
| 18. Perméabilité dépendante du Stress | non | * | * | non | * |
| 19. Trous de sondage verticaux | * | * | * | non | non |
| 20. Trous de sondage horizontaux | * | * | * | limité | * |
| 21. Trous de sondage en oblique | non | non | * | non | limité |
| 22. Effets de la stimulation | * | * | * | limité | * |
| 23. Vitesse de calcul rapide | non | non | non | non | * |
| 24. Facilité d'utilisation | limité | non | non | non | non |
| 25. Amélioration possible | limité | non | non | non | non |
| Modules utiles | | | | | |
| 26. Effets de la turbulence sur le mouvement de l'eau | non | * | non | non | non |
| 27. Effets de la turbulence sur le transport du gaz | non | * | non | non | * |
| 28. Phénomène de sorption d'un état non-permanent | non | non | non | non | non |

1 UP Université de la Pennsylvanie
2 BAM Bureau américain des mines
3 UN Université de Nottingham

* - oui

## TABLE OF CONTENTS


| | | Page |
|---|---|---|
| 1. | INTRODUCTION | 1-1 |
| 2. | REVIEW OF BACKGROUND FOR METHANE IN COAL SEAM MODELLING | 2-1 |
| 2.1. | Porosity of Coal | 2-1 |
| 2.1.1. | Background | 2-1 |
| 2.1.2. | Application to Methane in Coal Bed Modelling | 2-13 |
| 2.2. | Adsorption-Desorption of Gases | 2-15 |
| 2.3. | Diffusion | 2-25 |
| 2.3.1. | Background | 2-25 |
| 2.3.2. | Application to Methane in Coal Bed Modelling | 2-31 |
| 2.4. | Laminar and Non-Laminar Flow | 2-38 |
| 2.4.1. | Background | 2-38 |
| 2.4.2. | Application to the Modelling of Methane Flow in Coal Seams | 2-44 |
| 2.5. | Permeability | 2-47 |
| 2.6. | Flow through Porous Media | 2-52 |
| 2.6.1. | Background | 2-52 |
| 2.6.2. | Application to the Modelling of Methane Flow in Coal Seams | 2-54 |
| 2.7. | Effects of Stress on Porosity, Permeability and Gas Flow | 2-61 |
| 2.8. | Effects of Water Saturation on Gas Flow | 2-65 |
| 2.9. | Approximate or Numerical Methods | 2-73 |
| 2.9.1. | Background | 2-73 |
| 2.9.2. | Application to the Modelling of Methane Flow in Coal Seams | 2-81 |
| 3. | EVALUATION OF AVAILABLE MODELS | 3-1 |
| 3.1. | Fundamental Equations | 3-1 |
| 3.2. | Computer Models with Mine Activities | 3-11 |
| 3.2.1. | Pennsylvania State University Models | 3-12 |
| 3.2.2. | METGEN Model | 3-25 |

**TABLE OF CONTENTS**


| | | Page |
|---|---|---|
| | 3.2.3. University of Nottingham Models | 3-31 |
| | 3.2.4. United States Bureau of Mines Model | 3-35 |
| | 3.2.5. Empirical Models | 3-46 |
| 3.3. | Computer Models for Methane Well Degasing | 3-60 |
| | 3.3.1. Kovalev and Kuznetsov Model | 3-60 |
| | 3.3.2. ARRAY Model | 3-61 |
| 4. | SELECTED MODEL PARTS | 4-1 |
| 5. | PARAMETRIC STUDY OF A SELCTED MODEL | 5-1 |
| 6. | RESEARCH PLAN | 6-1 |
| 7. | CONCLUSIONS AND RECOMMENDATIONS | 7-1 |
| 8. | REFERENCES | 8-1 |

## LIST OF TABLES


| Table | | Page |
|---|---|---|
| 2.1. | PORE STRUCTURE OF SOME COALS | 2-12 |
| 2.2. | U.S. COAL SEAM CHARACTERISTICS | 2-51 |
| 3.1. | LIST OF FINITE-DIFFERENCE METHANE DRAINAGE MODELS INCORPORATING MINING ACTIVITY | 3-2 |
| 3.2. | LIST OF FINITE-DIFFERENCE METHANE DRAINAGE MODELS FOR SIMULATED WELLS | 3-3 |
| 3.3. | SELECTED EMPIRICAL CORRELATIONS FOR METHANE EMISSION | 3-48 |
| 4.1. | SUMMARY OF THE SELECTED MODEL PARTS, AND THEIR PRIORITIES AND AVAILABILITY | 4-2 |
| 5.1. | INPUT DATA USED IN THE RUNS | 5-2 |
| 5.2. | SUMMARY OF RESULTS FOR EXERCISE 1 | 5-9 |
| 5.3. | SUMMARY OF RESULTS FOR EXERCISE 2 | 5-18 |

## LIST OF FIGURES


| Figure | | Page |
|---|---|---|
| 2.1. | SCHEMATIC OF METHANE FLOW DYNAMICS IN A COAL SEAM | 2-2 |
| 2.2. | DUAL-POROSITY NATURE OF COAL SEAM | 2-14 |
| 2.3. | RELATIONSHIP BETWEEN RANK, DEPTH AND SORPTIVE CAPACITY | 2-17 |
| 2.4. | METHANE CAPACITY OF COAL AND INERT ROCK | 2-18 |
| 2.5. | SCHEMATIC REPRESENTATION OF THE MACROSCOPIC FLOW PROCESS, SELF-DIFFUSION FLOW PROCESS, AND THEIR INTERACTION | 2-37 |
| 2.6. | EFFECT OF SORPTION TIME CONSTANT ON GAS SORPTION RATE | 2-68 |
| 2.7. | THREE SETS OF RELATIVE PERMEABILITY CURVES USED FOR SYSTEMS A, B, AND C | 2-69 |
| 2.8. | EFFECT OF RELATIVE PERMEABILITY CHARACTERISTICS ON GAS SORPTION | 2-70 |
| 2.9. | EFFECT OF RELATIVE PERMEABILITY CHARACTERISTICS ON WATER PRODUCTION RATE | 2-71 |
| 2.10. | EFFECT OF RELATIVE PERMEABILITY CHARACTERISTICS ON GAS PRODUCTION RATE | 2-72 |
| 3.1. | DISTRIBUTION OF GAS, STRAIN AND $t_o$ IN COAL SEAM | 3-52 |
| 5.1. | RELATIVE PERMEABILITY CHARACTERISTICS IMPOSED ON THE COAL SEAM | 5-3 |
| 5.2. | MINE LAYOUT AND RELEVANT DIMENSIONS | 5-4 |
| 5.3. | FINITE-DIFFERENCE GRID IMPOSED ON THE COAL SEAM | 5-6 |
| 5.4. | VARIATION OF METHANE EMISSION RATE AT THE ACTIVITY MINE FACE AS A FUNCTION OF TIME FOR THREE COALS OF DIFFERENT METHANE CONTENT. RETREAT DIRECTION IS PARALLEL TO THE FACE CLEAT | 5-7 |
| 5.5. | VARIATION OF METHANE EMISSION RATE AT THE ACTIVITY MINE FACE AS A FUNCTION OF TIME FOR THREE COALS OF DIFFERENT METHANE CONTENT. RETREAT DIRECTION IS PERPENDICULAR TO THE FACE CLEAT | 5-8 |
| 5.6. | DEGASIFICATION OF METHANE WITH THE AID OF TWO BOREHOLES DRILLED FROM THE ROADWAYS | 5-11 |
| 5.7. | FINITE-DIFFERENCE GRID USED IN EXERCISE 2 | 5-12 |
| 5.8. | PRODUCTION PERFORMANCE BEHAVIOUR OF HORIZONTAL BOREHOLE. BOREHOLE IS DRILLED PERPENDICULAR TO THE FACE CLEAT DIRECTION (WELL #1) | 5-13 |

## LIST OF FIGURES


| Figure | | Page |
|---|---|---|
| 5.9. | PRODUCTION PERFORMANCE BEHAVIOUR OF HORIZONTAL BOREHOLE. BOREHOLE IS DRILLED PERPENDICULAR TO THE FACE CLEAT DIRECTION (WELL #2) | 5-14 |
| 5.10. | PRODUCTION PERFORMANCE BEHAVIOUR OF HORIZONTAL BOREHOLE. BOREHOLE IS DRILLED PARALLEL TO THE FACE CLEAT DIRECTION (WELL #1) | 5-15 |
| 5.11. | PRODUCTION PERFORMANCE BEHAVIOUR OF HORIZONTAL BOREHOLE. BOREHOLE IS DRILLED PARALLEL TO THE FACE CLEAT DIRECTION (WELL #2) | 5-16 |
| 6.1. | SIMPLIFIED DIAGRAM OF THE MODEL COMPONENTS | 6-6 |
| 6.2. | METHANE FLOW MODEL RESEARCH AND DEVELOPMENT PROGRAM | 6-9 |
| 6.3. | METHANE FLOW MODEL RESEARCH AND DEVELOPMENT PROGRAM - PHASE I | 6-10 |
| 6.4. | METHANE FLOW MODEL SELECTED APPLICATION MODULES | 6-13 |
| 6.5. | METHANE FLOW MODEL VERIFICATION PROGRAM | 6-15 |

## NOMENCLATURE

| | |
|---|---|
| A | cross-sectional area, $ft^2$ |
| a | shape factor, $ft^{-2}$ |
| b | slippage factor, psi |
| C | molar concentration, lb-mole/$ft^3$ |
| $C_L$ | Langmuir molar concentration, lb-mole/$ft^3$ |
| c | compressibility, $psi^{-1}$ |
| D | diffusivity coefficient, $ft^2$/day |
| k | permeability, md |
| L | length, ft |
| $M_w$ | molecular weight, lb/lb-mole |
| p | pressure, psia |
| $p_L$ | Langmuir pressure constant, psia |
| PF | geometric prefactor, $ft^{-2}$ |
| Q | flow rate, $ft^3$/day |
| R | real gas constant |
| | $10.73 \frac{\text{lb-mole } °R}{\text{psi } ft^3}$ |
| r | radius, ft |
| s | phase saturation, fraction |
| T | temperature, °R |
| t | time, day |
| V | volumetric concentration, SCF/$ft^3$ |
| $v_b$ | bulk, volume, $ft^3$ |
| v | velocity, ft/day |
| x | spatial coordinate (rectangular geometry), ft |

| | |
|---|---|
| $\alpha$ | bulk matrix compressibility, $psi^{-1}$ |
| $\alpha$ | constant |
| $\beta$ | turbulence coefficient, $ft^{-1}$ |
| $\lambda$ | flow coefficient |
| $\bar{\lambda}$ | mean free path, cm |
| $\mu$ | dynamic viscosity, cp |
| $\rho$ | density, $lb/ft^3$ |
| $\sigma$ | effective stress, psia |
| $\Phi$ | potential, psia |
| $\phi$ | porosity, fraction |

Subscripts

| | |
|---|---|
| a | apparent |
| ads | adsorbed |
| c | capillary |
| D | dimensionless |
| E | equilibrium |
| F | free |
| g | gas |
| ma | macropore |
| mi | micropore |
| $\infty$ | infinite |
| o | initial value |

Superscripts

| | |
|---|---|
| — | average |

# 1. INTRODUCTION

Emission of methane gas into mine workings poses a safety concern due to the explosive nature of the methane gas. It also affects mining production because it leads to work stoppages and influences the design of ventilation systems. The rate and pattern of methane emission depends on a combination of coal seam characteristics such as the seam gas content, the strata porosity and permeability, seam discontinuities, variations in permeability caused by the stress redistribution during mining operations, and on mining factors such as coal cutting rate, roof control, material handling methods, mine layout, and methane drainage scheme. The manner in which these factors influence the inflow of methane into coal mine workings cannot be completely identified; however, useful prediction methods have been developed and successfully applied to providing information for design of mine ventilation systems and methane drainage, as well as for mine operations.

The overall objective of this research program has been to develop a computer-based numerical model to simulate the time-dependent release of methane gas from the seam being worked, and from the adjacent seams and strata into longwall coal mine workings. The specific objectives of the project have been: 1) to conduct an in-depth review of the reported models of methane flow into longwall coal mine workings including their merits and shortcomings, 2) to identify model elements applicable to the

development of a multi-seam methane flow model for longwall coal mines; and 3) to define a research plan for the implementation of the computer-based models at the Canadian mines.

Chapter 2 of this report reviews the background material for modelling methane emission in coal seams. The reviewed topics include: 1) the porosity of coal, 2) adsorption-desorption of gases, 3) diffusion, 4) laminar and non-laminar flow, 5) permeability, 6) flow through porous media, 7) effects of stress on porosity, permeability and gas flow, 8) effects of water saturation on gas flow, and 9) approximate or numerical methods. Based on the background material, the physical representation and fundamental equations are recommended for modelling the flow of methane into coal mine workings. The physical representation and fundamental equations are listed in Section 3.1 of Chapter 3.

Five sets of reported models of methane flow into coal mine workings were reviewed in depth in Chapter 3. The selected models included: 1) the Pennsylvania State University models, 2) METGEN model, 3) University of Nottingham models, 4) United States Bureau of Mines model, and 5) Airey's empirical model. The review has considered the primary and secondary objectives of the models; the assumptions made in describing the physical phenomena and the subsequent governing equations, the numerical techniques and computer programs used to solve the model equations, the methods applied to validate the models, and the merits and limitations of the model. A discussion of the

findings is detailed in Section 3.2. Section 3.3 briefly reviews computer models which were developed for degasing coal seams and which may be of interest for the development of a computer model for prediction of methane flow into mine workings.

Twenty-nine model parts have been identified in Chapter 4 as being important for the prediction of methane flow into mine workings. The twenty-nine selected parts were listed in three groups: essential, important and useful, according to each model part priority and significance.

A series of simulation runs has been conducted in Chapter 5 using the PSU model. The parametric study included prediction of methane flow into an active mine, and degasing of the seam using horizontal boreholes.

The report is concluded with an outline of the required research and development work (Chapter 6) and a summary of major findings concerning application of the computer-based numerical models for simulation of methane flow into longwall coal mine workings (Chapter 7). Chapter 7 also discusses briefly the benefits that may be accrued by applying computer-based models to mine planning and operations.

# 2. REVIEW OF BACKGROUND FOR METHANE IN COAL SEAM MODELLING

## 2.1. Porosity of Coal

The porosity of coal and specifically its characteristic distribution gives rise to unique behaviour during mining and utilization. For example, porosity determines such coal properties as the amount of free and adsorbed methane, the physical strength, the amount of moisture, etc. Porosity determines the coal surface that is available for reaction or adsorption of gases.

Methods for determination of coal porosity were recently reviewed by Mahajan and Walker (1978). For clarification, however, we will review here basic concepts and terms used in describing coal porosity. Figure 2.1 is a schematic representation of flow mechanisms in coal pore structure as postulated by Ertekin et al. (1986).

### 2.1.1. Background

Pore structure of coal is characterized by pore volume, pore surface area and pore size distribution, which are determined from physical parameters like true density, particle density, physical sorption of gases and mercury porosimeter. A brief definition of each parameter is given below.

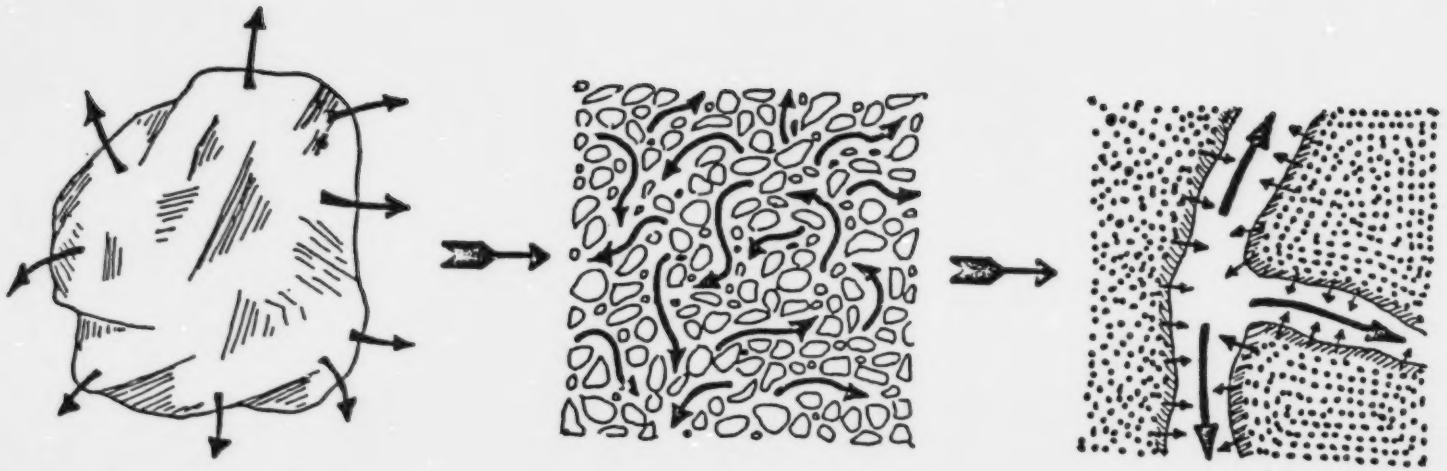




Figure 2.1. SCHEMATIC OF METHANE FLOW DYNAMICS IN A COAL SEAM

## True Density

True density of coal is determined by helium displacement assuming that helium is not adsorbed at room temperature and that all pore volume is accessible to helium. These assumptions were questioned by several studies; however, for most coals helium adsorption is negligible at room temperature and most pores are accessible.

Typical true densities for bituminous coals range from 1.38 g/cm³ to 1.59 g/cm³.

## Density Correction for Mineral Matter

Coal contains a variable amount of mineral matter which has a higher density than coal organic matter. To obtain the density of organic matter the density is corrected using equation (2.1.1):

$$\frac{f_m}{\rho_m} + \frac{(1-f_m)}{\rho_c} = \frac{1}{\rho} \qquad (2.1.1)$$

where $\rho_m$ = density of mineral matter (~2.7 g/cm³)

$\rho_c$ = the corrected density

$\rho$ = the uncorrected density

$f_m$ = the content of mineral matter, fraction by weight.

Particle Density (Mercury Density)

Mercury density of coal is determined from the volume of mercury that the sample displaces under given mercury porosimeter pressure. Gan et al. (1972) showed that the interparticle voids are filled with mercury at 413 kPa, and that further increase in pressure results in filling coal pores. Particle density includes coal pores and cracks.

Apparent Density

Apparent density of coal depends on the liquid that coal displaces using the pycnometric method. It depends on the size and properties of fluid, the degree of interaction between coal and fluid (swelling and surface effects), and time allowed for penetration (Mahajan and Walker, 1978). Apparent density of coal may exceed the true helium density because of adsorption of fluid, e.g. hydrocarbons. (Bond and Spencer, 1957).

Apparent density of coal is a function of particle size, moisture and fluid properties.

Pore Surface Area

Pore surface area is primarily associated with micropore structure (<300 Å radii) of coal. It is most often determined

using the BET (Brunauer, Emmett and Teller) adsorption isotherm (equation (2.1.2)):

$$\frac{P}{V(P_o-P)} = \frac{1}{V_m C} + \frac{C-1}{V_m C} \cdot \frac{P}{P_o} \qquad (2.1.2)$$

where $V$ = volume adsorbed at equilibrium pressure $P$

$P_o$ = saturation vapor pressure of nitrogen at -196°C

$V_m$ = monolayer capacity (caverage) in $cm^3$

$C$ = "net" heat adsorption.

In order to solve for $V_m$, $P/V(P_o-P)$ is plotted against $P/P_o$, and the resultant straight line gives slope $S = (c-1)/V_m C$ and intercept $I = 1/V_m C$. Solution of the two equations gives $V_m$ and $C$.

The pore specific surface area $S(m^2/g)$ can be calculated using equation (2.1.3):

$$S = \frac{V_m}{22414} \cdot N \cdot S_{N_2} \times 10^{18} \qquad (2.1.3)$$

where $N$ = Avogadro's number ($6.06 \times 10^{23}$)

$S_{N_2}$ = area in $nm^2$ (0.162 for $N_2$) occupied per molecule of adsorbed gas in the complete monolayer.

The BET method using nitrogen at -196°C does not determine the total micropore surface. At -196°C, not all micropores are

accessible to nitrogen molecules due to their narrow pore mouth. According to Anderson et al. (1965) nitrogen adsorption isotherm determines only pore surface area for pores with a diameter greater than 0.5 nm.

The difficulty with the activated diffusion of the adsorbate at low temperature can be overcome by the use of carbon dioxide as the adsorbate. Carbon dioxide has a larger molecular area (0.253 $nm^2$) than nitrogen, but also higher diffusional rates at adsorption temperature of 25°C. Coal surface obtained using carbon dioxide isotherms range from 100 to 200 $m^2/g$ versus 1 or 2 $m^2/g$ obtained using nitrogen. Unfortunately, the saturation pressure of carbon dioxide at 25°C is 6.4 MPa, which requires a high pressure adsorption system for the BET isotherms. This is not practical and, consequently, carbon dioxide adsorption apparatus is used only for special purposes.

Marsh and Siemieniewska (1965) proposed the Polanyi-Dubinin (P-D) equation for determining the micropore surface area in coals. The equation permits determination of the pore capacity with carbon dioxide at pressures less than the saturation pressure:

$$\log V = \log V_o - \frac{0.434\ BT^2}{\beta^2} (\log \frac{P_o}{P})^2 \qquad (2.1.4)$$

Equation (2.1.4) relates the amount of carbon dioxide adsorbed, V, at pressure P, to the micropore capacity, $V_o$. A plot of log V versus $(\log P_o/P)^2$ gives a straight line with the intercept of

log $V_o$. The micropore capacity is then converted to the micropore surface using equation (2.1.3).

Walker and Patel (1970) published coal surface data obtained using the BET equation with high pressure $CO_2$ adsorption isotherm and P-D equation at less than atmospheric pressure. The results showed a good agreement between the high pressure and vacuum experiments, thus facilitating the evaluation of coal micropore surface area using conventional adsorption apparatus and P-D equation for carbon dioxide.

Pore Size Distribution

Pore size distribution in coal is measured using nitrogen isotherms at -196°C up to relative vapor pressure ($P/P_o$) = 0.93, for radii up to 300 Å, and the mercury porosimetry for pores up to 75,000 Å radii.

Mercury Porosimetry (Macropores)

Pore size distribution can be determined from the volume penetration of mercury into coal at progressively increasing pressure. The relation between the radii of the penetrated pore (r) and mercury pressure (p) was derived by Washburn (1921) (equation (2.1.5)):

$$r = \frac{-2\,\gamma \cos\theta}{P} \quad \text{or} \quad r(\mu) = \frac{75{,}000}{P(\text{kPa})} \qquad (2.1.5)$$

where $\gamma$ is the surface tension of mercury (480 dynes/cm) and $\theta$ is the contact angle (140°) between mercury and the pore wall.

A major drawback in applying mercury porosimetry is that at high pressures coal pores collapse or widen due to high compressibility of coal. For this reason maximum pressure of only 68 MPa, which correspond to a pore diameter of 180 Å, is used.

Micropores System (Nitrogen Isotherms)

Barrett et al. (1951) developed a generalized method for determining pore volume and size distribution directly from the nitrogen adsorption data. The pore radii (r) corresponding to a given value of adsorption isotherm at given $P/P_o$ ratio is calculated using the Kelvin equation (2.1.6):

$$\ln (P/P_o) = - \frac{2V\gamma \cos \theta}{r\, RT} \qquad (2.1.6)$$

where V = molar volume of nitrogen

$\gamma$ = surface tension of nitrogen

$\theta$ = contact angle between nitrogen and the pore wall (assume zero)

R = gas constant

T = temperature (77°K).

Porosity

Porosity of coal can be calculated from the relationship:

$$P = 100\ \rho_p\ (\frac{1}{\rho_p} - \frac{1}{\rho_t}) \qquad (2.1.7)$$

$$\text{and}\quad V_T = \frac{1}{\rho_p} - \frac{1}{\rho_t} \qquad (2.1.8)$$

where subscripts p and t stand for particle and true densities and $V_T$ is the total open pore volume (volume that is occupied by pores).

For coals filled with water the porosity can be calculated from the following relations:

When particles are completely saturated with water:

$$P_W = 100 \cdot \frac{\rho_t - \rho_p}{\rho_t - \rho_W} \qquad (2.1.9)$$

where $\rho_W$ is the density of the water.

When particles are partly filled with gas and partly with water, for the pore filled with gas, $P_{gW}$:

$$P_{gW} = 100 \left[1 - \frac{\rho_p}{1+m} \cdot (\frac{m}{\rho_W} + \frac{1}{\rho_t})\right] \qquad (2.1.10)$$

Where m is the moisture content (kg/kg) for the pores filled with water:

$$P_{gW} = 100 \left[ \frac{\rho_p m}{(1+m)\rho_w} \right] \qquad (2.1.11)$$

and the total porosity is given by:

$$P_{TW_g} = 100 \left[ 1 - \frac{\rho_p}{(1+m)\rho_t} \right] \qquad (2.1.12)$$

Coal porosity consists of macropore and micropore systems (Zwietering et al., 1956). An example of the interrelation between macro and micropore systems for bituminous coals is given in Table 2.1. As apparent, there is a relationship between the micropore volume and surface area. This suggests that most of the coal surface area available for adsorption is due to the micropore system. Assuming cylindrical pores, calculation of a pore diameter from the coal surface area gives an average pore diameter of 20 Å. The relation between the surface area and pore volume is given by equation (2.1.13):

$$S \ (cm^2/g) = 1.8 \times 10^7 \ V_p \ (cm^3/g) \qquad (2.1.13)$$

Bond and Spencer (1957) studied the size distribution of the micropore system by measuring heat of wetting for liquids with a different molecular weight. The results showed bimodal distribution of micropore system determined by the pore mouth of

an approximate width of 5 to 8 Å. They proposed a model for a micropore system consisting of pores up to 40 Å in height and flat in shape, and separated by a network of narrower passages.

Gan et al. (1972) suggested the following classification for micro and macropore systems:

1. Total open pore volume, $V_T$, as determined from the true and particle densities (equation (2.1.7)).

2. Macropore volume as determined from mercury penetrometry (pore with radii greater than 150 Å).

3. Micropore volume as determined from the nitrogen capillary adsorption isotherms (pores with radii between 8 and 150 Å).

4. Pore volume for pores smaller than 8 Å and probably not accessible to methane.

**Table 2.1. PORE STRUCTURE OF SOME COALS (from Zwietering and Van Krevelen, 1956).**

| Coal | | % Moisture (air dried coal) | Porosity | Pore Volume ($cm^3/g$) | | | Internal surface $m^2/g$ |
|---|---|---|---|---|---|---|---|
| % C | % H | | | Total | Macro | Micro | |
| 84.7 | 4.9 | 2.7 | 0.139 | 0.121 | 0.039 | 0.082 | 120 |
| 81.2 | 4.4 | 2.7 | 0.146 | 0.125 | 0.042 | 0.083 | 128 |
| 80.5 | --- | 2.7 | 0.142 | 0.120 | 0.064 | 0.056 | 131 |
| 84.5 | 4.5 | 2.5 | 0.138 | 0.118 | 0.051 | 0.067 | 110 |
| 82.3 | --- | 2.1 | 0.100 | 0.090 | 0.052 | 0.038 | 90 |
| 88.6 | 4.9 | 1.4 | 0.125 | 0.107 | 0.042 | 0.065 | 90 |
| 88.0 | 4.8 | 1.3 | 0.120 | 0.102 | 0.043 | 0.059 | 82 |
| 85.5 | --- | 1.0 | 0.088 | 0.070 | 0.035 | 0.035 | 70 |
| 87.6 | 4.5 | 0.9 | 0.097 | 0.073 | 0.043 | 0.030 | 84 |
| 85.8 | 4.8 | 0.8 | 0.118 | 0.100 | 0.041 | 0.059 | 85 |
| 85.7 | --- | 0.6 | 0.070 | 0.058 | 0.038 | 0.020 | 40 |

### 2.1.2. Application to Methane in Coal Bed Modelling

The macropore system is made up of the volume occupied by the cleat. The fracture spacing is very uniform (ranging from a fraction of an inch to several inches) with the face and butt cleat generally intersecting at right angles. The face cleat is continuous throughout the seam, while the butt cleat in many cases is discontinuous, ending at an intersection with the face cleat. The total effective porosity to water is less than 2%, while the effective porosity to free gas in the same coal may be as high as 10% (Patching, 1970). Figure 2.2 is a schematic representation of the pore structures in coal.

Gas can exist in three states in a coal seam. The major portion of gas stored in coal exists as an adsorbed, liquid-like, molecular monolayer on the walls of the micropore system. Gas can also exist as free gas in both the micropores and macropores and to a lesser extent, in solution in resident brine. Therefore, in measuring the porosity of coal, it must be made certain that one is measuring the fractional volume of the coal that is capable of being occupied by free gas and not adsorbed gas. In general, the water porosities are considered to yield a better representation of the pore structure of the coal. In a more global sense the porosity of coal is found to be between 1% and 8%.

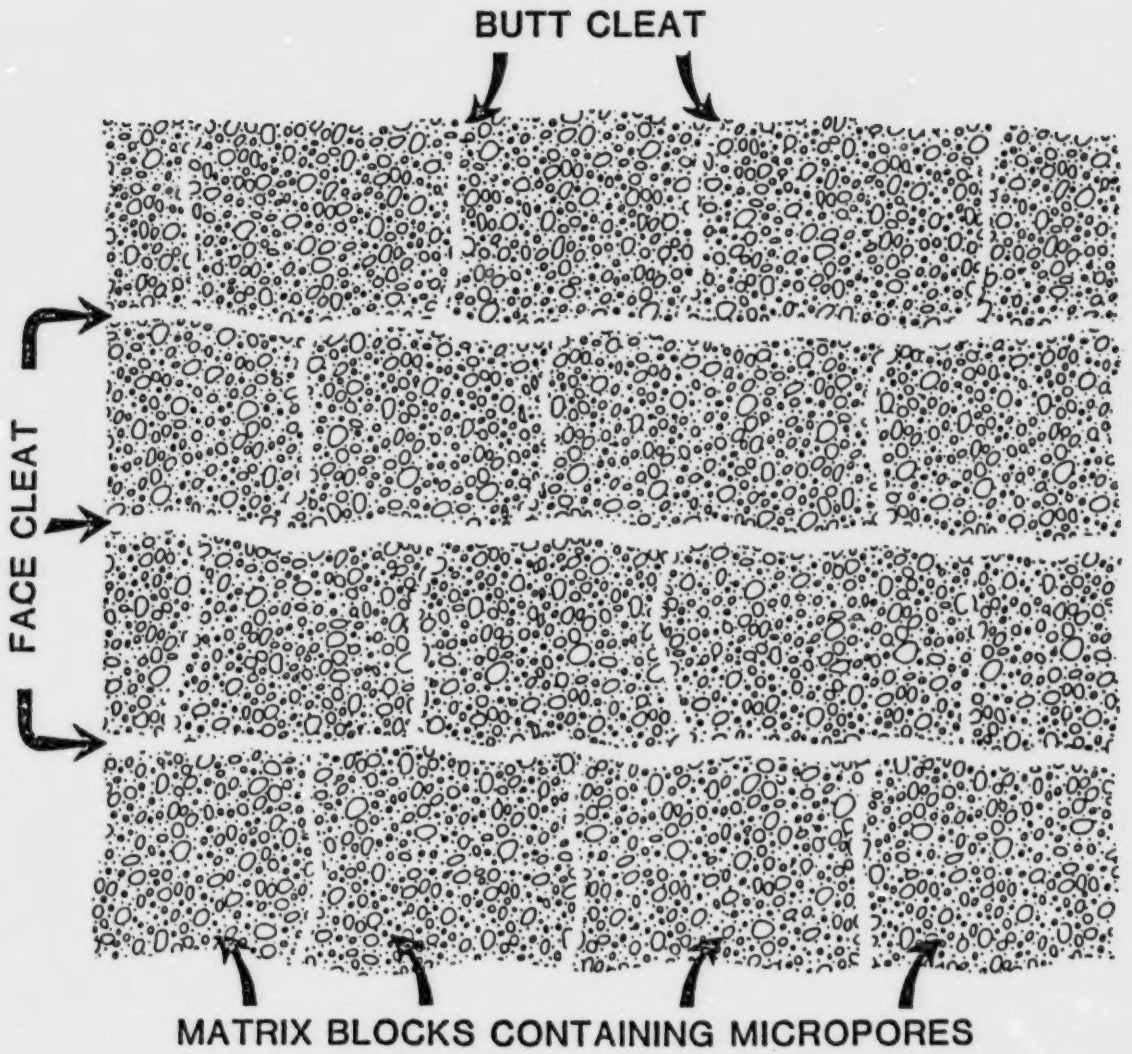


**Figure 2.2. DUAL-POROSITY NATURE OF COAL SEAM**

## 2.2. Adsorption-Desorption of Gases

Due to the small dimensions of the micropores, a large internal surface area exists within the coal matrix. When a methane molecule comes into contact with an internal surface, two storage mechanisms are possible (Gawuga, 1979). The first mechanism of entrapment occurs when the gas molecule penetrates the surface and resides within the molecular lattice of the coal. This is an absorption process. The second mechanism occurs when the gas molecule adheres to the surface. This is an adsorption process. Both storage mechanisms are theorized to occur in coal.

The adsorption process can be classified by the forces which cause the gas molecule to adhere to the surface. If these forces are chemical in nature, such as strong chemical bonding, then the process is a chemisorption process. If, however, the forces are physical, such as electrostatic forces or Van der Waal's forces, the process is a physical adsorption process. The major portion of the gas stored in coal exists as a physically adsorbed, molecular monolayer (Patching, 1970a).

Theoretically, the physical adsorption process is reversible. In coal, however, a small degree of absorption and chemisorption occurs along with the physical adsorption (Gawuga, 1979). Consequently, a hysteresis effect is often observed between experimentally determined adsorption and desorption isotherms.

The packing of methane molecules is thought to be only one molecule thick and its density increases with pressure. The large specific surface area which exists on the coal grain surfaces makes the coal grains able to hold large volumes of gas. As it can be seen from Figure 2.3, at low pressures the volume of adsorbed gas increases rapidly in a linear fashion. At higher pressures when the density of the packing increases, the adsorption slows and finally at extreme pressures, it stops.

Although no general correlation exists, it has been observed that the sorptive capacity of coal tends to increase with increasing rank (a measure of the coal's chemical structure) and increasing depth (Kim, 1978). Figure 2.3 shows the relationship between rank, depth, and sorptive capacity. Also, the sorptive capacity tends to decrease with increasing water content and temperature (Patching, 1970b). While the change of sorption characteristics with temperature is interesting, its implications for the practical applications of methane flow dynamics in coal seams is not interesting, since the process taking place can easily be considered as isothermal.

Along with the adsorbed gas, free gas exists in both the micropores and macropores of a coal seam. The relative contribution of the free and adsorbed gas to the overall storage is dependent on the seam. Two examples of this dependence are presented in Figure 2.4.

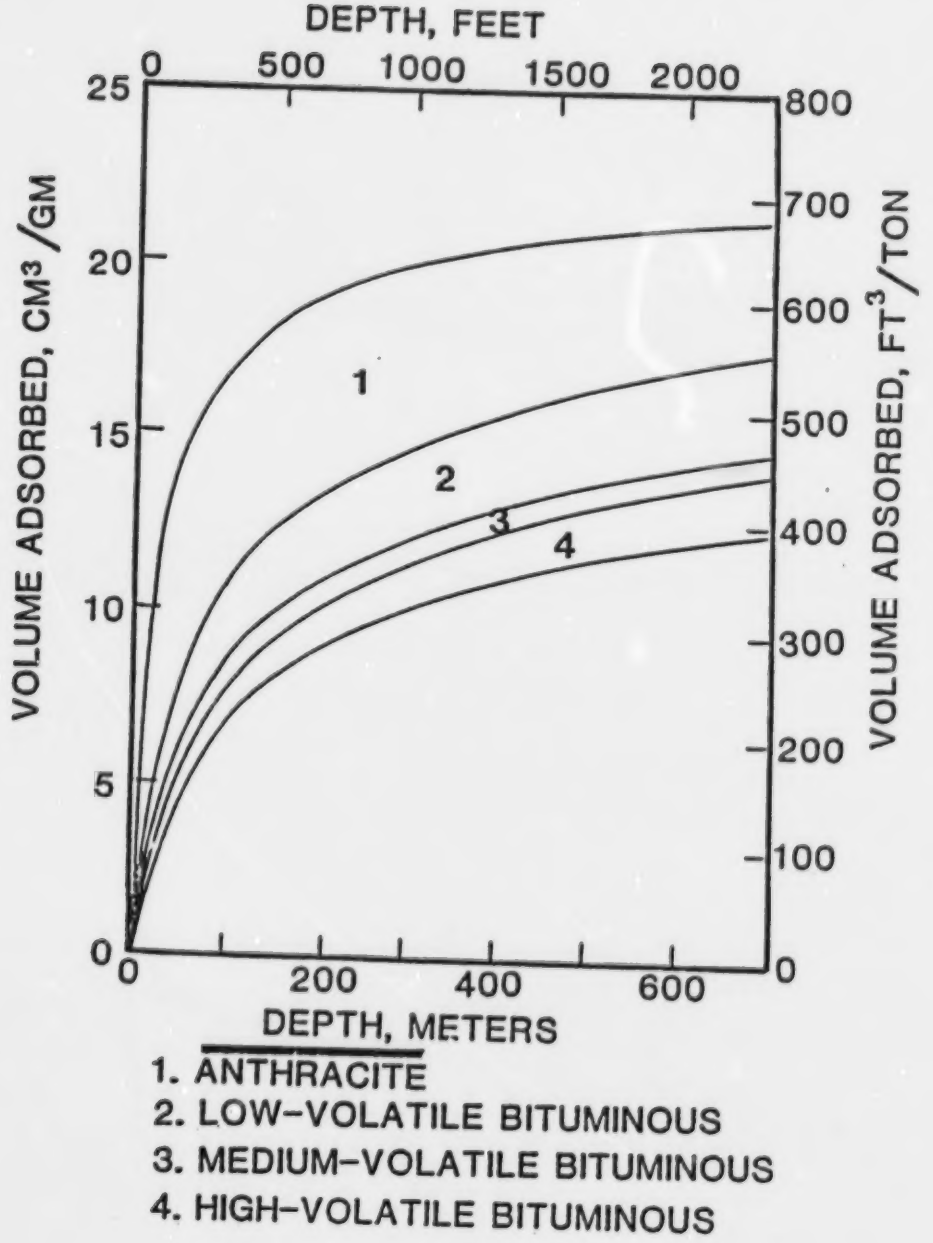


**Figure 2.3. RELATIONSHIP BETWEEN RANK, DEPTH AND SORPTIVE CAPACITY (after Kim, 1978).**

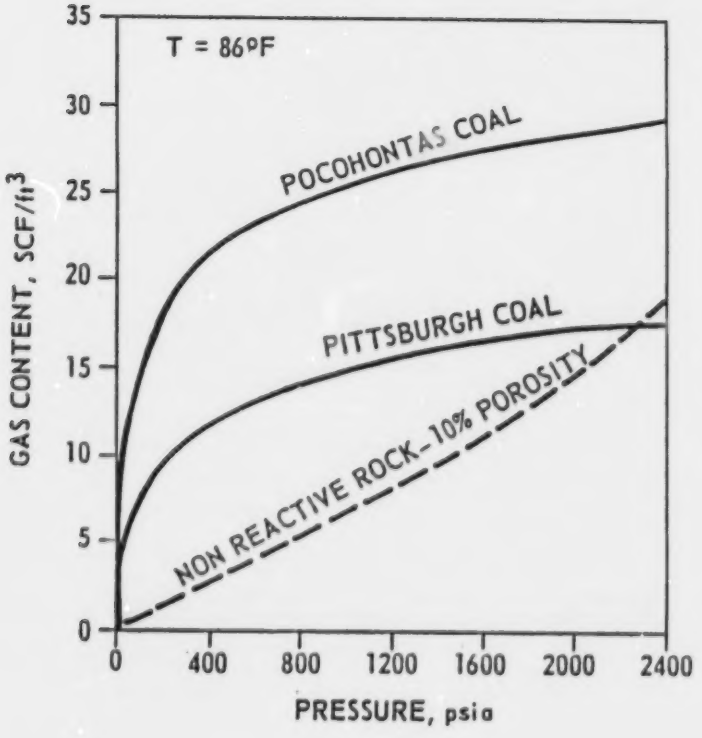


**Figure 2.4. METHANE CAPACITY OF COAL AND INERT ROCK (after Price and Ancell, 1976).**

Matrix sorption phenomena and two-phase flow in a matrix/fracture network make methane transport in coal a more complex problem than fluid transport in conventional dual-porosity reservoirs. Therefore, while many of the models developed for conventional naturally fractured reservoirs can be solved analytically, numerical solution techniques are generally required to solve coal-bed methane models. The complexity of the methane transport problem is significantly reduced by assuming that the coal matrix is in continuous equilibrium with the fracture system. In this type of model, the quantity of adsorbed gas in the matrix is only a function of the pressure in the fractures. Thus, as the fracture pressure declines over a discrete time interval, sorbed gas is released into the fractures.

Several models based on equilibrium, or pressure dependent, sorption have been developed to describe the single-phase release of methane gas from the coal matrix. In these models, the gas adsorbed onto the micropore walls is assumed to be in a constant state of equilibrium with the free gas phase in the macropore system. Models based on this approach are essentially single porosity models altered for coal seams by either the inclusion of a pressure dependent source term or by the modification of the storage term. These models generally predict optimistic results since, upon pressure decline, the adsorbed gas is assumed to immediately enter the macropore system.

For large coal masses, Airey (1968) derived the following partial differential equation for the gas emission from a stationary mine face:

$$\frac{\partial^2 P_D^2}{\partial^2 x_D} = \frac{\partial P_D^2}{\partial t_D} \qquad (2.2.1)$$

Researchers (Gorbachev et al., 1973, Vylegzhanin, 1974, Karagodin and Krigman, 1974, and Vorozhtsov et al., 1975) from the Soviet Union made use of the following model to simulate the single-phase flow of gas through coal:

$$\nabla \cdot (\lambda P_g \nabla P_g) = \frac{\partial}{\partial t} [\phi P_g + \frac{C_L P_g RT}{(P_L+P_g)}] \qquad (2.2.2)$$

The major difference between this model and Airey's (1968) model is in the storage term (partial derivative with respect to time). The ideal gas considered in equation (2.2.2) can be stored either as free gas, $\frac{\partial}{\partial t} [\phi P_g]$, or as adsorbed gas, $\frac{\partial}{\partial t} [\frac{C_L P_g RT}{(P_L+P_g)}]$. This is in contrast to Airey's model, which allowed only adsorbed gas storage. Also, the adsorbed gas in equation (2.2.2) obeys Langmuir's theory, which results in a nonlinear sorption isotherm. Henry's Law, which was used in the derivation of equation (2.2.1), predicts a linear isotherm.

Owili-Eger (1973) proposed a ventilation model, in which the following partial differential equation was used to govern the

rate of gas emission into the mine. It is derived in a two-dimensional (x-z) rectangular coordinate system:

$$\nabla\cdot(\lambda\nabla P_g^2) + \underset{\sim}{\alpha}q = 0 \qquad (2.2.3)$$

The associated boundary conditions with equation (2.2.3) gave the steady-state emission rate from the coal seam (when q(z)>0) and adjacent strata (when q(z)=0) into the mine being modelled.

O'Shaughnessy (1980) developed a model similar to that of Owili-Eger (1973) for the steady- and unsteady-state flow of gas towards a longwall face.

Price and Abdalla (1972) and Price et al. (1973) proposed a two-phase, equilibrium sorption model for field scale simulations. The equations used in this model had the form in two-dimensional (x-y) rectangular coordinate system:

$$\nabla\cdot(\lambda_k\rho_k\nabla\Phi_k) - \frac{1}{V_b}(Q_k - kq) = \phi\frac{\partial}{\partial t}(\rho_k S_k) \qquad (2.2.4)$$

where k = 0: water phase

1: gas phase.

A slightly more sophisticated approach to modelling methane transport in coal seams involves treating matrix sorption as a quasi-steady-state transport process, similar to the formulation

of Warren and Root (1963) for conventional naturally fractured reservoirs. In a quasi-steady-state model, the sorption rate is proportional to the difference between the concentration of the gas at the external matrix surface and the average concentration of the gas contained within the matrix.

Boyer et al. (1982) and Pavone and Schwerer (1984) used the non-equilibrium sorption formulation to derive a set of equations which described the simultaneous flow of water and gas through coal seams:

$$\nabla \cdot (\lambda_k \nabla p_k) + k \underset{\sim}{\alpha} \frac{q}{V_b} = \frac{\partial}{\partial t} (\phi R_k) \qquad (2.2.5)$$

where

$$\frac{q}{V_b} = - (PF)_{mi} \frac{dV_{mi}}{dt} \qquad (2.2.6)$$

$$\frac{dV_{mi}}{dt} = D \cdot a \cdot [V_E(p_g) - V_{mi}] \qquad (2.2.7)$$

Ertekin et al. (1983), King et al. (1986), Remner et al. (1986), and Sung et al. (1986) presented models similar to that of Pavone and Schwerer (1984). The major difference in these models was found to be in the numerical solution of the system of differential equations.

True unsteady sorption models, similar to the conventional dual-porosity model developed by DeSwaan (1976), relate the sorption rate to the concentration gradient at the external surface of the coal matrix.

A model for broken coal suggested by Smith and Williams (1982) used an unsteady-state formulation. In this model, the coal sample was assumed to have a spherical macropore geometry, and the micropore matrix subelements were also assumed to be spherical.

Kovalev and Kuznetsov (1974) formulated the following moving boundary value problem to calculate the rate of methane emission into an advancing longwall face. To describe the non-equilibrium diffusion/sorption of gas, the following equations were derived:

$$\frac{\partial}{\partial x}\left(\lambda_g \rho_g \frac{\partial p_g}{\partial x}\right) = \frac{\partial}{\partial t}\left[\phi_{ma}\rho_g + (1-\phi_{ma})M_{mi}\right] \qquad (2.2.8)$$

$$\frac{D_{mi}}{r_{mi}^2} \frac{\partial}{\partial r_{mi}} \left(r_{mi}^2 \frac{\partial C_{mi}}{\partial r_{mi}}\right) = \frac{\partial C_{mi}}{\partial t} \qquad (2.2.9)$$

$$M_{mi} = \frac{3(MW)}{R_{mi}^3} \int_0^{R_{mi}} C_{mi}(\hat{r}_{mi}, t)\ \hat{r}_{mi}^2\ d\hat{r}_{mi} \qquad (2.2.10)$$

Price and Ancell (1978) and Ancell et al. (1980) presented an unsteady-state, non-equilibrium sorption version of the model developed by Price and Abdalla (1972). The equations used in this two-phase, computer model were:

$$\nabla_{ma}\ (\lambda_k \rho_k \nabla_{ma} \Phi_k) - \frac{1}{v_{b_{ma}}}\ (Q_k - kq) = \frac{\partial}{\partial t}\ (\phi S_k \rho_k) \qquad (2.2.11)$$

$$\frac{d_{mi}}{r_{mi}^2}\ \frac{\partial}{\partial r_{mi}}\ \left(r_{mi}^2\ \frac{\partial C_{mi}}{\partial r_{mi}}\right) = \frac{\partial C_{mi}}{\partial t} \qquad (2.2.12)$$

$$\frac{q}{v_{b_{ma}}} = \frac{-3(MW)D_{mi}}{R_{mi}}\ \left.\frac{\partial C_{mi}}{\partial r_{mi}}\right|_{r_{mi} = R_{mi}} \qquad (2.2.13)$$

Kolesar and Ertekin (1986) presented the comparison of quasi-steady-state and unsteady-state matrix formulations in the slab, spherical, and cylindrical micropore structure of coal. They reported that unsteady-state models give significantly higher diffusion and production rates than quasi-steady-state micropore formulations during early simulation times. However, this early rate difference rapidly diminishes to less than 25% during the early stages of production.

## 2.3. Diffusion

### 2.3.1. Background

The diffusion process can be defined as "... the process by which matter is transported from one part of a system to another as a result of random molecular motions." (Crank, 1956). The process was quantified by Fick in 1855 with the following relationship:

$$\frac{q}{A} = - D \frac{dC}{dL} \qquad (2.3.1)$$

Fick's law states that the mass flux is directly proportional to the applied concentration gradient. The proportionality coefficient, D, is the diffusivity coefficient and is a property of the substance being transported, as well as the medium through which it is being transported.

Smith and Williams (1982) presented a detailed review of the mechanisms of gas diffusion through porous media. Their discussion determined that the diffusion of gases through a pore system can be the result of three distinct flow mechanisms that may act individually or simultaneously. The mechanisms are (1) bulk flow, where molecule/molecule interactions dominate; (2) Knudsen flow, where molecule/surface interactions dominate (as in the flow through a capillary); and (3) two-dimensional (2D) surface flow of adsorbed gas (when an adsorbed gas layer exists).

The following rules determine which flow mechanism dominates gas transport. If the diffusivity is inversely proportional to the flowing pressure, then bulk flow is the dominant diffusion mechanism. If, however, the diffusivity is independent of flowing pressure (i.e., constant), then gas transport is dominated by Knudsen flow. Finally, if the flux ratio satisfies:

$$\frac{Q_f}{Q_{ads}} < \sqrt{\frac{M_{w_{ads}}}{M_{w_F}}} \qquad (2.3.2)$$

then 2D surface diffusion dominates.

Another criterion for the determination of the type of diffusion is the Knudsen number which is calculated according to equation:

$$N_k = \frac{\lambda}{2\bar{r}} \qquad (2.3.3)$$

with typical numbers for a Knudsen flow above 10 and for a transition flow $N_k < 10$.

In 1937, Adzumi proposed the following approach to model the slip phenomenon through capillary tubes. The flow of a gas through a capillary, when the mean free path of the gas molecules is small compared to the capillary radius, is governed by the Hagen-Poiseuille law:

$$q = \frac{\pi r_c^4 \bar{p} \Delta p}{8 \mu p L} \qquad (2.3.4)$$

The criterion of the mean free path being smaller than the capillary radius is met for capillaries with large radii or flow at high pressures.

When the mean free path is large compared to the capillary radius, the flow is governed by the Knudsen equation (Gorbachev et al., 1973):

$$q = \frac{4}{3} \frac{r_c}{p} \sqrt{\frac{2\pi RT}{M_w} \frac{\Delta p}{L}} \qquad (2.3.5)$$

The criterion of the mean free path being larger than the capillary radius is met for capillaries with small radii or flow at low pressures.

For a given capillary, there is some intermediate or transitory pressure range where the two mechanisms act simultaneously. In this range, the flow rate is governed by the modification and addition of equations (2.2.3) and (2.2.4):

$$q = \frac{\pi r_c^4 \bar{p} \Delta p}{8 \mu p L} + K_2 \frac{4}{3} \frac{r_c^3}{p} \sqrt{\frac{2\pi RT}{M_w} \frac{\Delta p}{L}} \qquad (2.3.6)$$

where $K_2$ is a constant proportional to the relative volume of the mobile boundary layer. For the capillary/gas systems studied by Adzumi, this constant was about 0.9.

With this approach and assuming that a porous medium can be modelled as a bundle of capillaries, Rose (1962) derived the following expression for the mean-free-path length:

$$\bar{\lambda} \tilde{=} 2.13 \frac{\mu}{\bar{p}} \sqrt{\frac{RT}{M_w}} \qquad (2.3.7)$$

Substituting this equation into Klinkenberg's definition of the slippage factor yields:

$$b = \frac{8.52\ K_1\ \mu}{r_c} \sqrt{\frac{RT}{M_w}} \qquad (2.3.8)$$

or, more conveniently:

$$b = \frac{K_3}{\sqrt{M_w}}\ \mu\ (p) \qquad (2.3.9)$$

Although never stated explicitly in his paper, it appears that Rose assumed a constant gas viscosity. Actually, gas viscosity is an increasing function of pressure. Thus:

$$b(p) = \frac{K_3}{\sqrt{M_w}}\,\mu(p) \qquad (2.3.10)$$

is also an increasing function of pressure. Note that two compositional parameters, M and $\mu$, appear in Rose's definition of the slippage factor.

Gunn and King (1969) studied flow models that combine diffusion and hydrodynamic flow in porous materials. They stressed that the treatment of porous media as a bundle of long capillaries is not realistic. The flow of gas in most of the porous media differs from the flow in a bundle of capillaries. For example, for capillary flow a plot of the pressure gradient, N/(dP/d) versus pressure, P, always exhibits a curve with minimum at low pressures, whereas a similar plot for most porous materials yields a straight line. Gunn and King (1969) explained this phenomenon in the following way:

> In the Knudsen flow regime only a very small fraction of the molecules entering a long capillary emerge from the opposite end; most (molecules) exit from the end they entered . . . Molecules entering with flight paths nearly parallel to the axis of the tube have a higher probability of passing through than those (molecules) with other flight paths . . . Consequently, molecules with relatively long flight paths contribute a large fraction of the actual flux even though they represent only a small fraction of the total molecules present. As the pressure is increased to the point where the number of intermolecular collisions rivals the number of wall collisions, the number of long-flight-path molecules passing through decreases exponentially with pressure as these molecules are deflected toward the walls by collision with other molecules. This effect causes the molecular flux per unit pressure gradient to decrease with increasing pressure, before increasing

again at higher pressures because of the advent of Poiseuille or viscous flow.

Because of the tortuous flow paths in porous materials there is no possibility for a flight path between wall collisions to be more than a few pore diameters long. Therefore, the Knudsen permeability (in porous materials) is not controlled by very long flight paths and there is no mechanism present to cause a minimum permeability at pressures where wall collisions and intermolecular collisions are both important.

Gunn and King (1969) also developed an equation predicting flow in porous materials with gradients in composition and total pressure. The equation is based on the "dusty" gas model, originally proposed by Maxwell in 1860, later solved by Deriguin (1946). The model envisages porous mediums as a random collection of large particles fixed in space ("dust") in reference to diffusing gas molecules. For a binary mixture, the flow equation is:

$$N_A = - \frac{C_2 D^o_{AB} K_A P}{(C_2 D^o_{AB} + K_m P) RT} \nabla Y_A \qquad (2.3.11)$$

$$- \left[ \frac{K_A (C_2 D^o_{AB} + K_B P)}{C_2 D^o_{AB} + K_m P} + \frac{C_o P}{\mu m} \right] \frac{Y_A}{RT} \nabla P$$

which includes the Poiseuille flow. Equation (2.3.11) also combines the contributions of Knudsen and slip flow treating both as one diffusive phenomena.

## 2.3.2. Application to Methane in Coal Bed Modelling

The total flow of methane in coal consists of a viscous flow through large pores and cracks, Knudsen diffusion in the intermediate pores and activated diffusion in the smaller pores. For the flow by Knudsen diffusion, at a steady-state, the amount of flow, G, across a solid slab of thickness L and a sectional area A can be approximated by the relationship:

$$G = K_k \frac{\Delta P}{\Delta L} \qquad (2.3.12)$$

where G = steady-state flow, erg/s

K = Knudsen permeability, $cm^2/s$

$\Delta P$ = pressure gradient, $dyn/cm^2$.

Sevenster (1959) found $K_k$ to be dependent on molecular weight of adsorbed gas, temperature and for some adsorbates, pressure. The latter two were explained as evidence for surface flow of adsorbed molecules.

Another approach to measuring diffusion coefficient in coal is by sorption of gas on powder coal. Kinetic measurement of sorption of gases shows a relationship between the amount of gas and time following a relationship (Zwietering et al., 1956):

$$V(t) = \frac{2V(\infty)S}{V}\sqrt{\frac{Dt}{\pi}} \qquad (2.3.13)$$

where $V(t)$ = volume of adsorbed gas at time t

$V(\infty)$ = volume of adsorbed gas at infinite time

$D$ = apparent diffusion coefficient

$V$ = specific volume of the adsorbed

$S$ = surface area.

Plotting of $V(t)$ versus $\sqrt{t}$ yields a straight line from which the diffusion coefficient can be calculated if $V(\infty)$, S and V are known. Since a long measurement period is required for $V(\infty)$, the solution is either to use adsorption isotherms at high pressures or to reduce the pressure to measurement at 25°C by using the Claussius Clapeyron equation.

Zwietering et al. (1956) determined the effect of temperature on the sorption of methane by powdered coals. They determined the diffusion coefficient to be described by the relationship:

$$D = 6.3 \times 10^{-10} C^{\frac{-3870}{RT}} \text{ cm}^2/\text{sec} \qquad (2.3.14)$$

Thus at room temperature, T=293°K, the calculated diffusion coefficient would be $10^{-12}$ $\text{cm}^2/\text{sec}$ and the half-time to establish equilibrium conditions for adsorption of methane or coal:

$$t_{1/2} = \frac{V^2}{16SD} \tilde{=} 6 \text{ minutes} \qquad (2.3.15)$$

Recently, Mahajan and Walker (1978) reviewed the experimental methods used to measure molecular flow in coal; henceforth, our discussion of measurement of diffusion in coal will be limited to the two above methods. Some general comments are given below.

Thimons and Kissell (1973) discussed difficulties in modelling diffusion in coal. They pointed out that coal has a much broader range of pore size distribution than normally found in porous materials. The pore sizes range from a few angstroms to over a micrometer. In addition, coal lumps may contain a number of macro and microcracks. As a result, laboratory measurements are difficult to reproduce and the measured diffusion may depend on particle size and the history of the sample.

The assumption that, in measuring diffusion to and from fine ground coals, the effects of cracks and macropores are eliminated, is basically sound. It is difficult, however, to determine at what particle size these effects are not important. Also, equations used to calculate diffusion coefficients require knowledge of the particle volume and surface area. They are difficult to determine and are usually approximated by BET surface area measurement and sieving for particle size determination.

For measurement of diffusion coefficients from discs or slabs similar difficulties are encountered, since the larger the disc the more likely it is to contain cracks. To complicate the

matter further, when one considers flow of methane in coal beds, the flow is dendritic in nature and not steady-state. Flow starts in small pores, then travels through larger pores to flow in small cracks and finally through larger cracks to the working surface of the mine.

The model chosen by Ertekin et al. (1986) is similar to the approach of Adzumi and is based on the premise that gas is flowing under the simultaneous influence of a pressure field (macroscopic flow) and a concentration field (random molecular flow). In this approach it is assumed that the driving mechanisms exerted by these fields are acting in parallel; that is, their velocities are additive. The flow through the pressure field obeys Darcy's law, and as such, all assumptions inherent to this law apply. The flow through the concentration field obeys Fick's law and additional assumptions regarding this mode; because this approach is derived for low-permeability formations, the mean free path of the gas molecules is large compared with the capillary radii and, thus, the Knudsen (molecule-surface) flow is the dominant diffusion mechanism. This implies that the diffusivity coefficient is constant with pressure. This is actually a convenience used in this approach rather than an assumption. At high pressures, more molecule/molecule interactions will occur and bulk diffusion may dominate. If a relationship between diffusivity and pressure is known, then it may be used in the formulation discussed below. The use of a constant diffusivity coefficient will illustrate that the dual-

mechanism approach will yield a pressure and saturation-dependent slippage factor.

Furthermore, it can be assumed that the gas can be assigned a constant diffusivity coefficient and molecular weight. That is, chromatographic separation of the gas will not occur because of the individual diffusivities of the gas constituents. This ensures a diffusivity coefficient and molecular weight independent of time.

Finally, the diffusion taking place in the medium is considered to be self diffusion. This implies that the concentration gradient and density gradient are the same for single-phase flow.

It may be difficult to visualize the difference between the macroscopic, Knudsen, and self-diffusion flow processes, as well as their interrelations. The concepts are shown schematically in Figure 2.5.

Figure 2.5a represents the flow of an incompressible liquid across cross-section A-A'. The circles represent the fluid molecules. The large arrow indicates the macroscopic (Darcian) flow while the smaller arrows indicate the random (Fickian) flow. Because the densities are equal on both sides of the cross-section, the random molecular motion has a zero net effect.

Figure 2.5b represents the same cross-section; however, a compressible fluid is flowing. Again, the large arrow indicates the macroscopic flow, while the smaller arrows indicate the molecular flow. Because the density on the upstream side of the cross-section is greater than the density on the downstream side, the random motion has a positive net effect in the direction of flow. This density (concentration) gradient is the driving mechanism of the slip flow. Because Knudsen flow is the dominant diffusion process, the pore walls, not gas molecules, are the major impedance to molecular flow.

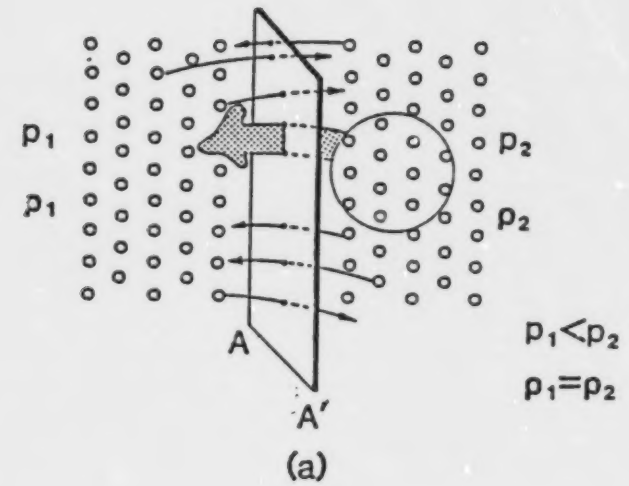


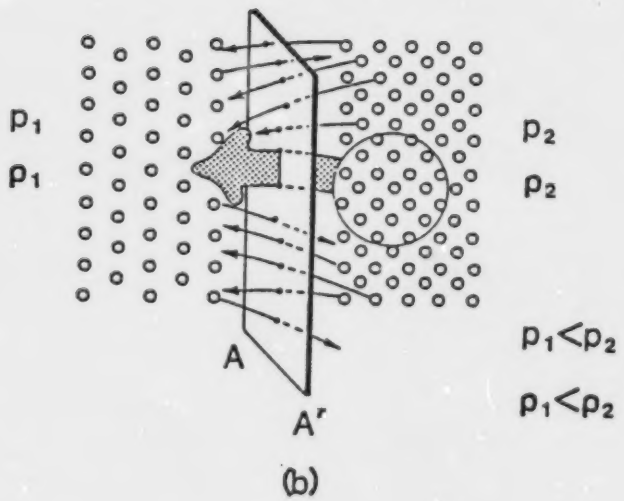


Figure 2.5. SCHEMATIC REPRESENTATION OF THE MACROSCOPIC FLOW PROCESS, SELF-DIFFUSION FLOW PROCESS, AND THEIR INTERACTION.

## 2.4. Laminar and Non-Laminar Flow

### 2.4.1. Background

A knowledge and understanding of the basic principles and concepts of fluid dynamics is required in the analysis of how methane moves in coal seams. This section presents the fundamental principles of fluid dynamics.

Mathematical Background and Notations

To represent, in an easier manner, the complex mathematical equations required to describe fluid flow the notation $D\alpha/Dt$ is used to represent the "material derivative" of $\alpha$ (Currie, 1974). It is the total change in the quantity of $\alpha$ as seen by an observer who is following and watching a particular mass of the fluid. Equation (2.4.1) relates the material derivative to the partial derivatives in an Eulerian reference frame as follows:

$$\frac{D\alpha}{Dt} = \frac{\partial\alpha}{\partial t} + u\frac{\partial\alpha}{\partial x} + v\frac{\partial\alpha}{\partial y} + w\frac{\partial\alpha}{\partial z} \qquad (2.4.1)$$

where $t$ = the time coordinate of an Eulerian reference frame

$x,y,z$ = the spatial coordinates of an Eulerian frame

$u,v,w$ = fluid velocities in the x, y, and z directions, respectively.

In vector form, equation (2.4.1) may be written as follows:

$$\frac{D\alpha}{Dt} = \frac{\partial \alpha}{\partial t} + (\bar{u} \cdot \bar{\nabla})\ \alpha \qquad (2.4.2)$$

where $\bar{u}$ = velocity vector $(u\,\hat{i} + v\,\hat{j} + w\,\hat{k})$

$\bar{\nabla}$ = the gradient $(\hat{i}\,\frac{\partial}{\partial x} + \hat{j}\,\frac{\partial}{\partial y} + \hat{k}\,\frac{\partial}{\partial z})$

$\cdot$ = scalar product of two vectors.

Using the Einstein summation convention where repeated subscripts are summed, the material derivative and the tensor notations shown in equations (2.4.1) and (2.4.2), respectively, may be written as follows:

$$\frac{D\alpha}{Dt} = \frac{\partial \alpha}{\partial t} + u_k \frac{\partial \alpha}{\partial x_k} \qquad (2.4.3)$$

Governing Equations

Using the Einstein summation notation, the equations which govern the motion of a newtonian fluid are listed as follows (Currie, 1974):

$$\frac{\partial \rho}{\partial t} + \frac{\partial}{\partial x_k}\ (\rho\ u_k) = 0 \qquad (2.4.4)$$

$$\rho \frac{\partial u_j}{\partial t} + \rho u_k \frac{\partial u_j}{\partial x_k} = - \frac{\partial p}{\partial x_j} + \frac{\partial}{\partial x_j} (\lambda \frac{\partial u_k}{\partial x_k}) + \frac{\partial}{\partial x_i} [\mu(\frac{\partial u_i}{\partial x_j} + \frac{\partial u_j}{\partial x_i})] + \rho f_j \qquad (2.4.5)$$

$$\rho \frac{\partial e}{\partial t} + \rho u_k \frac{\partial e}{\partial x_k} = - p \frac{\partial u_k}{\partial x_k} + \frac{\partial}{\partial x_j} (k \frac{\partial T}{\partial x_j}) + \lambda(\frac{\partial u_k}{\partial x_k})^2 + \mu(\frac{\partial u_i}{\partial x_j} + \frac{\partial u_j}{\partial x_i}) \frac{\partial u_j}{\partial x_i} \qquad (2.4.6)$$

$$p = p(\rho, T) \qquad (2.4.7)$$

$$e = e(\rho, T) \qquad (2.4.8)$$

Equation (2.4.4) is known as the continuity equation which is derived from the principle of the conservation of mass. Equation (2.4.5) represents in vector form the famous Navier-Stokes equation which is derived from combining the principle of momentum conservation with the constituitive relation for a newtonian fluid. Symbols $\mu$ and $\lambda$ represent the dynamic viscosity and the second viscosity coefficient of the fluid, respectively.

Equation (2.4.6) is called the energy equation, and is derived from the principle of energy conservation. The symbol e denotes the internal energy, and k represents the thermal conductivity of the fluid. Equations (2.4.7) and (2.4.8) represent, in a general format, the thermal and caloric equations of state, respectively. An example of the thermal equation of state is the ideal gas law

$p = \rho RT$, and the most frequently encountered form of the caloric equation of state is $e = C_v T$ where $C_v$ is the specific heat at constant volume.

The above set of seven equations describes the relationships between seven unknowns (note: equation (2.4.6) is a vector equation consisting of three scalar equations). The seven unknowns are the pressure p, density $\rho$, internal energy e, temperature T, and the three velocities $u_j$. The parameters $\lambda$, $\mu$ and k are considered to be known from experimental data. They may be constants or specified functions of temperature and/or pressure.

Physical Assumptions for Simplification Purposes

Depending on the physical system under investigation, different assumptions are used to reduce the complexity of the mathematical equations. The physical meanings of a few common assumptions are discussed as follows:

(1) The difference between unsteady and steady flows is that the fluid and flow properties of the latter case are not time dependent.

(2) Flows in which variations in density are negligible are termed incompressible. One is tempted to make the general statement that all liquid flows are incompressible or

slightly compressible and all gas flows are compressible. For virtually all practical cases, the first portion of the statement is correct. However, under some situations, gas flows may be considered incompressible. One such situation occurs when flow velocities are small relative to the speed of sound in the fluid. The ratio of the flow speed to the speed of sound in the fluid is defined as the Mach number M. For values of $M < 0.3$, changes in density are only 2% of the mean value (Fox and McDonald, 1973). It should be noted from equations (2.4.7) and (2.4.8) that factors such as temperature T, pressure p and internal energy e, can affect whether or not a fluid flow can be considered incompressible.

(3) The difference between inviscid and viscous flows is that the fluid viscosity of the former case is assumed to be zero. If features such as flow separation, flow profile and shear stress in the vicinity of the solid boundary are important to the physical system under investigation, then the fluid viscosity should not be ignored. Viscous flows can be divided into laminar and turbulent flows. Because of their importance to this project, these flows are discussed in more detail as follows.

## Laminar and Turbulent Flows

The primary difference between a laminar and a turbulent flow is that the former moves in laminae or layers and there is no macroscopic mixing of adjacent fluid layers. Whether a flow is laminar or turbulent depends on the properties of the particular flow. One non-dimensional group frequently used to differentiate laminar and turbulent flows is the Reynolds number, $Re = \rho L\bar{V}/\mu$ where $\rho$ is the density of the fluid, L is some characteristic length such as pipe diameter, $\bar{V}$ is the average flow velocity, and $\mu$ is the viscosity of the fluid. In general, two critical Reynolds numbers are important; $Re_{low}$ below which the flow is laminar and $Re_{high}$ above which the flow is turbulent. When the Reynolds number of a flow lies in the range of $Re_{low}$ and $Re_{high}$, a transition from laminar to turbulent flow can occur.

The macroscopic mixing of fluid layers in a turbulent flow is due to small, high frequency, and random velocity fluctuations superimposed on the mean motion of a turbulent flow. These random velocity fluctuations can be a consequence of inlet and outlet conditions as well as other sources of disturbances such as elbows and flow restrictions. The presence of such random velocity fluctuations makes theoretical studies of turbulent flows extremely difficult. Thus, analysis of turbulent flows relies very heavily on semi-empirical theories and on experimental data.

Many flow characteristics such as flow profile, shear stress distribution and pressure drop depend on whether the flow is laminar or turbulent. Due to the importance to this project, one difference related to pressure drop between laminar and turbulent flows is described as follows. For internal flows, such as through a capillary, the pressure drop of a laminar flow is proportional to the mean velocity of the flow, and the pressure drop of a turbulent flow is proportional to the square of the mean velocity (Fox and McDonald, 1973).

### 2.4.2. Application to the Modelling of Methane Flow in Coal Seams

The phenomena of laminar and turbulent flows have been applied to the modelling of methane flow in coal. Two fundamental equations which have been used and are important in describing how methane moves through the macropores and cleats of coal are described in this section.

#### Hagen-Poiseuille Flow Equation

The steady flow of a viscous fluid in a conduit, such as a capillary, of arbitrary but constant cross-section is referred to as Hagen-Poiseuille flow. With the following assumptions, the basic fluid mechanics equations, presented in Section 2.4.1., can be reduced to equations (2.4.9) or (2.4.10).

(1) Steady-state, incompressible, isothermal, free of external forces (i.e., fluid pressure is the only driving force), and no chemical reaction between the fluid and the conduit.

(2) One-dimensional flow in a constant circular cross-section:

$$-\frac{\partial P}{\partial x} + \mu \left(\frac{\partial^2 u}{\partial y^2} + \frac{\partial^2 u}{\partial z^2}\right) = 0 \qquad (2.4.9)$$

$$-\frac{dP}{dx} + \mu \left[\frac{1}{r}\frac{d}{dr}\left(r\frac{du}{dr}\right)\right] = 0 \qquad (2.4.10)$$

It should be mentioned that equations (2.4.9) and (2.4.10) are, essentially, the same physical equation, but derived using different co-ordinate frames (cartesian and cylindrical for equations (2.4.9) and (2.4.10), respectively). If the assumption of non-slip boundary condition is used to solve the differential equation shown in equation (2.4.10) it becomes:

$$Q = -\left(\frac{\pi d^4}{128\ \mu}\right)\left(\frac{dP}{dx}\right) \qquad (2.4.11)$$

where Q = volumetric flowrate

d = diameter of the circular conduit.

Flow Restrictions

An understanding of how fluid moves through a flow restriction can be useful to the modelling of methane flow in coal. The

pressure drop across a flow restriction is related to the mass flowrate by equation (2.4.12), which can be derived from solving the Bernoulli and continuity equations simultaneously:

$$\dot{m} = C_d A_t \sqrt{2\rho \Delta P} \qquad (2.4.12)$$

where $C_d$ = discharge coefficient of the flow restriction

$A_t$ = cross-section area of the throat or restrictions.

The assumptions imposed on equation (2.4.12) are listed as follows:

(1) Steady-state, incompressible, isothermal, free of external forces (i.e., fluid pressure is the only driving force), and no chemical reaction between the fluid and the conduit.

(2) One-dimensional flow with uniform velocity at sections upstream and downstream of the flow restrictions.

## 2.5. Permeability

Two different permeability coefficients characterize the flow of methane through coal seams. At a steady-state, if the flow is by the Knudsen diffusion, e.g. in the coal microstructure, the rate of flow is given by equation (2.5.1):

$$G = K_k A \Delta P/L \qquad (2.5.1)$$

where $K_k$ = the Knudsen permeability ($cm^2/sec$)

$G$ = the rate of flow (ergs/sec)

$A$ = the cross-sectional area of the laboratory flow measurement for a disk of coal

$\Delta P$ = the pressure differential across the disk ($dyne/cm^2$)

$L$ = the disk thickness (cm)

If the flow is laminar, e.g. in the coal macropore structure, the Knudsen permeability no longer holds, and the flow rate across a solid disk is given by equation (2.5.2):

$$G = K_p A \bar{P} \Delta P/L \qquad (2.5.2)$$

where $K_p$ = the Poiseville permeability constant ($cm^2$ sec/g)

$P$ = the mean pressure in the disk ($dyne/cm^2$)

In order to determine which permeability coefficient is governing gas flow, a series of measurement of flow rate versus $\Delta P$, under

steady-state conditions, has to be made for the studied coal sample. That is, if Poiseville flow is absent, the plot of G versus $\Delta P$ will be linear. In practice, however, flow through a disk does not immediately reach a steady-state condition. There is a lag time before a steady-state flow can be reached because a certain amount of methane is accumulated in the micropore structure. This lag time can be determined and corrected for from pressure-time-flow measurements.

Laboratory measurements of coal permeability relate for the most part to the Knudsen permeability. Thimons et al. (1973) showed that permeabilities measured on disks of coal in the laboratory were much smaller than permeabilities determined in the coal seam. This suggests that in coal seams flow primarily takes place through macropores (cleats), whereas in laboratory disks flow takes place through the micropore structure.

Table 2.2 lists some of the reservoir properties of major U.S. coal seams. Although the permeabilities of the U.S. coal seams tend to be high ($k_{\infty}$ > 1.0 md), this is not the case for all coal beds. Jones et al. (1982) report samples of European coals with permeabilities as low as 0.003 md.

The dependence of the seam's permeability on cleat has two important consequences. The first is that the permeability is anisotropic, with the greatest permeability in the direction parallel to the face cleat. The second consequence is that the

permeability depends on the confining stress. For example, an increase in the confining stress causes crack (cleat) closure and reduces the absolute permeability. Permeability reductions of two orders of magnitude have been observed due to stress, with the greatest relative changes occurring in less permeable coals (Dabbous et al., 1974, Mordecai and Morris, 1974, Somerton et al., 1975).

More recently, Durucan et al. (1986) studied permeability of coal lumps in a triaxial cell as a function of different stress conditions. They showed that the rates of reduction of permeability under stress is similar for different coals and can be expressed by an empirical equation (2.5.3):

$$K = (1.12 - 0.003\ \sigma_3)\ K_i \exp[-(1.12-0.03\sigma_3)\ C\sigma_3] \qquad (2.5.3)$$

where $K_i$ and C are constants and $\sigma_3$ is the radial stress.

A large variation of permeability around the abutment zone also makes it difficult to correlate laboratory measurements of permeability with the seam permeability measurements in the zone of the highest methane emission, i.e. in front of the face. An approach that may be adapted for predicting methane flow in front of the abutment zone requires that several types of permeability measurements, and their interpretation be carried out, including:

1. Laboratory measurements of the Knudsen permeability to determine methane diffusion in coal micropores.

2. Laboratory measurements of the effect of stress on permeability and fissures developed to determine the magnitude of permeability change due to stress.

3. Field tracer experiments to determine the distribution of the permeability.

4. A detail calculation and field verification of the stress distribution in the worked seam.

The recommended experimental methods for the laboratory measurements of coal permeability are procedures described for the solid disks (Thimons et al., 1973 and Durucan, 1986) The recommended methods for the field permeability measurements are procedures reported by Richards (1984).

**Table 2.2. U.S. COAL SEAM CHARACTERISTICS (Compiled by Jones et al., 1982).**

| Gas Source | Rank | Geologic Era | Overburden (Feet) | Adsorbed Gas (c.ft/ton) | Virgin Reservoir Pressure (psi) | Permeability (md) |
|---|---|---|---|---|---|---|
| Pittsburgh | High Volatile Bituminous | Pennsylvanian Series (Carboniferous) | 500-900 | 218 | 275 | 10 |
| Pocahontas #3 | Low Volatile Bituminous | Pennsylvanian Series (Carboniferous) | 1600 | 430 | 650 | 2 to 9 |
| Mary Lee | High Volatile Bituminous | Pennsylvanian Series (Carboniferous) | 2100 | 512 | 750 | 7 |
| Sunnyside | High Volatile Bituminous | Mesaverde Group (Cretaceous) | 2500 | 160 | 620 | -- |

## 2.6. Flow Through Porous Media

### 2.6.1. Background

In order to understand how methane moves in coal, the porous nature and matrix of coal need to be studied. With reference to Section 2.1., coal is considered to have dual-porosity consisting of micropores and macropores. Methane is transported from micropores to macropores by the mechanism of diffusion, which is covered in detail in Section 2.3. This section, therefore, focuses on how methane moves through the macropores and the cleats.

#### Flow Through a Capillary

One approach to modelling the macropores of coal is to consider them as capillaries of various sizes. The Hagen-Poiseuille flow equation discussed in Section 2.4.2. can be used to describe how fluid moves through a capillary. Without listing the assumptions associated with the Hagen-Poiseuille flow equation again, equation (2.4.11) of Section 2.4.2. is re-written as follows:

$$Q = - \left(\frac{\pi\, d^4}{128\, \mu}\right) \left(\frac{dP}{dx}\right) \qquad (2.6.1)$$

where $Q$ = volumetric flowrate

$d$ = diameter of the capillary.

Darcy's Law

Darcy's Law states that the apparent velocity, u, of a flowing fluid is inversely proportional to its dynamic viscosity, $\mu$, and directly proportional to the applied pressure gradient, dP/dx. That is:

$$u = - \frac{k_a}{\mu} \frac{dP}{dx} \qquad (2.6.2)$$

where $k_a$ = permeability of the medium, which is a macroscopic property.

There are a few assumptions inherent to Darcy's Law. The similarities between equations (2.6.1) and (2.6.2) can indicate that these two equations bear the same kinds of assumptions described in Section 2.4.2.

Fluid Flow Through Restrictions

The proportional relationship between flowrate and pressure gradient is a consequence of the assumption that the flow is a fully-developed laminar flow. In order to relax this assumption to certain degree, one consideration is to include flow restrictions in the modelling of coal cleats. The relationship between flowrate and pressure drop across a flow restriction is described in equation (2.4.12) of Section 2.4.2., and it is re-written as follows:

$$\dot{m} = C_d A_t \sqrt{2\rho \Delta P} \qquad (2.6.3)$$

where $\dot{m}$ = mass flowrate

$C_d$ = discharge coefficient of the flow restriction

$A_t$ = cross-section area of the throat or restriction.

The assumptions inherent to equation (2.6.3) are listed in Section 2.4.2.

Boundary Layer Separation

Suction beneath porous surfaces is well-known in preventing or delaying boundary layer separation (Schlichting, 1979). In the case of methane flow in coal, the micropores surrounding the cleat surfaces are fluid sources instead of sinks through the mechanism of diffusion. Therefore, boundary layer separation tends to occur sooner, and the methane flow tends to become turbulent at a lower Reynolds number. Consideration can be made to include boundary layer theories in the analysis of methane flow in coal seams.

### 2.6.2. Application to the Modelling of Methane Flow in Coal Seams

Klinkenberg (1941) found from his experiments that the permeability of a porous medium, defined by Darcy's Law, is not

only a property of the medium, but can also be dependent on the flow through the porous medium. He attributed this phenomenon to the slipping of the fluid in contact with the solid surface.

By extrapolating the experimental results, Klinkenberg found that the permeability constant at infinite gas pressure, $k_\infty$, depended only on the porous medium and was independent of the fluid. Using the molecular theory developed by Kundt and Warburg (1875), he derived the relationship between the flow parameters and the permeability of an idealized porous medium consisting of randomly oriented capillaries of equal diameter:

$$k_a = k_\infty \left(1 + \frac{b}{p}\right) \tag{2.6.4}$$

$$b = \frac{4c\lambda\bar{P}}{r_c} \tag{2.6.5}$$

where $b$ = slippage factor

$c$ = a constant approximately equal to unity

$\bar{P}$ = average pressure

$\bar{\lambda}$ = mean free path

$r_c$ = radius of a straight capillary.

Klinkenberg also presented some physical and chemical factors that could affect the permeability constant of a porous medium. These possible factors are:

(1) Reactions between the flowing gas with the constituent of the core material resulting in swelling and shrinking of the pores.

(2) Poorly consolidated core material resulting in plugging the pores caused by the loose material eroded by the moving fluid.

(3) Adsorpability of the solid surface resulting in the build-up of rigid layers and subsequently reducing the effective pore diameter.

(4) Electro-kinetic phenomenon, also known as the streaming potential, resulting in electro-endosmotic flow and subsequently opposing the hydrodynamic flow.

In his experiment investigating the gas emitted from broken coal as a function of time, Airey (1968) also found that the permeability constant defined by Darcy's Law was not a constant. He considered that the phenomenon being attributed to the non-homogenous nature of coal was in fact, caused by the existence of cracks in coal. He, subsequently, developed a model in which coal was built up of small slabs of various sizes instead of considering coal as one homogenous slab. The total gas emission from coal was then considered to be the algebraic sum of the gas emitted from these small slabs.

Based on Epstein's work (1947), Airey considered that, within a lump of coal, the size of the small slabs was distributed in a log-normal manner. Mathematically, the log-normal distribution used by Airey was:

$$m = \ln (a/a_o) \tag{2.6.6}$$

$$W(m) = \frac{1}{(2\pi)^{1/2}\sigma} \exp (-m^2/2\sigma^2) \tag{2.6.7}$$

where $m$ = non-dimensional parameter to represent slab size

$a$ = half-thickness of the coal slab

$a_o$ = average value of $a$

$W(m)$ = probability density function of the distribution

$\sigma$ = standard derivation of $m$.

Airey applied equation (2.6.7) as a weighting function to $V(t,m)$ resulting in the total gas emission from coal shown in equation (2.6.8), where $V(t,m)$ represents the fraction of coal emitted from time 0 to $t$ by a slab of coal of size $a = ma_o$. It should be mentioned that Airey developed the equation governing $V(t,m)$ from Darcy's Law, Boyle's Law and the continuity equation. Airey reported that such an approach to modelling how gas moved through the porous media of coal provided better correlation with the experimental data.

$$f(t) = \int_{-\infty}^{+\infty} V(t,m)\ W(m)\ dm \tag{2.6.8}$$

$$f(t) = \frac{1}{(2\pi)^{1/2}\sigma} \int_{-\infty}^{+\infty} V(t,m) \exp(-m^2/2\sigma^2)\, dm \qquad (2.6.9)$$

where $f(t)$ = total fraction of methane emitted by all coal slabs of various sizes from time 0 to t.

It is our opinion that the improved correlation found by Airey can be attributed to two possible factors listed in descending significance as follows:

(1) Considering coal to be built up of small slabs of various sizes provides a closer representation of the porous nature of coal than considering it as one homogenous slab.

(2) An additional coefficient or constant parameter denoted by $\sigma$ was used to correlate the experimental data.

The use of Darcy's Law to describe high-speed gas flows in porous media (especially in the vicinity of sources and/or sinks) has been found to be inadequate by a few researchers (Tek et al., 1962, Wattenbarger and Ramey, 1968, Firoozabadi and Katz, 1979). To account for turbulence-related effects associated with high-speed gas flows, the quadratic corrective term proposed by Forchheimer (1901) has been used to supplement Darcy's Law as follows:

$$-\frac{dP}{dx} = \frac{\mu}{k_a} u + \beta\rho u^2 \qquad (2.6.10)$$

where $\beta$ = turbulence coefficient.

It should be noted that the quadratic corrective term $\beta\rho u^2$ of equation (2.6.10) is similar to the velocity term of equation (2.6.3) describing the pressure drop across a flow restriction. However, one significant difference between these two terms should not be ignored. In equation (2.6.10), the pressure drop is distributed along the path of the fluid flow. The pressure drop described by equation (2.6.3) occurs suddenly at a particular location which is at the throat of the flow restriction.

There is no doubt that as compared to Darcy's Law, equation (2.6.10) can provide a better correlation to the experimental and/or field data related to high-speed gas flows in porous media. However, prior to applying equation (2.6.10) to the modelling of methane flow in coal, consideration should perhaps be made to determine which of the following two factors attributes more to the improved correlation.

(1) Equation (2.6.10) provides a closer representation of the nature of fluid flow in a porous medium than Darcy's Law.

(2) An additional coefficient or constant parameter denoted by $\beta$ is applied to correlate the experimental and/or field data.

## 2.7. Effects of Stress on Porosity, Permeability and Gas Flow

Coal-bed methane production is initiated by the removal of formation water in quantities sufficient to accomplish a large reduction of fluid pressure in the cleat system. Pressure reduction causes gas to be desorbed from the coal; the cleat system channels this gas to the wellbore. The rate and quantity of water removal is limited by the permeability of the cleat system which is usually stimulated to facilitate dewatering and gas production.

A number of investigators (Patching, 1965, Gunther, 1965, Jones, 1973, Hantush, 1964, and Walsh, 1981) have shown the effect of stress on permeability.

Patching (1965) measured the permeability of a number of coals at various confining pressures and found that in some cases permeability may decrease by as much as three orders of magnitude on increasing confining pressure from 10 to 3000 psi. When data was plotted on log-log coordinates, nearly straight line relations resulted. The confining pressure was applied only in the radial direction perpendicular to flow direction and may thus not be representative of subsurface stress conditions.

Gunther (1965), in connection with his study of diffusion of gas in coal, also reported results of permeability measurements with the application of 'mechanical stress'. Although somewhat

difficult to interpret, it appears that the tests were run under hydrostatic pressure. Again, a large decrease in permeability with an increase in stress was noted. As much as five orders of magnitude reduction in permeability for stress to 700 bars was noted for some coals.

Large reduction of permeability with increase in stress is not unique to coal; other fracture systems show similar behavior. Jones (1973) measured permeabilities of a number of fracture systems (Carthage marble, Smackover limestone, Ellenberger dolomite, and Portland cement with an artificial fracture) and found a straight line relationship between the cube root of normalized permeability (permeability at stress divided by permeability at reference stress of 50 psi) and the log of confining pressure. All tests were run under hydrostatic stress.

Hantush (1964) notes that a change in fluid pressure results in an opposite change in effective stress of the same magnitude:

$$dp = - d\sigma \qquad (2.7.1)$$

Walsh (1981) gives the following relationship between effective stress, confining stress, and pore (fluid) pressure:

$$\sigma = p_c - sp \qquad (2.7.2)$$

He assumes and justifies that s is a constant for linearly elastic materials, and also for rocks. Differentiation of equation (2.7.2) yields:

$$d\sigma = - sdp \qquad (2.7.3)$$

where confining stress, $p_c$, due to the overburden is taken as constant. Using this equation, the dependence of permeability on fluid pressure can be expressed as:

$$k = k_o \left[1 - \frac{\bar{\alpha}s(p_o-p)}{\phi_o}\right]^3 \qquad (2.7.4)$$

When compressibility of individual grains of a solid is small compared to the change in porosity, Hantush (1964) gives the following relationship for the change in porosity with respect to change in compressive (effective) stress:

$$d\phi = -\alpha(1-\phi)\, d\sigma \qquad (2.7.5)$$

where $\alpha$ is the bulk compressibility of the matrix. When equation (2.7.5) is integrated, the following porosity-effective stress relationship is obtained:

$$\phi = 1 - (1-\phi_o)\, \exp\left(\int_{\alpha_o}^{\alpha} \alpha\, d\sigma\right) \qquad (2.7.6)$$

Somerton et al. (1975) observe that bulk compressibility (and therefore pore matrix compressibility) is dependent on stress. To reduce the complexity of the following equations, we introduce the notation:

$$\bar{\alpha} = \frac{1}{\sigma-\sigma_o} \int_{\alpha_o}^{\alpha} \alpha \, d\sigma \qquad (2.7.7)$$

Based on the Kozeny-Carman (1956) equation, the following relationship between permeability and porosity can be written:

$$k \propto \frac{\phi^3}{(1-\phi)^2} \qquad (2.7.8)$$

For coals, cleat porosity is on the order of a few percent, and therefore an approximation, $1-\phi \simeq 1$, can be used to simplify equation (2.7.8). This simplification introduces a small error -- less than the scatter in experimental data. Jones (1973) has observed this simplification for his data.

Jones (1973), and Rose et al. (1975) suggests that:

$$\frac{k}{k_o} = \left(\frac{\phi}{\phi_o}\right)^n \qquad (2.7.9)$$

where $k_o$ and $\phi_o$ are the cleat permeability and porosity at the initial coal seam fluid pressure, $p_o$. Theoretical considerations predict an exponent of n=3; however, some experimental evidence suggest a much stronger dependence.

In a recent study, McKee et al. (1987) presented relationships which were developed from fundamental principles regarding permeability and porosity changes in coal and other porous materials as a function of effective stress. The following equations were proposed to express the effect of stress on coal porosity and permeability:

$$\phi = \phi_o \frac{e^{-\bar{c}_p \Delta\sigma}}{1-\phi_o(1-e^{-\bar{c}_p \Delta\sigma})} \qquad (2.7.10)$$

and

$$k = k_o \frac{e^{-3\bar{c}_p \Delta\sigma}}{1-\phi_o(1-e^{-\bar{c}_p \Delta\sigma})} \qquad (2.7.11)$$

In the above equations, subscript o refers to values at initial conditions and pore compressibility, $c_p$, is related to bulk matrix compressibility through $c_m = \phi c_p$, and finally $\Delta\sigma$ represents the increase in effective stress.

## 2.8. Effects of Water Saturation on Gas Flow

In coal seams, when a well is opened to production, a low pressure area is created, and gas desorbs only in this area. Desorbing gas collects in the low-pressure area until a critical

gas saturation at which gas can start to flow is reached. As the gas saturation increases, a gas bank is formed that decreases the relative permeability to water, thus restricting the water production. The formation of this gas bank, therefore, may trap water in the external regions of the coal seam. Because the diffusion/sorption rate governs the formation of this gas bank, the faster sorption process (smaller sorption time constant) creates a stronger and more efficient trap.

As water is a slightly compressible liquid, its removal at a high rate would more effectively reduce reservoir pressure than the removal of gas, because the reduction of reservoir pressure is the principal cause of desorption. This is the reason gas sorption rate levels off at early times for small values of a sorption time constant (Figure 2.6).

Later in the life of the reservoir, the desorption of gas acts as an internal pressure-maintenance mechanism, which creates competing effects between the water relative permeability and sorption characteristics of the coal seam.

In order to show the effects of relative permeability characteristics on gas flow, three systems are considered (Figure 2.7). The effect of water production on the gas desorption rate can be seen in Figure 2.8. During the early-time period, desorption rate was greatest for the system that was most permeable to water. This reinforces the proposed explanation

that water removal has a greater effect on reservoir pressure reduction than does gas removal.

Figures 2.9 and 2.10 show graphs of water and gas production rates as a function of time. While the water production rates approach one single value at large times, the gas flow rates approach different values. This is a result of the structuring of the relative permeability curves. The system that can transport the greatest reservoir fluid volumes will possess the highest gas sorption rate. Because the water flow rates are essentially the same for later times, the highest desorption rate was observed in the system which had the greatest conductivity to gas.

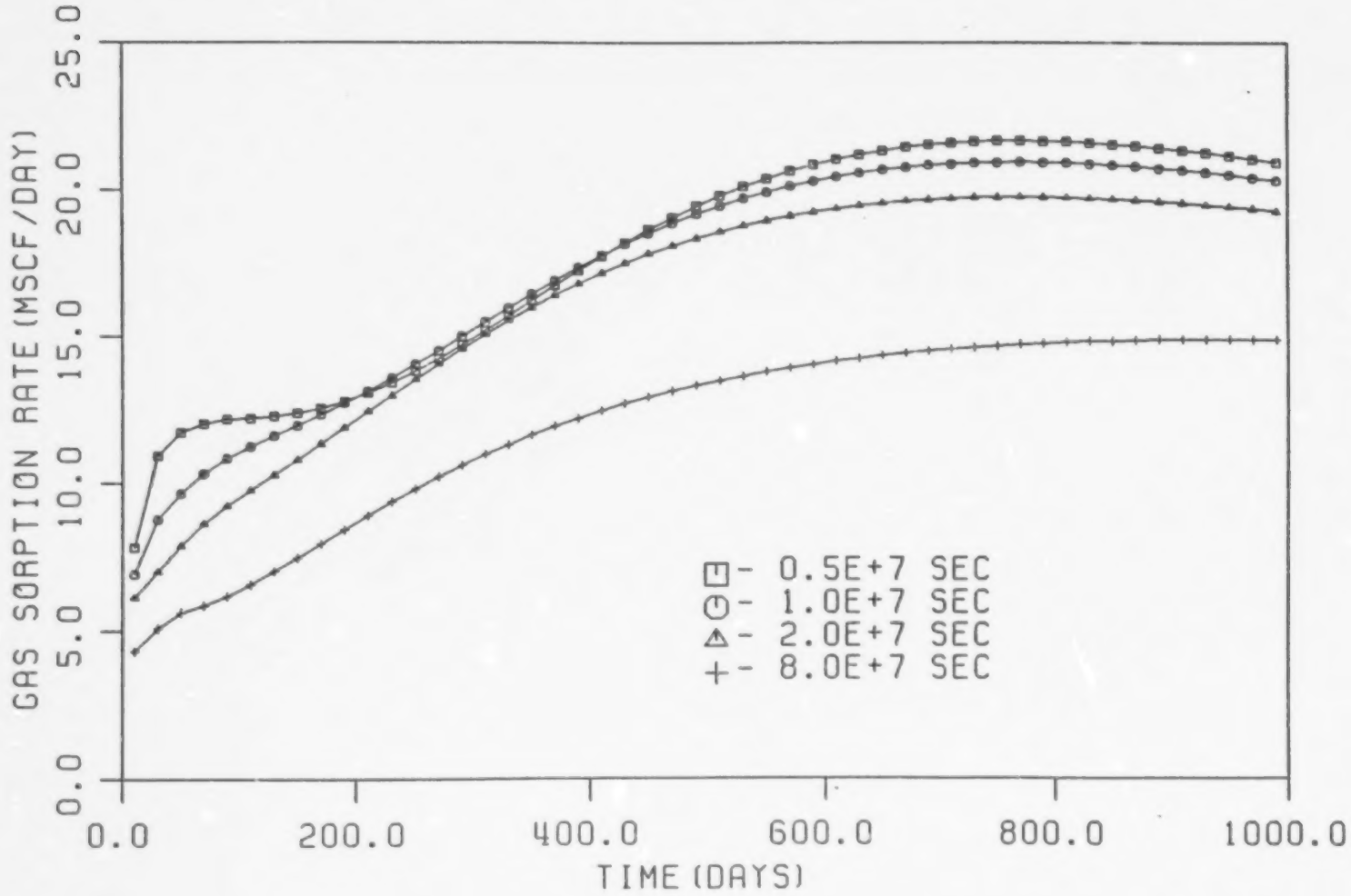


**Figure 2.6. EFFECT OF SORPTION TIME CONSTANT ON GAS SORPTION RATE**

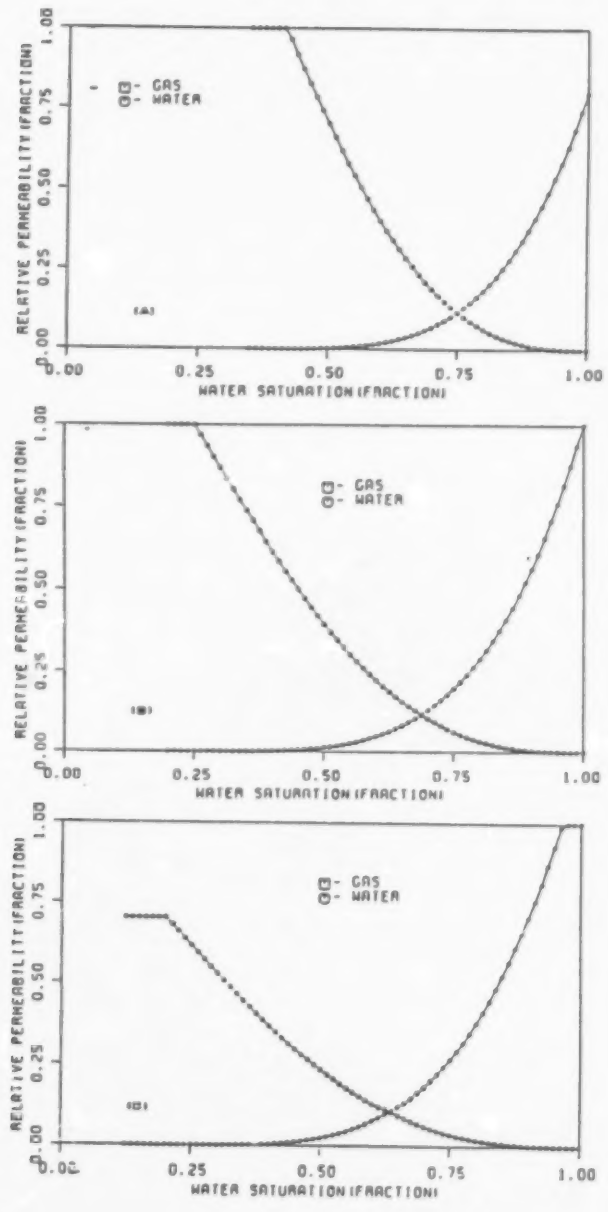


Figure 2.7. THREE SETS OF RELATIVE PERMEABILITY CURVES USED FOR SYSTEMS A, B, AND C

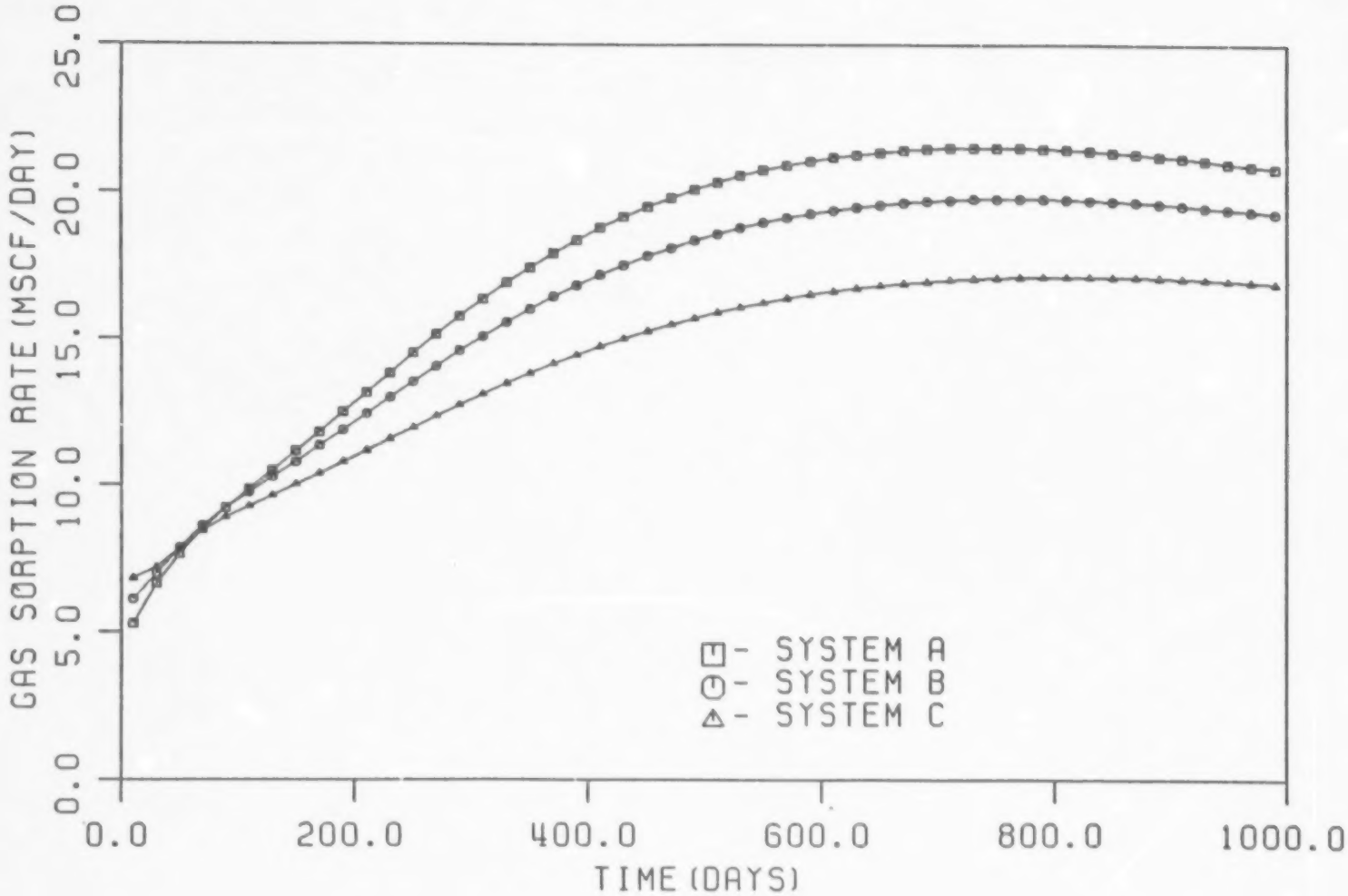


**Figure 2.8. EFFECT OF RELATIVE PERMEABILITY CHARACTERISTICS ON GAS SORPTION RATE**

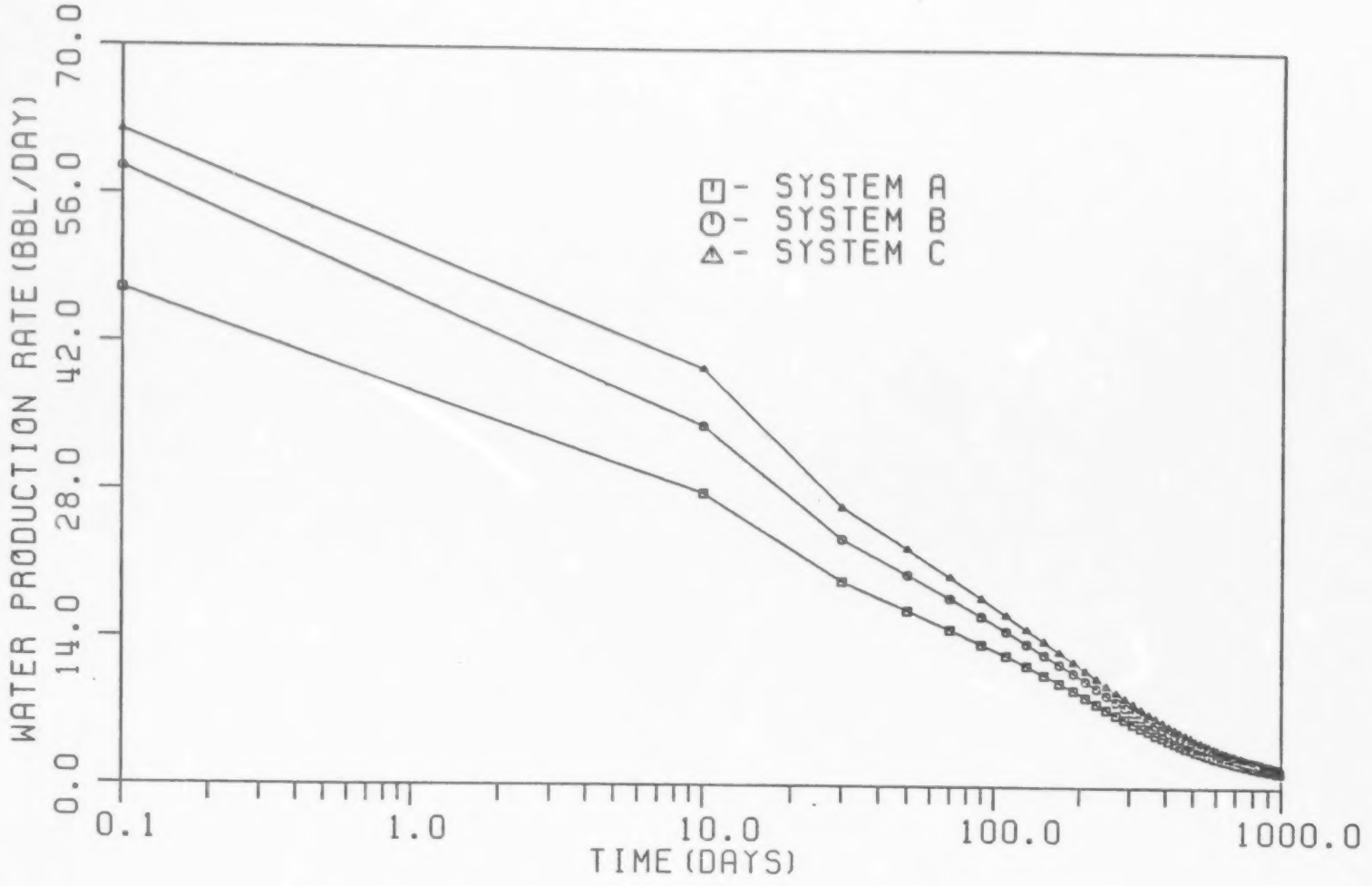


**Figure 2.9. EFFECT OF RELATIVE PERMEABILITY CHARACTERISTICS ON WATER PRODUCTION RATE**

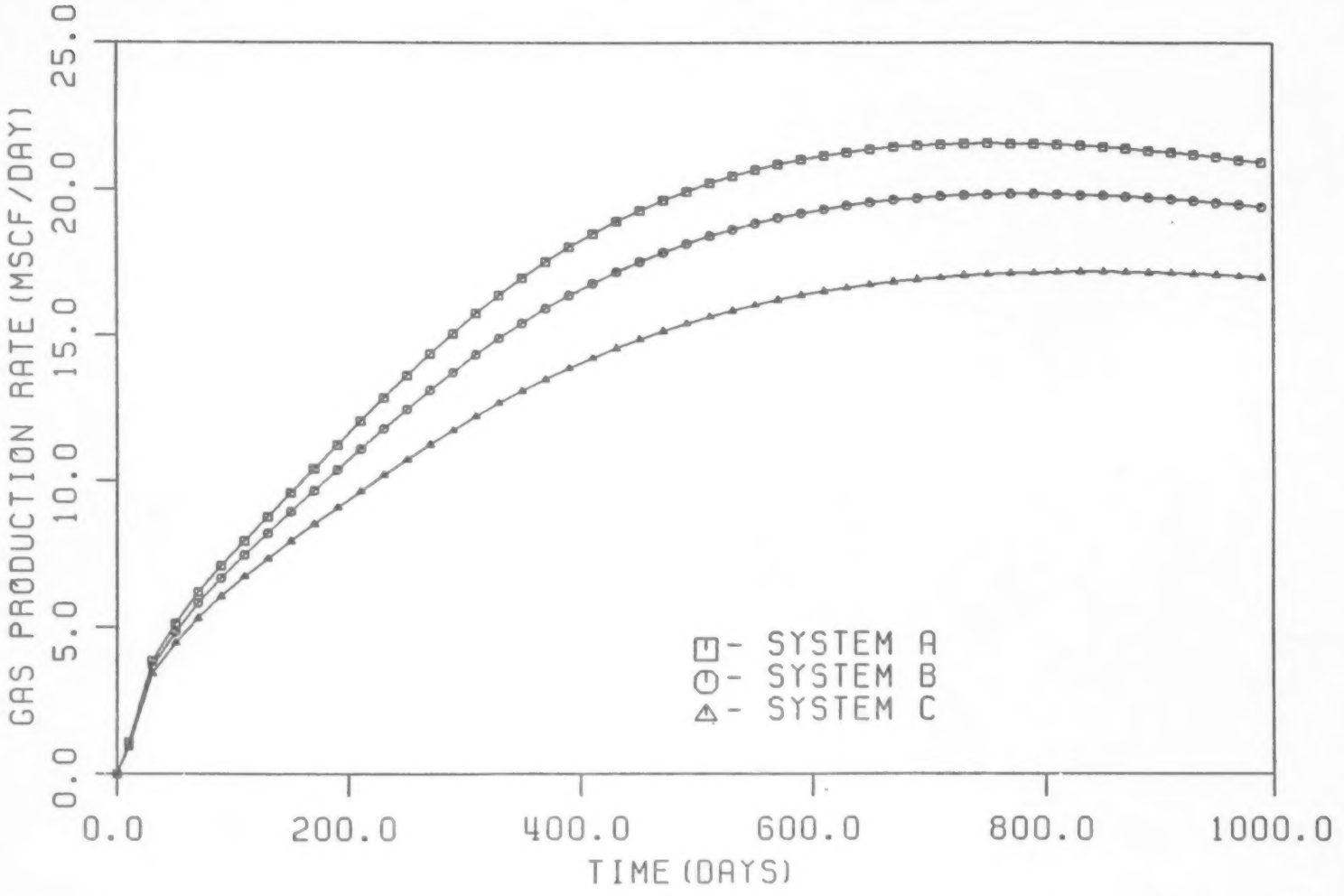


**Figure 2.10. EFFECT OF RELATIVE PERMEABILITY CHARACTERISTICS ON GAS PRODUCTION RATE**

## 2.9. Approximate or Numerical Methods

### 2.9.1. Background

While the derivation of the governing equations for a complex physical system is not unduly difficult, solving the governing equations by exact or analytical methods can be a formidable task. Approximate methods of analysis provide alternative means of finding solutions. Among these approximate methods, the finite-difference method and the variational methods such as the Ritz and weighted-residual methods are frequently used. In recent years, the finite-element method has received a great deal of attention (Reddy, 1984).

The finite-difference method is simple in concept. However, it suffers from several disadvantages such as difficulty in imposing the boundary conditions along non-straight boundaries and in accurately representing geometrically complex domains, etc..

In the variational method, the approximate solution is assumed to be a combination ($\Sigma\ C_j\ \phi_j$) of given approximation functions $\phi_j$. The parameters $C_j$ are determined from the variational form of the governing differential equations. The variational method suffers from the disadvantage that the approximate functions $\phi_j$ for problems with arbitrary domains are difficult to construct.

The finite-element method can be viewed as a piecewise application of the variational method. In general, the approximation functions $\phi_j$ are algebraic polynomials and the undetermined parameters $C_j$ represent the values of the solution at a finite number of preselected points, called nodes, on the boundary and in the interior of the given domain. The disadvantage of the finite-element method is that it requires a large amount of computation.

## $\theta$-Family of Approximation

One effective approach to converting a continuous function to its corresponding discrete or finite-difference form is described as follows. The $\theta$-family of approximation is a weighted average of the first derivative of a dependent variable y(x) at two consecutive steps of the independent variable x (Reddy, 1984). If y = f(x) and if y(n) denotes the value of y at x = x(n) the first derivative of y(x) in numerical form becomes [y(n+1) - y(n)]. The $\theta$-family approach represents this value to be equal to the weighted average of $\dot{y}(x)$ at x = x(n) and x = x(n+1) as follows:

$$\theta\, \dot{y}(n+1) + (1-\theta)\, \dot{y}(n) = \frac{y(n+1) - y(n)}{x(n+1) - x(n)} \qquad (2.9.1)$$

where $\theta$ = lies between 0 to 1

$\dot{y}$ = first derivative of y with respect to x.

It can be seen from equation (2.9.1) that with $\theta$ equal to 0 to 1, equation (2.9.1) becomes the forward-difference and the backward-difference schemes, respectively. Furthermore, with $\theta$ equal to 1/2 and 2/3, equation (2.9.1) becomes the Crank-Nicolson scheme and the Galerkin method, respectively.

The $\theta$-family approximation can be extended to the second derivative of the dependent variable y(x) in the following manner, which is known as the Newmark direct integration method (Reddy, 1984):

$$\dot{y}(n+1) = \dot{y}(n) + [\alpha\, \ddot{y}(n+1) + (1-\alpha)\, \ddot{y}(n)\, \Delta x \qquad (2.9.2)$$

$$y(n+1) = y(n) + \dot{y}(n)\Delta\omega + [\beta\, \ddot{y}(n+1) + (1/2-\beta)\, \ddot{y}(n)]\, (\Delta x) \qquad (2.9.3)$$

where $x,\beta$ = lies between 0 to 1

$\Delta x$ = size of the x increment, i.e., x(n+1) - x(n)

$\ddot{y}$ = second derivative of y with respect to x.

The choice of x = 1/2 and $\beta$ = 1/4 is known as the constant-average-acceleration method. Choosing x = 1/2 and $\beta$ = 1/6 corresponds to the linear acceleration scheme.

Runge-Kutta Method

In addition to the finite-difference, variational and finite-element methods mentioned at the onset of this section, there are many other types of numerical methods useful to the evaluation of an approximate solution of the governing equations. One conventional type is based on the Taylor series or expansion, which can be demonstrated by the derivation of the second order Runge-Kutta method (Pearson, 1986).

It should perhaps be mentioned that after a set of ordinary differential equations is generated from the governing partial differential equations, the Runge-Kutta method can be applied.

If $\dot{y} = f(x,y)$ where $x$ is the independent variable and $y$ is the dependent variable, then denote:

$$k_1 = f(x_n, y_n) \tag{2.9.4}$$

$$k_2 = f(x_n + x\Delta x,\ y_n + \beta k_1 \Delta x) \tag{2.9.5}$$

$$y_{n+1} = Y_n + (A_1 k_1 + A_2 k_2)\ \Delta x \tag{2.9.6}$$

where $x_n$ = nth step of x

$y_n$ = y value at $x=x_n$

$\Delta x$ = size of the x increment, i.e., $x_{n+1} - x_n$

$x, \beta, A_1, A_2$ = constants to be determined.

By means of Taylor expansion in two variables, and substituting equations (2.9.4) into equation (2.9.6) and re-arranging the terms in ascending order of $\Delta x$, yields equation (2.9.7) as follows:

$$y_{n+1} = y_n + (A_1 f + A_2 f)\ \Delta x + A_2(f_x \alpha + f_y \beta f)\ (\Delta x)^2 + 1/2\ A_2(f_{xx}\alpha^2 + 2f_{xy}\alpha\beta + f_{yy}\beta^2 f^2)\ (\Delta x)^3 + \text{--- etc ---} \qquad (2.9.7)$$

The usual Taylor expansion of $y_{n+1}$ yields:

$$y_{n+1} = y_n + f\ \Delta x + 1/2(f_x + f_y f)\ (\Delta x)^2 + 1/6(f_{xx} + 2f_{xy}f + f_{yy}f^2 + f_y f_x + f_y^2 f + f)\ (\Delta x)^3 + \text{--- etc ---} \qquad (2.9.8)$$

Comparing the coefficient of $\Delta x$ and $(\Delta x)^2$ of equations (2.9.7) and (2.9.8) yields:

$$A_1 + A_2 = 1 \qquad (2.9.9)$$

$$A_2 = 1/2 \qquad (2.9.10)$$

$$A_2 \beta = 1/2 \qquad (2.9.11)$$

The two popular choices are $A_1 = A_2 = 1/2$, $x = \beta = 1$ and $A_1 = 0$, $A_2 = 1$, $x = \beta = 1/2$. The first choice leads to:

$$k_1 = f(x_n, y_n)$$

$$k_2 = f(x_n + \Delta x,\ y_n + k_1 \Delta x)$$

$$y_{n+1} = y_n + 1/2\ (k_1 + k_2)\ \Delta x \qquad (2.9.12)$$

The second choice leads to:

$$k_1 = f(x_n, y_n)$$
$$k_2 = f(x_n + \Delta x/2,\ y_n + k_1 \Delta x/2)$$
$$y_{n+1} = y_n + k_2\ \Delta x \qquad (2.9.13)$$

It can be seen from equations (2.9.12) and (2.9.13) that the advantage of the Runge-Kutta method is elimination of the need to evaluate the derivatives of f. As a compromise between accuracy and computational labor, the most common choice is the fourth order Runge-Kutta method such as (Pearson, 1986):

$$k_1 = f(x_n, y_n)$$
$$k_2 = f(x_n + \Delta x/2,\ y_n + k_1 \Delta x/2)$$
$$k_3 = f(x_n + \Delta x/2,\ y_n + k_2 \Delta x/2)$$
$$k_4 = f(x_n + \Delta x,\ y_n + k_3\ \Delta x)$$
$$y_{n+1} = y_n + 1/6\ (k_1 + 2\ k_2 + 2\ k_3 + k_4)\ \Delta x + \mathrm{ERR}[(\Delta x)^5] \qquad (2.9.14)$$

where $\mathrm{ERR}[(\Delta x)^5]$ means with an error of order $(\Delta x)^5$.

Newton-Raphson Method

This is an iterative method to solve for x and y to satisfy equations $f(x,y) = 0$ and $g(x,y) = 0$ simultaneously. To start, an initial guess $(x_1, y_1)$ has to be made. The values $f(x_1, y_1)$ and $g(x_1, y_1)$ are then calculated. These values are called the

residues and they are normally non-zero. The purpose is to alter x from $x_1$ to $x_2$ and y from $y_1$ to $y_2$ to bring the residues of f and g to zero. The choice of $x_2$ and $y_2$ is described as follows:

Using the relationship between total derivative and partial derivatives, the expected changes in f and g caused by altering x from $x_1$ to $x_2$ and y from $y_1$ to $y_2$ are governed by equations (2.9.15) and (2.9.16), respectively:

$$df = f_x \cdot (x_2 - x_1) + f_y \cdot (y_2 - y_1) \qquad (2.9.15)$$

$$dg = g_x \cdot (x_2 - x_1) + g_y \cdot (y_2 - y_1) \qquad (2.9.16)$$

where df = total change in f

$f_x = \partial f/\partial x$

$f_y = \partial f/\partial y$

dg = total change in g

$g_x = \partial g/\partial x$

$g_y = \partial g/\partial y$.

To bring the residues $f(x_1,y_1)$ and $g(x_1,y_1)$ to zero, the approximate equations for determining $x_2$ and $y_2$ are, therefore, given by:

$$f_x \cdot (x_2 - x_1) + f_y \cdot (y_2 - y_1) = - f(x_1,y_1) \qquad (2.9.17)$$

$$g_x \cdot (x_2 - x_1) + g_y \cdot (y_2 - y_1) = - g(x_1,y_1) \qquad (2.9.18)$$

The values for $x_2$ and $y_2$ can be solved from the above two simple equations. In matrix form, equations (2.9.17) and (2.9.18) can be written as follows:

$$\begin{bmatrix} f_x & f_y \\ g_x & g_y \end{bmatrix} \cdot \begin{bmatrix} (x_2 - x_1) \\ (y_2 - y_1) \end{bmatrix} = - \begin{bmatrix} f(x_1,y_1) \\ g(x_1,y_1) \end{bmatrix} \qquad (2.9.19)$$

The coefficient matrix containing the partial derivatives of f and g is known as the Jacobian matrix, and it is often denoted by J.

This method can be extended to solve for more variables. For example, the iteration process to solve (f(x, y, z) = 0, g(x, y, z) = 0 and h(x, y, z) = 0 becomes:

$$\begin{bmatrix} f_x & f_y & f_z \\ g_x & g_y & g_z \\ h_x & h_y & g_z \end{bmatrix} \cdot \begin{bmatrix} (x_{j+1} - x_j) \\ (y_{j+1} - y_j) \\ (z_{j+1} - z_j) \end{bmatrix} = - \begin{bmatrix} f(x_j,y_j,z_j) \\ g(x_j,y_j,z_j) \\ h(x_j,y_j,z_j) \end{bmatrix} \qquad (2.9.20)$$

Interpolation Techniques

Numerical methods such as the finite-difference approach yield the approximate values of the dependent variable y at the preselected x values or so-called mesh points. Many interpolation techniques such as polynominal, Newton and Spline interpolations are available for curve fitting purposes. A compromise between flexibility and economy of calculation, one popular choice is probably the cubic spline approach.

## 2.9.2. Application to the Analysis of Methane Flow in Coal Seams

In his study of gas emission from broken coal, Airey (1968) used an infinite series to solve the governing partial differential equation. He then proved that for his intended purpose, the ratio of the nth term to the (n+1)th term was greater than $148^n$ where $n = 1$ to $\infty$. He, therefore, reported that the series converged rapidly and only the first term needed to be considered.

King et al. (1986) and Sung et al. (1986) applied the finite-difference approximations to the governing differential equations. Mathematical manipulations were then applied to the subsequent algebraic equations resulting in two non-linear equations with two principal unknowns. The Newton-Raphson method described in Section 2.9.1. was applied by both King et al. (1986) and Sung et al. (1986) to solve the unknowns in the non-linear equations.

In their investigation of the transient behaviour of coal-seam degasification wells, King et al. (1986) placed mesh points on the boundaries of the reservoir. Additional points were placed in the interior of the reservoir. To assure a relatively fine grid near the fracture where large pressure gradients were expected to exist in the vicinity, they applied a combination of

arithmetic and logarithmic spacing between the mesh points (in cylindrical co-ordinates).

To discretize the time co-ordinate, King et al. (1986) used an automatic time step selector similar to that of Todd et al. (1972). Through observations obtained from numerical experimentation, King et al. (1986) found that numerical instability could occur when the ratio of the time step size to the quasi-steady-state time constant reached a critical value of 50.

# 3. EVALUATION OF AVAILABLE MODELS

Chapter 2 reviewed background materials and the state-of-the-art of methane flow in coal seam modelling. In this chapter, the fundamental equations useful to the modelling of methane flow from coal seams into mine workings are described. The existing computer models for predicting the flow of methane into mine workings are reviewed. Also, elements of well gasification models which can be applied to the development of improved multi-seam methane flow models for longwall workings are evaluated.

Table 3.1 provides a summary of the computer models which simulate methane flow and mining activities. Table 3.2 presents a summary of models that predict methane flow in coal seams but do not account for mine activities. These models were developed for well degasification of coal seams. A more detailed description of these two types of computer models is provided in Section 3.2 and 3.3.

## 3.1. Fundamental Equations

Based on the background materials reviewed and discussed in Chapter 2, the following physical representations and fundamental equations are suggested for use in modelling the flow of methane into mine workings.

**Table 3.1. LIST OF FINITE-DIFFERENCE METHANE DRAINAGE MODELS INCORPORATING MINING ACTIVITY**

| Model | Developed by | Main Frame or PC | Computer Language | Type of Model | Model Validation | Features and Options |
|---|---|---|---|---|---|---|
| PSU/FORV | PSU/USS/GRI | IBM 370/3003<br>PRIME 2250<br>CDC/CYBER 810 | Standard FORTRAN V | Numerical Model | History Matches/prediction comparison against analytical solutions | Multi-dimensional, multi-well, two-phase finite-difference model in rectangular coordinates, fully implicit formulation multi-mechanistic flow dynamics, quasi-steady-state desorption model.<br>Mining activity<br>Unstimulated vertical well<br>Horizontal well<br>Stimulated vertical/horizontal well |
| METGEN | A.S.C. Owili-Eger (PSU) | IBM/360 | FORTRAN IV | Numerical Model | Comparison against analytical model | Two-dimensional, single-phase, finite-difference model, simulates quantity and quality control in mine ventilation. |
| PAFEC '75 | Univ. of Nottingham, United Kingdom | University ICL 1906A Computer | | Numerical Model | | Two-dimensional, single-phase, finite-element model (the computer simulation of methane flow through strata adjacent to a working longwall coalface). |

Table 3.2. LIST OF FINITE-DIFFERENCE METHANE DRAINAGE MODELS FOR SIMULATED WELLS

| Model | Developed by | Main Frame or PC | Computer Language | Type of Model | Model Validation | Features and Options |
|---|---|---|---|---|---|---|
| PSU/FORV | PSU/USS/GRI | IBM 370/3003 CDC/CYBER 170/750 | Standard FORTRAN IV | Numerical Model | History Matches/prediction comparison against analytical solutions | Multi-dimensional, single-well, two-phase finite-difference model in rectangular, radial, and elliptical coordinates, fully implicit formulation, multi-mechanistic flow dynamics, quasi-steady-state desorption model.<br>Unstimulated vertical well<br>Horizontal well<br>Stimulated vertical well |
| Well 1D | USS/GRI | CDC/CYBER 170/750 | USSTRAN | Numerical Model | History Matches | One-dimensional, single-well model. |
| ARRAY | USS/GRI | CDC/CYBER | USSTRAN | Numerical Model | History Matches | Two-dimensional, multi-well, two-phase model. |
| PAFEC '75 | Lewin/GRI | PC with a minimum of 512 K memory | Standard FORTRAN 77 | Numerical Model | History Matches | Fully implicit formulation, radial and rectangular coordinates, menu-driven pre-processor, interactive graphics. |
| | E.M. Airey | | | Analytical/ Empirical Model | Comparison with existing model and experimental model | Gas emission from broken coal. |
| UNSW | S.J. Spencer<br>M.L. Somers<br>W.V. Pinczewski<br>I.D. Doig<br>(Univ. of New South Wales, Australia) | Personal desktop calculator | | Numerical Model | Comparison with existing numerical model of PSU/USS/GRI | Multi-dimensional, two-phase, finite-difference model, implicit pressure explicit saturation formulation, unsteady-state desorption model. |

1. The dual-porosity approach consisting of micropores inside the matrix blocks and macropores between the matrix blocks should be used to represent the porosity of coal.

2. Two-phase (water and gas) flow should be modelled.

3. The continuity equation shown in equation (3.1.1) is recommended for use when describing the mass balance in the macropore system. It should be noted that in equation (3.1.1), the porosity, $\phi$, is a function of stress.

$$- \nabla \cdot (\rho \vec{\vartheta}) + \frac{Q}{V_b} = \frac{\partial}{\partial t} [\phi(\sigma)\ \rho\ S] \qquad (3.1.1)$$

where $\nabla = \frac{\partial}{\partial x} \hat{i} + \frac{\partial}{\partial y} \hat{j} + \frac{\partial}{\partial z} \hat{k}$

$x$, $y$ & $z$ = spatial axes (ft)

$\cdot$ = dot product of two vectors

$\rho$ = density (lbm/ft$^3$)

$\vec{\vartheta}$ = superficial velocity vector (ft/day)

$Q$ = mass flowrate (lbm/day)

$V_b$ = bulk volume (ft$^3$)

$t$ = time (day)

$\phi(\sigma)$ = macropore porosity, a function of stress (fraction)

$S$ = phase saturation (fraction)

4. It is suggested that the state of the water phase be represented by equation (3.1.2) as follows:

$$\rho_w = \frac{\rho_{wsc}}{B_w(P_w, T)} \qquad (3.1.2)$$

where $\rho_{wsc}$ = density of water at standard conditions ($lbm/ft^3$)

$B_w\ (P_w, T)$ = a function of water phase pressure and temperature (dimensionless)

5. For water flow in the macropore system, Darcy's law shown in equation (3.1.3) is recommended. It should be noted that in equation (3.1.3), the permeability relative to water, $k_{rw}$, is a function of the water phase pressure. The absolute permeability, $k_i$, is a function of stress. The dynamic viscosity of water, $\mu_w$, is a function of pressure. It is suggested that the physical terms be grouped as shown in equation (3.1.5).

$$\vartheta_{wi} = -\frac{\alpha\ k_{rw}\ (S_w)\ k_i(\sigma)}{\mu_w\ (P_w)}\ \nabla\ \phi_w \qquad (3.1.3)$$

where $\vartheta_{wi}$ = velocity of water in the $\hat{i}$ direction (ft/day)

$\alpha$ = conversion factor to match the dimensions

$k_{rw}\ (S_w)$ = permeability relative to water, a function of water phase saturation (dimensionless)

$k_i(\sigma)$ = principle permeability in the $\hat{i}$ direction, a function of stress (md)

$\mu_w\ (P_w)$ = dynamic viscosity of water, a function of water phase pressure (cp)

$\phi_w$ = pressure including depth effect (psi)

$$= P_w - \frac{\rho_w}{144} d \qquad (3.1.4)$$

d = depth below datum (ft)

Denote:

$$\lambda_{wi} (P_w, S_w, \sigma) = \frac{k_{rw} (S_w) \; k_i(\sigma)}{\mu_w (P_w)} \qquad (3.1.5)$$

where $\lambda_{wi} (P_w, S_w, \sigma)$ = water phase mobility in the $\hat{i}$ direction a function of $P_w$, $S_w$ and $\sigma$ (md/cp)

Substituting equations (3.1.4) and (3.1.5) into equation (3.1.3) yields equation (3.1.6) as follows:

$$\vartheta_{wi} = - \alpha \lambda_w (\nabla P_w - \frac{\rho_w}{144} \nabla d) \qquad (3.1.6)$$

6. It should be noted that substituting the equation of state shown in equation (3.1.2) and the flow equation shown in equation (3.1.6) into the mass balance shown in equation (3.1.1) yields the transport equation of water as follows:

$$\nabla \cdot \left[ \frac{\alpha \lambda_w}{B_w} (\nabla P_w - \frac{\rho_w}{144} \nabla d) \right] + \frac{5.615 \; q_{STB}}{V_b} = \frac{\partial}{\partial t} (\frac{\phi \; S_w}{B_w}) \qquad (3.1.7)$$

where 5.615 = conversion factor from $ft^3$ to STB

$q_{STB}$ = volumetric production rate of water at standard conditions (STB/day)

7. It is suggested that the real gas law described in equation (3.1.8) be used to describe the state of the gas phase.

$$\rho_g = \frac{(MW)\ P_g}{Z\ R\ T} \qquad (3.1.8)$$

where $\rho_g$ = density of the free gas ($lbm/ft^3$)

MW = molecular weight (lbm/lb - mole)

$P_g$ = pressure of the free gas (psi)

Z = gas supercompressibility factor (fraction)

R = universal gas constant

T = temperature (°R)

8. Equation (3.1.9) is derived from considering the gas velocity as the sum of the Darcy's and Fick's components. It is recommended that this equation be applied to describe the gas flow in the macropore system.

$$\vec{v}_g = \frac{-\alpha\ k_\infty}{\mu_g} \nabla P_g + \frac{-(MW)}{\rho_g} D \nabla C_g \qquad (3.1.9)$$

where $\vec{v}_g$ = gas velocity vector (ft/day)

$\alpha$ = conversion factor to match the dimensions

$k_\infty$ = permeability at infinite pressure (md)

D = macropore diffusion coefficient ($ft^2$/day)

$C_g$ = molar concentration (lb-mole/ft³)

Defining the gas mobility as $\lambda_g = k_\infty/\mu_g$ and using the real gas law described in equation (3.1.8) to re-write equation (3.1.9) yields equation (3.1.10) as follows:

$$\vec{v}_g = - \alpha \lambda_g \nabla P_g - \frac{Z}{P_g} D \nabla \left(\frac{P_g S_g}{Z}\right) \qquad (3.1.10)$$

where $S_g$ = gas saturation (fraction)

9. It should be noted that substituting equations (3.1.8) and (3.1.10) into equation (3.1.1) yields the transport equation of gas as follows:

$$\nabla \cdot \left[ \frac{\alpha \lambda_g P_g}{Z} \nabla P_g + D \nabla \left(\frac{P_g S_g}{Z}\right) \right] + \frac{1000 P_{sc} T}{T_{sc}} \frac{q_{gsc}}{V_b} + \frac{P_{sc} T}{T_{sc}} \frac{q_t}{V_b} = \frac{\partial}{\partial t} \left(\frac{\phi P_g S_g}{Z}\right) \qquad (3.1.11)$$

where 1000 = conversion factor to match the dimension

$P_{sc}$ = standard pressure (psi)

$T$ = temperature (°R)

$T_{sc}$ = standard temperature (°R)

$q_{gsc}$ = volumetric production rate of gas at standard conditions (MSCF/day)

$q_t$ = volumetric matrix/fissure transfer (SCF/day)

10. It should, perhaps, be summarized that equations (3.1.7) and (3.1.11) are the transport equations of water and gas, respectively. There are five unknowns in these two equations. They are $P_w$, $P_g$, $S_w$, $S_q$ and $q_t$. Therefore, three auxiliary equations are required. Two of them are shown in equations (3.1.12) and (3.1.13) as follows:

$$S_w + S_g = 1.0 \qquad (3.1.12)$$

$$P_{cgw}\ (S_g) = P_g - P_w \qquad (3.1.13)$$

where $P_{cgw}\ (S_g)$ = capillary pressure between gas and water phases, a function of $S_g$ (psi)

11. It is suggested that the third auxiliary equation be derived from the pseudo-steady-state diffusion/sorption model. In the derivation of this model, two extra unknowns, $V_{mi}$ and $V_E\ (P_g)$, are introduced and the following three equations result:

$$q_t = -\ (PF)_{mi}\ \frac{d\ V_{mi}}{dt} \qquad (3.1.14)$$

$$\frac{d\ V_{mi}}{dt} = D_{mi}\ a\ [V_E\ (P_g) - V_{mi}] \qquad (3.1.15)$$

$$V_E\ (P_g) = \frac{V_L\ P_g}{P_L + P_g} \qquad (3.1.16)$$

where $(PF)_{mi}$ = geometric prefactor in micropore subelement (dimensionless) (by comparing the pseudo-steady-state and unsteady-state equations, a value of 6 is chosen)

$V_{mi}$ = volumetric concentration in the micropores (SCF/ft³)

$D_{mi}$ = micropore diffusion coefficient (ft²/day)

$a$ = shape factor ($ft^{-2}$) (by comparing the pseudo-steady-state and unsteady-state equations, $a = \pi^2/R_{mi}^2$ where $R_{mi}$ is the radius of the spherical micropore sub-element)

$V_E(P_g)$ = equilibrium volumetric concentration, a function of $P_g$ (SCF/ft³)

$V_L$ = a constant Langmuir volumetric concentration (SCF/ft³)

$P_L$ = a constant Langmuir pressure (psi)

12. In summary, the seven model governing equations are equations (3.1.7), (3.1.11) and (3.1.12) to (3.1.16). The seven unknowns to be solved are $P_w$, $P_g$, $S_w$, $S_g$, $q_t$, $V_{mi}$ and $V_E$.

It should be noted that after $P_w$ and $P_g$ are solved, the velocities (and hence, flowrates) of the water phase and gas phase can be calculated from the flow equations shown in equations (3.1.6) and (3.1.10), respectively.

## 3.2. Computer Models with Mine Activities

A detailed review was carried out of the following five sets of computer models:

1. the Pennsylvania State University models developed by Professor T. Ertekin and his researchers during the late seventies and mid eighties;

2. the METGEN model developed by Owili-Eger at the Pennsylvania State University in the early seventies;

3. the University of Nottingham models developed in the late seventies;

4. the United States Bureau of Mines model developed in the late seventies and early eighties; and

5. the empirical models.

The results of the evaluation of the five sets of computer models are presented in Sections 3.2.1 to 3.2.5. The presentation of the findings is organized in the following manner:

1. primary and secondary objectives of the model;

2. assumptions imposed in describing the physical phenomena and the subsequent governing equations;

3. numerical techniques and computer programs used to solve the model equations;

4. methods applied to validate the computer model; and

5. merits and limitations of the model.

### 3.2.1. Pennsylvania State University Models

The Pennsylvania State University models were developed by Professor T. Ertekin and his students during the late seventies and mid eighties. The model PSU/FORV, including mine activities, gradually evolved from a series of finite-difference models, PSU/FORIV, which simulated the unsteady-state behaviour of coal seam degasification from wells.

The primary objectives of the initial models were to simulate the multi-dimensional, unsteady-state flow of water and methane through coal seams for unstimulated vertical wells, hydraulically stimulated vertical wells, and horizontal wells from a shaft bottom. Later, some elements of mine working were incorporated into the initial models. The recent model, PSU/FORV, can predict methane inflow into the mine face based on the methane and water

contents of the seam, and the assigned porosity and permeability of the seam.

Assumptions and Model Equations

In the description of the PSU models, King (1985) listed the following assumptions:

1. The coal seam can be idealized by using regular geometric blocks to represent the coal matrix and by using the spaces between these blocks to represent the coal seam's cleat.

2. The co-ordinate axes of the model coincide with the principal permeability axes of the coal seam.

3. Water is a slightly compressible fluid.

4. Water transport obeys Darcy's Law for laminar flow in porous media.

5. Methane is a real gas.

6. Gas in the macropores is stored as free gas. Therefore, there is no adsorbed gas or solution gas in the macropores.

7. The free gas and the adsorbed gas have the same molecular weight.

8. Over geologic time, the gas in the micropores has reached equilibrium with the gas in the macropores.

9. No selective adsorption or diffusion occurs in the micropores.

10. Desorption at the surfaces of the regular geometric subelements of the idealized reservoirs is sufficiently rapid so that equilibrium between the free gas and adsorbed gas is maintained.

11. Diffusion through the micropores is in the pseudo-steady-state regime.

12. The flow is isothermal.

13. Gas transport obeys a combined form of Darcy's and Fick's laws.

14. The capillary end effects at the wellbore and fracture are negligible.

It can be seen from the above assumptions that the PSU model treats the coal seam as a dual-porosity reservoir. A pseudo-steady-state, time-dependent sorption model is used to describe methane desorption from the coal matrix. Gas transport is governed by two fields:

1. a concentration field within the coal matrix which is modelled with Fick's Law of diffusion; and

2. a pressure field describing flow in the fracture system and modelled with Darcy's Law.

It should be mentioned that in the PSU model, the combination of the two flow mechanisms (i.e., concentration and pressure) yields a pressure, saturation and composition dependent slippage factor.

This approach is in contrast to Klinkenberg's theory which predicts a constant slippage factor (see Chapter 2).

The model treats water as a slightly compressible fluid which obeys Darcy's Law for laminar flow through porous media. The compressibility is assured to be constant over the entire pressure range. The effects of water saturation on gas flow and permeability are introduced through two auxiliary macropore equations. Equation (3.2.1) describes the water and gas saturation, and equation (3.2.2) governs the interrelation between the pressures of the two phases.

$$S_w + S_g = 1.0 \qquad (3.2.1)$$

$$P_{cgw}\,(S_w) = P_g - P_w \qquad (3.2.2)$$

where subscripts w and g stand for water and gas.

The effect of seam characteristics on the gas flow is introduced in the model through the input property values. These input values include formation compressibility, temperature, density, fracture half-length and half-width, and so on.

King (1985) summarized the PSU's governing equations as follows:

$$\nabla_{ma} \cdot \left[\frac{\alpha\lambda_w}{B_w} \left(\nabla_{ma} P_g - \nabla_{ma} P_{cgw} - \frac{\rho_w}{144} \nabla_{ma} d\right)\right] + \frac{5.615\ q_{STB}}{V_{bma}}$$

$$= \frac{\partial}{\partial t} \left[\frac{\phi_{ma}(1-S_g)}{B_w}\right] \qquad (3.2.3)$$

$$\nabla_{ma} \cdot \left[\frac{\alpha\lambda_g P_g}{Z} \nabla_{ma} P_g + D_{ma} \nabla_{ma} \left(\frac{P_g S_g}{Z}\right)\right] + \frac{1000\ P_{SC}\ T}{T_{SC}} \frac{q_{gSC}}{V_{bma}}$$

$$+ \frac{P_{SC}\ T}{T_{SC}} \frac{q_t}{V_{bma}} = \frac{\partial}{\partial T} \left(\frac{\phi_{ma} P_g S_g}{Z}\right) \qquad (3.2.4)$$

$$q_t = -(PF)_{mi} \frac{dV_{mi}}{dt} \qquad (3.2.5)$$

$$\frac{dV_{mi}}{dt} = D_{mi}\ a[V_E(P_g) - V_{mi}] \qquad (3.2.6)$$

$$V_E(P_g) = \frac{V_L P_g}{P_L + P_g} \qquad (3.2.7)$$

or;

$$V_E(P_g) = H\ P_g \qquad (3.2.8)$$

With reference to the above set of equations, the five dependent variables are $P_w$, $P_g$, $S_w$, $S_g$ and $V_{mi}$. These five dependent variables are governed by two non-linear partial differential equations (3.2.3 and 3.2.4) and three auxiliary macropore equations (3.2.5 to 3.2.8).

The initial and boundary conditions used to solve the above governing equations are listed as follows:

For t=0 and over the reservoir volume,

$$P_g = P_g^{\circ} \tag{3.2.9}$$

$$S_g = S_g^{\circ} \tag{3.2.10}$$

$$V_{mi} = V_{mi}^{\circ} = V_E\ (P_g)^{\circ} \tag{3.2.11}$$

For t>0 and on the internal boundary,

$$P_g = P_{wf}(t) \tag{3.2.12}$$

or;

$$q_{gsc} = \frac{-\alpha\lambda_g\ A}{1000}\ \frac{P_g\ T_{SC}}{Z\ P_{SC}\ T}\ \nabla_{ma}\ P_g - \frac{D_{ma}\ A}{1000}\ \nabla_{ma}\ \left(\frac{P_g\ S_g}{Z}\right) \tag{3.2.13}$$

$$\nabla_{ma}\ S_g = 0 \tag{3.2.14}$$

For t>0 and on the external boundary,

$$\nabla_{ma} S_g = 0 \qquad (3.2.15)$$

$$\nabla_{ma} P_g = 0 \qquad (3.2.16)$$

The PSU FORIV model was recently upgraded to include multi-well situations and mine activities. A convective type boundary condition was used to quantify the methane emissions in the vicinity of an active working area. This boundary condition describes the pressure gradient close to the mine face and the pressure in the active working area. To accommodate a moving mine face, the recent PSU model treats the physical boundaries of a coal seam as functions of the velocity of the moving mine face.

Numerical Technique and Computer Programming

The finite-difference method was used to solve the model transport equations for water and methane. The numerical procedure was implemented by superimposing a finite-difference grid over an idealized heterogeneous and anisotropic coal seam.

The set of non-linear partial differential equations was approximated using Taylor series expansion of the dependent variable in the vicinity of the grid point. This resulted in a system of non-linear algebraic equations which were then solved using the Newton-Raphson method. A similar approach was taken

with respect to the time domain and the unsteady-state source/sink equations.

Five computer programs were developed for unsteady-state, single- and two-phase flow in one- to three-dimensional space. These programs were written in standard FORTRAN IV for use by IBM 370/3033 series and CDC Cyber 170/750 series computers, and they are listed as follows:

1. Single-phase, one-dimensional model;
2. Two-phase, one-dimensional model;
3. Two-phase, two-dimensional, areal model;
4. Two-phase, two-dimensional, cross-sectional model; and
5. Two-phase, three-dimensional model.

The computer programs were recently upgraded to include multi-well situations and mine activities. The upgrading was carried out by implementing a convective type boundary condition to describe the pressure gradient area. The physical boundaries of a coal seam were implemented as functions of the velocity of the moving mine face. The recent computer programs were written in standard FORTRAN V for use by IBM 370/3033 series, PRIME 2250 series and CDC Cyber 810 series computers.

## Model Validation

The validity of the computer models was tested by comparing the results generated from the programs to:

1. the results generated from the existing analytical models;

2. the results generated from the existing numerical models; and

3. the existing field data.

The single-phase model was compared to the analytic solution of Jacob and Lohman (1952), as well as the analytical solution of Aziz and Flock (1963). These two analytical solutions simulated unstimulated wells in infinite and bounded reservoirs, respectively. For hydraulically stimulated wells the model was compared to the analytical solutions of Kucuk (1978) and Gringarten et al. (1975).

All the comparisons above showed quantitative agreement between the numerical and analytic solutions with the exception of some discrepancies in the constant terminal pressure case for stimulated wells. The source of the discrepancy was identified as being caused by the two different types of equations (non-linear vs linear) used by the numerical and analytical models.

The numerical model ARRAY was used to test the validity of the PSU's computer models. In this comparison, a well stimulated by an infinite conductivity fracture was modelled using both the PSU/FORV and ARRAY models. The geometry used in the PSU/FORV model was a two-dimensional, cylindrical system. The geometry used in the ARRAY model was a one-dimensional, elliptical system. The different geometries were chosen to examine the effects of using different grids. By comparing the subsequent results, the PSU/FORV model showed good quantitative agreement with the well degasification model ARRAY developed by Pavone and Schwerer (1984) for GRI.

The third approach used to test the validity of the PSU/FORV model was to compare the results of the models to the observed field data. The histories of an unstimulated and stimulated well in the Blue Creek coal seam (Mary Lee coal group) in the Warrier Basin were used for such a comparison. These two history matches were successfully completed for well degasification. However, no comparison was given to the methane emission at a mine face.

The recent computer programs which upgraded the PSU/FORIV model to include multi-well situations and mine activities were tested up to the inclusion of 121 wells. No stability problem was encountered.

Merits and Limitations

The PSU models have the capabilities of simulating methane flow in coal seam subject to the following various environments:

1. unstimulated vertical wells;

2. stimulated vertical and horizontal wells;

3. horizontal boreholes originating from a common vertical shaft or drilled from a mine face;

4. mine activities; and

5. impermeable geological barriers within the system.

The most significant contribution of the PSU models is their success at including and connecting an extensive amount of basic physical phenomena in the modelling of methane flow in a coal seam subject to conditions such as unstimulated and stimulated wells. The success of the models demonstrates that the developed mathematical and computational tools handle the interactions of numerous physical phenomena in the modelling of methane flow in coal seams. To achieve sufficient accuracy at predicting methane flow in coal seams the model relies on:

1. the choice of the appropriate physical phenomena to describe the flow;

2. the validity of the assumptions to reduce the complexity of the physical phenomena; and

3. the choice of the basic parameters such as porosity and permeability for specific applications.

The important features included in the PSU models are:

1. unsteady-state, three-dimensional, two-phase flow;

2. dual-porosity (matrix and fissure) to represent the nature of coal;

3. two mechanisms (concentration and pressure) to represent the methane flow;

4. pseudo-steady-state sorption based on Langmuir isotherms for coal matrix subelements;

5. pressure, situation and composition dependent slippage factor which is in contrast to the constant slippage factor predicted from Klinkenberg's theory;

6. superimposing the slip velocity on the Darcy velocity and the use of Fick's law to describe the methane flow in macropores; and

7. the real gas law to describe the PVT relationship of the free gas storage and flow.

Features which <u>are not</u> included in the PSU models or which may require further improvement are:

1. effects due to variations in natural seam compaction, pressure distribution fracture and content of methane;

2. effects of stress and water concentration on porosity and permeability;

3. interactions or communications between multiple seams;

4. porosity and permeability distributions;

5. assumption that the directions of the principal permeabilities coincide with the co-ordinate axes; and

6. relative advantages and disadvantages of using the finite-difference and finite-element methods for solving the model transport equations.

It is recommended that these features be the focus of further studies.

### 3.2.2. METGEN Model

The primary objective of the computer model METGEN was to simulate methane flowrates into the mine workings for mine ventilation applications. The secondary objectives were:

1. to modify the ventilation network simulator developed by Wang and Saperstein (1970) to accommodate the methane flowrates predicted by METGEN; and

2. to determine the free split (longest pressure drop path) of a ventilation network.

#### Assumptions and Model Equations

The mathematical model developed in the METGEN project was modified from a diffusion model for flow through porous media. Several assumptions were made in the mathematical model to represent the physical phenomena in a less complicated manner and to reduce the complexity of the governing equations. These assumptions are summarized as follows:

1. The medium is assumed to be porous, anisotropic and fully saturated.

2. The directional permeabilities $k_x$ and $k_y$ are assumed to be dependent on the pressure and position co-ordinate only. For small pressure and temperature variations, the directional emissivities are considered to be constant. The effects of asymmetric components $k_{xy}$, $k_{yx}$ and $k_{xz}$ are assumed to be negligible.

3. Temperature variations over the media are assumed to be insignificant.

4. Variations in the density of methane throughout the porous medium are considered to be small.

5. The methane pressure is assumed to be much greater than the gravity head.

6. The flow system is considered to be in dynamic equilibrium.

7. Methane is assumed to flow along the seam except when an injection and production term are involved.

8. Two-dimensional, single-phase and steady-state flow conditions are assumed.

The physical laws or equations applied to derive the model-governing equation are:

1. the two-dimensional mass balance equation (3.2.17);

2. Darcy's Law to describe the fluid velocities in the x and y directions shown in equations (3.2.18) and (3.2.19); and

3. the gas law shown in equation (3.2.20).

$$-\frac{\partial(V_x\rho)}{\partial x} - \frac{\partial(V_y\rho)}{\partial y} + q_{vol} = \phi\frac{\partial\rho}{\partial t} \qquad (3.2.17)$$

$$V_x = -\frac{k_x}{\mu}\frac{\partial P}{\partial x} \qquad (3.2.18)$$

$$V_y = -\frac{k_y}{\mu}\frac{\partial P}{\partial x} \qquad (3.2.19)$$

$$\rho = \frac{PM}{ZRT} \qquad (3.2.20)$$

Rearranging equations (3.2.17) to (3.2.20) and applying the previously mentioned assumptions to reduce the complexity of the mathematical equations yields the model-governing equation as follows:

$$\frac{\partial}{\partial_x}\left(k_x\frac{\partial U}{\partial_x}\right) + \frac{\partial}{\partial_y}\left(k_y\frac{\partial U}{\partial_y}\right) + \frac{29.4\ \mu\ Z\ T}{2919.8\ h\ \Delta x\ \Delta y}\ q = 0 \qquad (3.2.21)$$

where $U = P^2$

$P$ = fluid pressure

The boundary conditions applied to solve equation (3.2.21) are:

1. the atmospheric pressure at the mine face, i.e., $P = P_f$ at $x = x_f$;

2. reservoir pressure at 1000 feet away from the mine face, i.e., $P = P_r$ at $x = x_r$; and

3. the non-slip conditions at the rocks above and below the coal seam, i.e., $\partial P/\partial x = 0$ at $y = y_{top}$ and $y = y_{bottom}$.

Numerical Technique and Computer Programming

The computer program METGEN was developed to solve the governing equation shown in equation (3.2.21) in a numerical manner. This program was written in FORTRAN IV for IBM 360 machines. The grid system used by METGEN is constant in spacing in the x and y directions. It should be mentioned that the spacing in the x direction can be different from that in the y direction. The numerical technique used in METGEN to solve the governing equation is known as the finite-difference method. Using the central difference scheme of the method, equation (3.2.21) was transformed into a set of finite-difference equations. The Gauss-Seidal iterative approach with a relaxation factor equal to

1.15 was used to estimate the solutions of the finite-difference equations.

The input parameters required by METGEN can be divided into five categories as follows:

1. Model size: number of grid nodes plus one in the x and y directions, as well as the length, width and thickness of the medium.

2. Initial conditions: initial pressure and quantity values in the interior nodes of the model area.

3. Boundary conditions: reservoir and face pressure values.

4. Medium properties: directional permeability, porosity and temperature of the medium.

5. Miscellaneous: viscosity and gas deviation factor, as well as the maximum number of iterations and the maximum allowable error required for convergence.

The METGEN program outputs the pressure values at all interior and boundary nodes of the selected test area. It also outputs the rate of methane emission from the mine face in standard cubic feet per day as well as in cubic feet per minute.

## Model Validation

The validity of the METGEN model was tested by applying special input parameter values such as $k_y = 0$ to reduce the two-dimensional flow to one-dimensional, as well as by applying simple boundary and initial conditions. Analytical solutions for such simplified conditions could exist. The results obtained from METGEN and from the analytical solutions were then compared. Two model test runs were performed, and the results showed quantitative agreement with the analytical solutions. The METGEN model has not been field tested.

## Merits and Limitations

The METGEN model was aimed at the planning and design of the mine ventilation system. In the METGEN project, the ventilation network simulator developed by Wang and Saperstein (1970) was modified to accommodate the methane flowrates predicted by METGEN. The most significant contribution of the METGEN project is, therefore, its readiness for use by mine ventilation engineers. The second significant contribution of the METGEN model is the demonstration of the importance and usefulness of predicting methane flow in coal seams for coal mine applications.

The METGEN model was modified from a steady-state, two-dimensional, single-phase diffusion system. Many features such as the existence of various wells and/or boreholes were not

implemented in the model. The METGEN model is, therefore, much less complicated and much less complete than the PSU models discussed in the preceding section.

### 3.2.3. University of Nottingham Models

In 1977, Keen developed a computer program called METNET1 to "simulate real life situations and prove or disprove previous theories by a controlled analysis of assumptions". He indicated that METNET1 was not intended to be the final solution to methane prediction for the mining ventilation engineer. METNET1 was intended to be used by subsequent researchers to develop better and more commercially-oriented computer programs.

In 1980, Keen's work was further improved by O'Shaughnessy. The objective of O'Shaughnessy's project was to explore possible computer-aided techniques for the prediction of methane migration patterns through strata adjacent to a moving longwall coal face.

#### Assumptions and Model Equations

The assumptions made by O'Shaughnessy in the derivation of the mathematical model were as follows:

1. The effects of adsorption may be ignored.

2. The Klinkenberg and Sowier effects may be ignored.

3. The flow is single-phase, isothermal and laminar in nature.

4. Darcy's Law is valid.

5. Methane does not exhibit abnormal compressibility and obeys the perfect gas law.

In the studies of the effects of a borehole, two further assumptions were made:

6. Permeability does not change in the vicinity of the borehole.

7. The flow remains laminar in the vicinity of a borehole.

8. In the computer simulation, O'Shaughnessy further assumed that the flow was two-dimensional.

Based on assumptions 1 to 5, the model-governing equation was:

$$\frac{\partial P}{\partial t} = \frac{1}{2\mu\phi}\left[\frac{\partial}{\partial x}\left(k_x \frac{\partial P^2}{\partial x}\right) + \frac{\partial}{\partial y}\left(k_y \frac{\partial P^2}{\partial y}\right) + \frac{\partial}{\partial z}\left(k_z \frac{\partial P^2}{\partial z}\right)\right] \quad (3.2.22)$$

The first case studied by O'Shaughnessy was a steady-state field equation for anisotropic porous media with variable permeability.

This was achieved by assuming $\partial P/\partial t$ of equation (3.2.22) to be equal to zero. That is,

$$\frac{\partial}{\partial x}\left(k_x \frac{\partial \phi}{\partial x} + k_y \frac{\partial \phi}{\partial y} + k_z \frac{\partial \phi}{\partial z}\right) = 0 \qquad (3.2.23)$$

where $\phi = P^2$ (3.2.24)

One boundary condition for equation (3.2.23) was the $\phi$ values specified on the boundary as shown in equation (3.2.25).

Since the principal directions of the permeability tensor might not necessarily coincide with the directions of the co-ordinate axes, equation (3.2.26) was used as the second boundary condition.

$$\phi = \phi_B \qquad (3.2.25)$$

$$k_x \frac{\partial \phi}{\partial x} l_x + k_y \frac{\partial \phi}{\partial y} l_y + k_z \frac{\partial \phi}{\partial z} l_z + M = 0 \qquad (3.2.26)$$

where $M$ = the mass flux of gas across the unit surface area

$l_x$, $l_y$ and $l_z$ = the direction cosines of the outward normal to the boundary surface.

## Numerical Technique and Computer Programming

Based on Keen's (1977) conclusion that the finite-difference method was inadequate for solving the field equations as applied to longwall mining, O'Shaughnessy applied the finite-element approach to solve the model-governing equation. The computer package called PAFEC '75 (Program for Automatic Finite-Element Calculations) developed at the University of Nottingham was used to aid solution of the finite-element model. The PAFEC '75 package used the method of variational calculus to develop the finite-element model.

## Model Validation

The developed models were not field validated.

## Merits and Limitations

O'Shaughnessy's computer model is an unsteady-state, two-dimensional (three-dimensional in the mathematical formulation), single-phase, finite-element model for the prediction of methane migration patterns from adjacent strata to a moving longwall coal face. It also has the capability of predicting the methane flux into boreholes drilled at the coal face. The important features included in this computer model are as follows:

1. An empirical relationship is used to describe the effects of stress on the permeability of coal.

2. The directions of the principal permeabilities need not coincide with the co-ordinate axes.

3. Variational calculus is used to develop the finite-element model which is then solved by the routines of PAFEC '75.

4. A time-marching approach is used to approximate the unsteady-state condition.

The most significant contribution of O'Shaughnessy's model is the use of the finite-element method in approximating the solution of the methane flow equation. With this method, the directions of the principal permeabilities do not have to coincide with the co-ordinate axes and the boreholes can be treated as the nodal boundaries of the affected elements (see Chapter 2).

### 3.2.4. United States Bureau of Mines Model

The United States Bureau of Mines (BOM) model was developed by the United States Steel Corporation (USSC) under a contract initiated by the United States Department of Energy and later transferred to the United States Bureau of Mines. The primary objective of this BOM project was to develop a mathematical model

to describe and, hence, to predict the inflow of methane gas into active mine workings. The model was based on fundamental information available on the coal seam and on both the rate and extent of mining. The output of this project is a two-dimensional, numerical, mathematical model capable of predicting the methane influx into coal mines under a variety of mining conditions. The mathematical model was programmed using a structured dialect of FORTRAN called USSTRAN to result in a computer simulation model.

Assumptions and Model Equations

Based on the description of the BOM model, the following assumptions existed:

1. The coal seam is idealized as an array of regular blocks. The spaces between the blocks represent the natural fracture network or cleat.

2. Methane production occurs by a three-stage process in which gas: 1) is desorbed from the internal surfaces, 2) diffuses through the unfractured matrix to the cleat, and 3) flows through the cleat.

3. The flow is two-dimensional and isothermal.

4. In addition to being present as free gas in the pores and fracture network and as dissolved species in the pore water, methane is also stored in coal by a sorption process identified as physical adsorption of the methane molecules on to internal coal surfaces.

5. Water transport in the cleat system obeys a modified Darcy's Law which contains a Forschheimer-type term to account for turbulent effects.

6. Gas transport in the cleat system can be modelled using Darcy's Law and three additional terms. A Forschheimer-type term is used to account for possible turbulent effects. A Klinkenberg-type term is applied to describe gas slippage, and a source/sink term is used to describe methane diffusion from the micropores to the cleats.

7. The pseudo-steady-state adsorption model based on Langmuir's theory of monolayer adsorption is considered to be adequate to describe the equilibrium adsorption properties.

8. Fluid properties are calculated from correlations based on published data.

The BOM model considers the pore gas saturation $S_g$, gas pressure $P_g$, and volume of adsorbed gas $V_g$ as the primary dependent variables. The secondary dependent variables are the pore water

saturation $S_w$, water pressure $P_w$, gas velocity $U_g$, and the water velocity $U_w$. These secondary dependent variables are related to the primary dependent variables by the following equations.

$$S_w = 1 - S_g \tag{3.2.27}$$

$$P_w = P_g - P_{cgw} \tag{3.2.28}$$

$$U_g = - \frac{k}{\mu_g} \left(1 + \frac{b}{P_g}\right) (1 + \epsilon_g) F_{Dg} \tag{3.2.29}$$

$$U_w = - \frac{k}{\mu_w} (1 + \epsilon_w) F_{Dw} \tag{3.2.30}$$

where $P_{cgw}$ = capillary pressure

$k$ = permeability

$\mu$ = viscosity

$b$ = Klinkenberg factor to account for gas slippage

$\epsilon$ = $[(1 + 4\ Re)^{1/2} - 1] / 2$ to account for turbulent effects

$F_D$ = Darcy flow force due to pressure gradients and gravitational forces

g & w = subscripts to represent gas and water, respectively

To complete the basic equation set, the flow equations described above are supplemented with the equations describing the gas sorption process. The model equations become:

$$v\, C_{ss}\, \dot{S}_g + v\, C_{sp}\, \dot{P}_g = + \nabla \cdot \lambda_w\, k_{rw}\, (1 + \epsilon_w)^{-1}\, \nabla P_g + \nabla \cdot \lambda_w\, k_{rw}\, (1 + \epsilon_w)^{-1}\, P_c'\, \nabla S_g - \nabla \cdot \lambda_w\, k_{rw}\, (1 + \epsilon_w)^{-1}\, \gamma_w^{\circ}\, \rho_w\, \nabla z - Q_w \qquad (3.2.31)$$

$$C_{ps}\, \dot{S}_g + C_{pp} + \dot{V}_g = + \nabla \cdot \lambda_g\, k_{rg}\, (1 + \epsilon_g)^{-1}\, (1 + b/P_g)\, P_g\, \nabla P_g - \nabla \cdot \lambda_g\, k_{rg}\, (1 + \epsilon_g)^{-1}\, (1 + b/P_g)\, C_g\, P_g^2\, \nabla z - Q_g \qquad (3.2.32)$$

$$\dot{V}_g = t_s^{-1}\, (V_E - V_g) \qquad (3.2.33)$$

It should be mentioned that equations (3.2.31), (3.2.32) and (3.2.33) are similar to equations (3.2.3), (3.2.4) and (3.2.6) of the PSU model reviewed in Section 3.2.1. The only three differences between these two sets of equations are as follows:

1. The PSU model neglects the turbulent effects, while the BOM model applies the term $(1 + \epsilon)$ to account for the turbulent effects.

2. The BOM model uses a constant gas slippage factor based on Klinkenberg's theory, while the PSU model derives a pressure, saturation and composition dependent slippage factor.

3. The BOM model groups some of the terms in a different manner than the PSU model.

The BOM model uses a general format shown in equations (3.2.34) and (3.2.35) to represent the boundary conditions required to solve the model equations. The values $\alpha_p$, $\beta_p$, $\gamma_p$, $\alpha_s$, $\beta_s$, and $\gamma_s$, shown in the boundary conditions depend on the physical situation or system under consideration.

$$\alpha_p P + \beta_p \nabla P = \gamma_p \qquad (3.2.34)$$

$$\alpha_s S + \beta_s \nabla S = \gamma_s \qquad (3.2.35)$$

In the BOM model, the moving mine face was described mathematically in terms of a moving co-ordinate system or finite-difference grid. The degasification wells were modelled using well-block source/sink functions.

Numerical Techniques and Computer Programming

Two computer programs, MINE1D and MINE2D, were developed in the BOM project. The MINE1D program considers two one-dimensional cases. One case is an isolated mine pillar approximated by a cylinder with the same cross-sectional area and height. A second case is an advancing mine face with an optional horizontal or vertical degasification well ahead of the face.

The MINE2D program is a two-dimensional simulation model developed to describe the transient flow of gas and water through a horizontal coal seam in two space directions. MINE2D includes a mine face which can be held stationary or advanced according to a user-specified schedule. MINE2D also includes the possibility of one or more degasification wells. The degasification wells may be horizontal or vertical, and the vertical wells may be associated with induced infinite-conductivity vertical fractures.

Both the MINE1D and MINE2D programs were written using a structured dialect of FORTRAN called USSTRAN. The structured programming operations such as IF-ELSE, DO-WHILE and DO-UNTIL may not be available in standard FORTRAN. A pre-compiler also named USSTRAN was developed to translate the basic structured programming operations into standard FORTRAN. Theoretically speaking, any computer capable of executing ANSI standard FORTRAN codes is capable of executing the MINE1D and MINE2D programs. However, depending on the configuration of the computer system and the peripherals, problems may exist in the input/output (I/O) section.

The finite-difference method was used in the BOM project to solve the model equations shown in continuous form in equations (3.2.31) to (3.2.35). Using the method-of-lines, the space variables are discretized and the differential operators are approximated by the finite-difference operators.

## Model Validation

The simulation results obtained from the BOM model were compared with the methane measurements made in three coal mines in the eastern United States. One test site was the Cumberland mine of the United States Steel Mining Company, Inc. (USM) located in southwestern Pennsylvania. The Cumberland mine operates both longwall and continuous-mining sections in the Pittsburgh Seam. Methane measurements were made only in the longwall section. A second site was the Oak Grove mine of USM located in Alabama near Birmingham. This mine operates continuous-mining sections in the Blue Creek Seam. A third site was the No. 50 mine of USM located in West Virginia. The No. 50 mine operates both continuous-mining and longwall sections. Methane measurements were made only in a continuous-mining section.

In-mine measurements of methane concentration and air velocity were made to quantify the methane emission. Methane concentration was measured with both hand-held methanometers and continuous-recording methanometers. The hand-held units allowed portability and spot readings, while the continuous-recording methanometers allowed recording of all changes in methane concentration at selected locations. A vane anemometer was used to determine air velocity in the entries and returns in the test areas.

From the methane emission data and air volumes, the relative volumes of methane liberated from the rib, the gob and the mine face were calculated. The highest and lowest methane emissions were found to be from the gob and from the mine face, respectively. The methane emission from the rib was found to be intermediate between the two. It is because of these findings that the BOM report (1984) mentions:

> The overall release of methane during mining will depend on many factors including the average rate of advancement of all sections in a mine, the extent of mine workings, degasification practice, the age, and the mining history. Furthermore, gas emission from gob areas resulting from caving of overlying seams may be significant. Because these factors are difficult to quantify, measurements in the face area are more appropriate for evaluation of the model than measurement of total mine methane.

It is stated in the BOM report that detailed comparison of model predictions with field measurements proved difficult because data were incomplete; however, results of the simulation of methane emission during advance of the mine face following idle periods were in general agreement with observed values. Hyman and Stahl (1985) compared predictions of the one-dimensional model, MINE1D, with published accounts of methane emissions and pressure profiles from active mine workings in the Pocahontas coal seam. Good agreement was obtained when the default coalbed properties contained in the computer program for the Pocahontas coal seam were used.

The model predictions regarding the effects of degasification by horizontal and vertical wells have not been tested with the field data.

Merits and Limitations

One significant contribution of the BOM model is the use of empirical equations or models to describe the effects of compaction on porosity and permeability. Using a constant compressibility value, the porosity of coal is related to the stress. The effective stress acting to compress the coal structure is the overburden load minus the pore fluid pressure. The variation of permeability is calculated from the variation in porosity according to a power law. An analysis by Jones (1973) based on the theory of fluid flow between parallel plates suggests that the exponent in the power law should be 3. Ostensen (1982) has proposed a value of 2 based on tri-axial deformation studies of porous sandstones. Many experimental studies are generally more consistent with larger values for n (Somerton et al., 1975 and Ostensen, 1983).

A second significant contribution of the BOM model is the detailed modelling of the transport of water and methane in the cleat system. Water transport is modelled using two terms. One term is Darcy's Law which is valid for laminar flow conditions. The second term is Forschheimer's approach to account for turbulent effects. Gas transport is modelled using four terms.

One term is Darcy's Law. A Forschheimer-type term is used to compensate for possible turbulent effects. A Klinkenberg-type term is applied to account for gas slippage, and a source/sink term is used to describe methane diffusion from the micropores to the cleats.

The important features included in the BOM model are:

1. unsteady-state, two-dimensional, two-phase flow;
2. dual-porosity to represent the nature of coal;
3. two mechanisms (concentration and pressure) to represent the methane flow;
4. pseudo-steady-state sorption based on Langmuir isotherms;
5. Klinkenberg's theory to account for gas slippage;
6. Forschheimer's approach to account for turbulent effects; and
7. empirical equations to describe fluid properties.

The limitations of the BOM model are as follows:

1. As mentioned in the BOM report, the computer codes are not fully optimized and some further work will be required to adapt the computer codes to a wide range of mining problems.

2. The BOM model does not account for three-dimensional phenomena. A three-dimensional model is felt to be important in predicting the methane emission from thick coal

seams with inhomogeneous properties in the vertical direction. A three-dimensional model is also felt to be important in the investigations of the effects of adjacent seams and impermeable geological barriers on the methane emission.

3. The BOM model does not account for the effects of other strata. As discussed in the previous point, it is recommended that the BOM model be extended so that it is three-dimensional prior to incorporating the strata effects.

### 3.2.5. Empirical Models

Several empirical models were proposed for predicting methane emission into mine workings (Curl, 1978). These models are based on empirical formulas incorporating the amount of methane adsorbed in the seam, and consideration of the mining parameters such as the height (h) and depth (d) of the emission zone, face length ($\ell$), extracted seam thickness (t), etc.

As a general formulation, the degree of gas emission[1] in the roof $A_R$ or in the floor $A_F$ is calculated using mathematical functions denoted by equation (3.2.36) as follows:

[1] The degree of gas emission is the percentage of the gas contained within the strata at a specific level which flows into the workings

$$A_{R(F)} = f(h, d, t, \ell) \qquad (3.2.36)$$

The most common functional form f(h, d, ...) is a combination of linear, quadratic and exponential terms of variables h, d, t, and $\ell$. A summary of the selected models is given in Table 3.3.

A different approach was proposed by Airey in 1971. Although the theoretical approach uses an empirical equation for predicting the emission of methane from broken coal (Airey, 1968), the theoretical development of Airey's model was based on a phenomenological description of methane emission in the mine workings. The model has shown to successfully correlate a number of cases where methane emissions were determined at the mine face at different face advancement rates. It has been also adapted as a MRDE prediction method in the U.K. Therefore, it was felt that the more detailed evaluation of Airey's model would be helpful to the overall review of the computer-based numerical method for the prediction of methane emissions into longwall mines.

Assumptions and Model Equations

The development of Airey's model is based on an empirical equation derived for the methane emission from broken coal (Airey, 1968).

**Table 3.3. SELECTED EMPIRICAL CORRELATIONS FOR METHANE EMISSION (Curl, 1978)**

| METHOD | HEIGHT OF ZONE OF GAS EMISSION, m | DEGREE OF GAS EMISSION, % |
|---|---|---|
| Gunther | $h_R$ = + 100 | $A_R$ = 100 % |
| | $h_F$ = - 100 | $A_F$ = 100 + h |
| Schultz | $h_R = 0.5\ \ell$ | $A_R = \frac{100}{\ell}\sqrt{\ell^2 - 4h^2}$ |
| | $h_F$ = - 20 | $A_F$ = 100% to h = -5, then linear decrease to 0% at h = -20 |
| Koppe | $h_F$ = - 50 to 64 | $A_F = 142 + 4\ h + 0.027\ h^2$ |
| Barbara Mine | $h_R$ = 120 h/t | $A_R$ = 64.7 exp(-0.03957 h/t) |
| | $h_F$ = 120 h/t | $A_F$ = 54.1 exp(0.03721 h/t) |

$$V(t) = A \{1 - \exp[-(t/t_o)^n]\} \qquad (3.2.37)$$

where $V(t)$ = amount of methane released from a coal lump ($m^3$/tonne)

$A$ = initial methane content in coal seam ($m^3$/tonne)

$t_o$ = characteristic time for methane desorption (sec)

$t$ = time after start of desorption

$n$ = empirical coefficient

The assumptions underlying equation (3.2.37) are:

1. At the initial time, the rate of methane release is infinite. In a strict sense, this assumption is incorrect since the rate has to be finite at all times.

2. At the infinite time, the amount of total methane released approaches a constant value.

$$\frac{dv(t)}{dt} \rightarrow \infty \text{ at } t \rightarrow \infty$$

Review of the application of equation (3.2.37) showed that:

1. The empirical coefficient, n, is a relatively constant value of 0.31 and it cannot be correlated using a simple function of variables such as particle size, coal properties, etc.

2. The characteristic time, $t_o$, is a function of particle size up to about 0.1 inch, above which it increases non-linearly and assumes a constant value of about 140 hours for large coal lumps.

Parameters n and $t_o$ should be viewed as correlation constants since there is no supporting data to suggest that they depend, in a regular manner, on seam or coal property variables. Also, the amount of methane released is not sensitive to parameter n. This suggests that there is no theoretical significance underlying this parameter.

Airey (1971) also proposed a phenomenological model for methane emission which incorporated the empirical equation (3.2.36). The theory postulates the following phenomenological model for the methane emission process:

1. A coal seam consists of an assembly of closed packed "coal lumps" (grains), with the spaces (fissures) between grains offering a negligible resistance to the methane flow. The permeability of the fissures is assumed to be unaffected by the stress distribution.

   In a sense, Airey introduced a dual-porosity model; however, the assumption of stress-independent permeability is incorrect for most coal seams (McPherson, 1975).

2. The size of lumps varies with the distance from the coal surface. The size of lumps is represented by a characteristic time $t_o(t)$, which is assumed to vary in a prescribed fashion (equations (3.2.38) and (3.2.39)).

$$\text{for } x > 0 \quad t_o(t) = t_o \exp(x/x_o) \tag{3.2.38}$$

$$x < 0 \quad t_o(t) = t_o \tag{3.2.39}$$

where $x_o$ and $t_o(t)$ are further defined in Figure 3.1.

3. Gas emission per unit mass of coal is determined by the empirical equation (3.2.36) so that a low emission from the coal away from the face is associated with a large lump size. For example, gas emission at the distance of $x = x_o$ would have a characteristic time $t_o(t) = 2.7\ t_o$, or 2.7 x 140 hours = 378 hours. The characteristic time $t_o(t)$ at $x = 5\ x_o$ would be equal to 150 x 140 hours = $2.1 \times 10^4$ hours.

Since the longwall face advances in the x direction, Airey's model requires that coal grains decrease in mesh size with time, and that $t_o(t)$ for a specific grain also decreases with time.

The above treatment resembles somewhat an application of Lagrangian coordinates by following each coal grain with time, at different space coordinates, rather than using Eulerian coordinates and following the same space coordinate

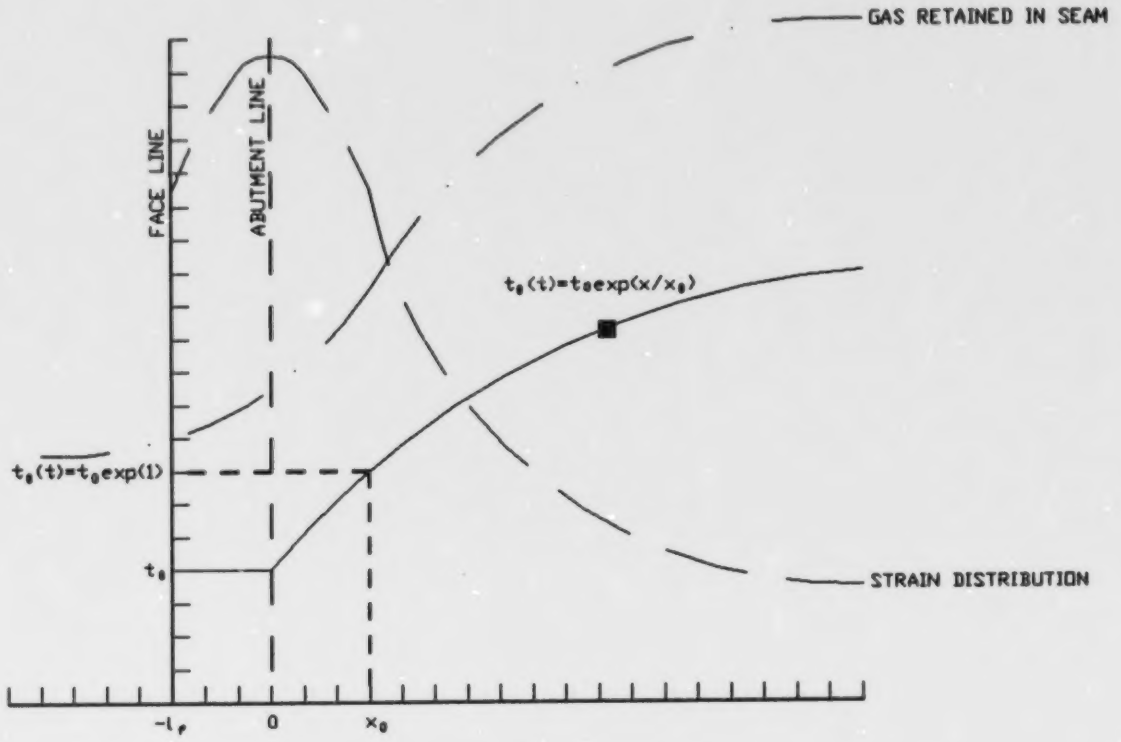


**Figure 3.1. DISTRIBUTION OF GAS, STRAIN AND $t_o$ IN COAL SEAM**

at different times. Assuming that the empirical equation (3.2.37) is an approximation of a finite-element solution for the methane emission from coal grain, the theoretical results would then not differ significantly from a finite-difference method. This analogy would hold, however, only for the coal matrix and not for the coal porosity. Also, another consequence of using Lagrangian coordinates is a requirement for a different time delay for methane emission from coal grains located along the x coordinate. This introduces a certain awkwardness and complexity to the treatment.

Assuming a uniform rate of face advance, the rate of gas emission at the face is given by Airey (equation (3.2.40)).

$$\frac{dv(t)}{dt} = \frac{dw}{dx}\ A(t)\ r\ \{1 - \exp[-(\frac{x_o + L_{\gamma_s}}{r\ t_o})^{1/2}]\} \qquad (3.2.40)$$

where $\frac{dw}{dx}$ = the weight of coal removed per unit advance rate (m/s)

$A(t)$ = gas content in the seam ($m^3$/tonne)

$L_{\gamma_s}$ = the distance between the face and the position of maximum abutment load ($x_o$)

Equation (3.2.40) is a weak function of $L_{\gamma_s}$ and $x_o$. For small values in the terms in parenthesis ( ), equation (3.2.40) can be approximated by equation (3.2.41) as follows:

$$\frac{dv}{dt} = \text{constant } r^{0.8} \qquad (3.2.41)$$

Model Capabilities

Airey's model can provide the following information on methane emission:

1. Emission from the mine face is given by equation (3.2.40). For low exponent values, equation (3.2.41) predicts the effect of the rate of face advancement on the methane emission.

2. Emission from the adjacent seams is treated in a similar fashion as from the worked seam. Equation (3.2.40) requires adjustment of parameter values $L_{\gamma_s}$ depending on whether emission to the face or the gob is calculated.

   Interestingly enough in his report, (Airey, 1971) does not consider the changes of parameter $\frac{dw}{dx}$, which would imply that the emission from the adjacent seams does not depend on the adjacent seam thickness. This could explain, perhaps, why in some instances Airey's model significantly under-predicts the methane emission from the adjacent seams.

3. Gas content of the seam can be calculated by mathematical extension of equation (3.2.40). The portion of gas retained

at the face can be evaluated using equation (3.2.40) and X = $-L_{fs}$ suggested to be equal to 2 m.

4. Pressure in the seam is derived from the distribution of gas content in the seam, assuming a proportional relationship (Henry's Law) between the gas content and gas pressure. For high gas pressures these assumptions are not accurate and tend to under-estimate the amount of gas in coal.

5. Methane emission after stoppage of the mine face can be calculated from a combination of equation (3.2.40) and its derivatives.

6. It is proposed that gas emission from the cut coal be calculated using a modified empirical equation (3.2.42).

$$V(t) = 1 - \exp[-(CT^3)^n] \qquad (3.2.42)$$

where $V(t)$ = fraction of gas lost, $V(t)/A$

$c$ and $n$ = parameter dependent on the lump size distribution

$T = t_o(t) / t_o$

For a narrow size distribution n = 0.33 and c = 1, and for a normal size distribution c = 0.82 and n = 0.24.

Model Validation

Airey (1971) provides an example of the predictive capabilities of the model by comparison of the predicted values, using equation (3.2.41), to the actual measurement of methane emission at two different mine faces. The measured data are quite scattered, however, and do not necessarily validate the value of the exponent 0.8. Also, no information is provided concerning whether or not the value of constants would correspond to the theoretical predicted values using equation (3.2.37). In fact, the value for $A(\frac{dw}{dx})(t)$ was adjusted to give the best fit to the field results.

The value of $t_o$ was derived using laboratory tests for methane emission from different sized coal. It was shown that $t_o$ can be correlated with the mesh size for coal lumps smaller than 0.1 inch ($t_o$ ~ 100 hours). For larger pieces, the value of $t_o$ was found to scatter significantly and a value of 140 hours was assumed for mine methane emission predictions.

The distribution of the $t_o(t)$ as a function of distance from the mine face is not known and was assumed to have a functional form of equations (3.2.38) and (3.2.39). Later, Airey (1979) derived an expression for $t_o(t)$ based on the stress distribution within the seam. The proposed functional form is:

$$t_o(t) = T\ (\frac{\sigma_1}{\sigma_3})$$

where T = a function of a principal stress $\sigma_1$ and $\sigma_3$ in x and y directions

The value of $t_o(t)$ can be calculated numerically from the stress distribution in the worked and adjacent seams, and as a function of the depth of the worked seams. It is assumed that the lines of equal $(\frac{\sigma_1}{\sigma_3})$ values correspond to lines of equal time constant $t_o(t)$. The total methane emission can be calculated from the distribution of $t_o(t)$.

The values of $L_{fs}$, $L_{fa}$ and $l_{ga}$ (the distance between the face and the position of maximum abutment, and the length of waste) were found to be not critical and were assumed to be:

- for the worked seam face, $L_{fs}$= 2 m
- for the adjacent seams methane emission into face, $L_{fa}$ = 10 m
- for the adjacent seams methane emission into waste, $L_{ga}$= 100 m

The value of $x_o$ is defined as the characteristic length at which $t_o(t) = t_o \exp(1)$. In practice, this correlation constant determines how steep the pressure gradient is in the vicinity of the maximum load abutment. A value of X = 4 m was found to yield a satisfactory fit of the model equations to experimental emission.

## Numerical Techniques and Computer Programs

A combination of numerical techniques and hand calculation methods can be used with Airey's model. For calculation of stress distribution and the lines of equal characteristic time $t_o(t)$ in the worked and adjacent seams, numerical techniques such as finite-difference were used. For calculation of the methane emission, manual methods using graphs of the integrated model functions can be used. Since the calculations are easily amenable to programming on a computer, a series of mainframe and microcomputer programs were developed and adopted as MRDE methane prediction methods in the U.K. (Dunmore et al, 1984).

## Model Limitations

Despite the flexibility of the model it has several limitations inherent to the development of the model governing equations.

1. The model cannot determine the amount of methane drainage from drainage boreholes. Also, since all calculations are based on the original methane content in the seam, it is not clear whether methane predictions are equally accurate for the predrain seams. It is possible, in principle, to carry out calculations for a predrain seam, but one would have to know the distribution of the methane content in the seam.

2. There is some confusion about the application of the Airey model to the calculation of methane emission from the adjacent seam. Specifically, the characteristic length parameter L seems to be redefined. In later developments, the methane emission from the adjacent seams that come into the face is calculated based on coal deposited only in front of the abutment zone. The waste emission from the adjacent seams is calculated based on coal deposits behind the abutment zone. This resulted in a simplification of the model equation, with the emission into the face described by a function of the district age, methane content in the seams, and the rate of the face advancement.

3. There is a controversy concerning the application of Airey's model to seams with medium methane pressure (Owili-Eger et al., 1973). The controversy arises from Airey's assumption that the amount of gas adsorbed is proportional to methane pressure (Henry's Law). At relatively low or high pressures, the amount of adsorbed gas at saturation can be given by Henry's Law; however, at a range of pressure typically observed in mines, the Langmuir isotherm described the amount of adsorbed gas more accurately.

4. A much weaker feature of Airey's model is the neglect by the model of the pressure gradient that exists within the coal grains, thus the calculated pressure is an average or equivalent pressure for coal lumps.

## 3.3. Computer Models for Methane Well Degasing

A number of computer models for degasing coal seams have recently been developed with the overall objective of simulation of degasification boreholes. These models have various degrees of complexity and sophistication. Some of them may be of interest for the development of a computer model for prediction of methane flow into mine workings. A summary of the available models is presented in Table 3.2. A discussion of those elements of the models that may be of interest is presented below.

### 3.3.1. Kovalev and Kuznetsov Model

Kovalev and Kuznetsov (1974) formulated a moving boundary value problem to determine the rate of methane emission into an advancing longwall face. The model includes a non-equilibrium diffusion/sorption term for the matrix/fissure transfer. It assumes a steady-state pressure and methane concentration distribution in longwall face direction. The final equations governing methane flow into the mine workings are:

$$\frac{d}{dx}\left[\frac{\alpha k_{ma}}{\mu_g}\rho_g\frac{dP_g}{dx}\right] - \dot{x}_{ma}\frac{d}{dx}\left[\phi_{ma}\rho_g + (1-\phi_{ma})M_{mi}\right] = 0 \qquad (3.3.1)$$

$$\frac{D_{mi}}{r_{mi}^2} \frac{\partial}{\partial r_{mi}} \left(r_{mi}^2 \frac{\partial C_{mi}}{\partial r_{mi}}\right) = \dot{x}_{ma} \frac{\partial C_{mi}}{\partial x} \qquad (3.3.2)$$

$$M_{mi} = \frac{3(MW)}{R_{mi}^3} \int_0^{R_{mi}} C_{mi} (\hat{r}_{mi}, t) \hat{r}_{mi}^2 d\hat{r}_{mi} \qquad (3.3.3)$$

With the following boundary conditions:

$$P_g = \text{Const} \quad ; x = 0 \qquad (3.3.4)$$

$$P_g \rightarrow P_g^o \quad ; x = \infty \qquad (3.3.5)$$

$$C_{mi} = C_E(P_g) = \frac{C_L P_g}{P_L + P_g} \quad ; r_{mi} = R_{mi} \qquad (3.3.6)$$

$C_m$ is finite ; $r_{mi} = 0$

The solution of the differential equation was presented in a graphical form.

### 3.3.2. ARRAY Model

USS and GRI have developed computer-based numerical models to simulate the release of methane gas from coal and to model two-phase flow of water and methane gas through the coal seam to gas production wells. USS developed two simple one and two-dimensional single-well models designated WELL1D and WELL2D, and a more complex computer model, ARRAY, capable of simulating degasification of coal seams using a two-dimensional array of

wells. Some of the capabilities of the ARRAY model are discussed below.

Variable Permeability Model

ARRAY includes relative permeability models to account for the effects caused by variations in pressure and saturation on permeability. The relative permeabilities are calculated from the compressibility and relative permeability models based on the modified Corey equations (Corey, 1954):

$$k_{rw} = R_w \, s^4 \qquad (3.3.7)$$

$$k_{rg} = R_g \, (1 - s)^2 \, (1 - s)^2 \qquad (3.3.8)$$

$$P_c = P_c^o \, s^{-1/2} \qquad (3.3.9)$$

where $k_{rw}$ = relative permeability to water

$k_{rg}$ = relative permeability to gas

$s = (1 - S_g - S_{wr}) / (1 - S_{gr} - S_{wr})$, the saturation variable

$R_g$ = the relative permeability to gas at the residual water saturation ($s = 1 - S_{wr}$)

$R_w$ = the relative permeability to water at the critical gas saturation ($s = S_{gr}$)

$P_c^o$ = capillary pressure factor

The ARRAY user has the option of selecting parameters for the relative permeability model including a capillary pressure

factor. Several options corresponding to different assumptions about stratification of fluids in the fracture can also be selected by the user. The model accounts for the flow in the third dimension by assuming equilibrium between gravitational and capillary forces in the vertical direction.

In addition to the relative permeability models using the modified Corey relations, ARRAY allows the user to enter appropriate saturation-dependent properties.

Compaction Model

ARRAY's description of the effect of stress and compaction on seam porosity and permeability uses Terzaghi's effective-stress model (Terzaghi, 1943). The model assumes a constant compressibility seam structure in which the stress is equal to the overburden load minus the pore fluid pressure, P. For a fixed overburden load the porosity is given by the following equation:

$$C_\phi = \frac{1}{\phi}\left(\frac{d\phi}{dP}\right) = C_s \frac{(1-\phi)}{\phi} \qquad (3.3.10)$$

where $C_\phi$ = effective compressibility of the pore volume

$C_s$ = coal seam compressibility

$\phi$ = porosity

P = pressure

The variation of porosity ($\phi$) with pressure (P) is obtained by integrating the above equation. The variation of permeability (k) is calculated from the variation in porosity ($\phi$) according to:

$$\left(\frac{k}{k^o}\right) = \left(\frac{\phi}{\phi^o}\right)^n \qquad (3.3.11)$$

where n = the porosity permeability exponent.

Based on an analysis using the theory of fluid flow between parallel plates, Jones (1973) suggested the porosity permeability exponent (n) to be equal to 3. More recently, Ostensen (1982) proposed a value of 2 based on the tri-axial deformation studies of porous sandstones. However, many experimental studies are generally more consistent with higher values for the porosity permeability exponent (Somerton et al., 1975 and Ostensen, 1983).

# 4. SELECTED MODEL PARTS

Based on the review of the background materials (Chapter 2) and the study of the existing models (Chapter 3), twenty-nine model parts are identified as being important to the prediction of methane flow into mine workings. These twenty-nine selected model parts can be separated into three groups according to their priorities. One group consists of the model parts that must be implemented in order to provide an adequate prediction of methane flow into mine workings. Seventeen model parts belong to this group. A second group consists of nine model parts which can either improve the prediction or enhance the use of the computer model. A third group consists of three model parts which may be required by a few unique or uncommon applications.

Some of the twenty-nine model parts are available in the four computer models reviewed and discussed in Chapter 3 (Sections 3.2.1 to 3.2.4). However, none of the four computer models contain all the twenty-nine selected model parts. Table 4.1 provides a summary of the twenty-nine selected model parts as well as their priorities and availabilities. The reasons why these selected model parts are important and the adverse effects of not implementing the model parts are as follows:

**Table 4.1. SUMMARY OF THE SELECTED MODEL PARTS, AND THEIR PRIORITIES AND AVAILABILITY**

| | Selected Model Part | Priority[1] | Availability[2] |
|---|---|---|---|
| 1. | Dual-porosity to represent coal | I | PSU, BOM |
| 2. | Two-phase flow | I | PSU, BOM |
| 3. | Three-dimensional flow | I | PSU, BOM[3], UON[3] |
| 4. | Unsteady-state flow | I | PSU, BOM, UON |
| 5. | Stress-dependent porosity | II | BOM |
| 6. | Stress-dependent permeability | II | BOM, UON |
| 7. | Darcy's Law for water transport | I | PSU, BOM |
| 8. | Effects of turbulence on water | III | BOM |
| 9. | Real gas law for the gas state | I | PSU, BOM, UON, METGEN |
| 10. | Dual-mechanism for gas flow | I | PSU, BOM |
| 11. | Effects of gas slippage on gas transport | I | PSU, BOM |
| 12. | Effects of turbulence on gas transport | III | BOM |
| 13. | Pseudo-steady-state sorption phenomenon | I | PSU, BOM |
| 14. | Unsteady-state sorption phenomenon | III | N/A |
| 15. | Interactions between multiple seams | I | N/A |

[1] I is the highest priority and III is the lowest priority
[2] PSU = Pennsylvania State University Model
BOM = United States Bureau of Mines Model
UON = University of Nottingham Model
N/A = not available
[3] The mathematical model is three-dimensional, but not the computer model

**Table 4.1. SUMMARY OF THE SELECTED MODEL PARTS, AND THEIR PRIORITIES AND AVAILABILITY (Continued)**

| | Selected Model Part | Priority[1] | Availability[2] |
|---|---|---|---|
| 16. | Mine layout | I | N/A |
| 17. | Vertical borehole | II | PSU, BOM, UON |
| 18. | Horizontal borehole | II | PSU, BOM, UON |
| 19. | Slanted borehole | II | UON |
| 20. | Effects of stimulation | II | PSU, BOM, UON |
| 21. | Emission from mine face | I | PSU, BOM, UON, METGEN |
| 22. | Emission from gob | I | N/A |
| 23. | Coal face advance rate | I | PSU, BOM, UON |
| 24. | Atmospheric pressure in mine workings | I | PSU, BOM, UON METGEN |
| 25. | History matching procedures | I | N/A |
| 26. | Executable in IBM PC compatible microcomputers | I | COMET PC[3] |
| 27. | Fast computational speed | II | See footnote[4] |
| 28. | User friendly | II | See footnote[4] |
| 29. | Ease of future improvements | II | See footnote[4] |

---

[1] I is the highest priority and III is the lowest priority

[2] PSU = Pennsylvania State University Model
BOM = United States Bureau of Mines Model
UON = University of Nottingham Model
N/A = not available

[3] This software was developed by ICF-Lewin Energy, Virginia for maximizing gas recovery from coal seams instead of for mining applications

[4] Improvements regarding these computer-related aspects can be made to the existing computer models

Dual-Porosity

The accuracy of predicting the methane flow into mine workings depends on the adequacy of modelling the nature of coal. If coal is not considered to have a dual-porosity nature, the dual-mechanism (pressure and concentration) that exists in the transport of gas cannot be modelled. The amount of gas emitted from the coal seam and from the cut coal would be underestimated.

Two-Phase, Three-Dimensional and Unsteady-State Flow

If a steady-state condition is assumed in the model, difficulties can arise in the prediction of the effects of the mine face velocity on the methane emission. The requirement of a two-phase flow model depends on the original water saturation or content in the coal seam. A three-dimensional flow model is required in order to accurately predict the methane emission from thick coal seams with inhomogeneous properties in the vertical direction. A three-dimensional flow model also enables accurate prediction of the effects of adjacent seams and impermeable geological barriers on the methane emission.

Stress-Dependent Porosity and Permeability

A moving mine face can alter the stress distribution of the main and adjacent seams. Therefore, stress distribution which affects the porosity and permeability of coal is time-dependent. Without

considering porosity and permeability as functions of stress, the time-dependent functions governing porosity and permeability would be in error. The subsequent methane emission prediction would only be accurate within a limited time interval.

Darcy's Law for Water Transport and Turbulent Effects

For most mining applications, the assumptions inherent in Darcy's Law are felt to be valid for the transport of water in coal. However, if the water flowrate is high, the effects of turbulence will become significant and they should be modelled.

Dual-Mechanism for Gas Flow, Gas Slippage and Turbulent Effects

The release of methane from the micropores to the macropores is caused by the concentration gradient or diffusion. The transport of the desorbed methane through the macropore system is caused by the pressure gradient and can be modelled using a modified Darcy's Law to compensate for gas slippage. Therefore, dual-mechanism is required to model the flow of methane in coal. If the methane flowrate is high such as in the vicinity of a borehole, an additional term is required to supplement the modified Darcy's Law in order to account for the turbulent effects.

Pseudo-Steady-State or Unsteady-State Sorption Phenomenon

Based on the PSU results, the pseudo-steady-state approach to modelling the sorption phenomenon does not result in excessive error in estimating the methane flow at time beyond the initial value, $t^+$, as compared to the unsteady-state approach. Therefore, it is suggested that the pseudo-steady-state approach be used to describe the sorption phenomenon.

Interactions Between Multiple Seams and Mine Layout

The existing models reviewed in Chapter 3 are not capable of predicting the effects of these two physical configurations on the methane emission rate. However, the adjacent seams and the mine layout can affect significantly the emission rate of methane into the mine workings. A high priority should, therefore, be assigned to the development of these two model parts.

Vertical, Horizontal, Slanted, Stimulated and Unstimulated Boreholes

For gassy coal seams, boreholes are commonly used to drain the methane prior to mining. Therefore, the computer model should allow the user to study the effectiveness of using various kinds of boreholes to degasify gassy coal seams.

Methane Emission From Mine Face and Gob

The amount of methane to be emitted from the mine face and from the gob is key information for the user. Output of these predictions should be user friendly.

Effects of Coal Face Advance Rate and Atmospheric Pressure

From the mine operation viewpoint, these two parameters are the controllable parameters. Therefore, the computer model should allow the user to study the effects of these two parameters on methane emission in order to optimize the mining operations.

History Matching Procedures

Stochastic analyses such as the correlations of the field data provide insights into what has happened. Results obtained from such analyses are often extrapolated to predict what will happen in the future. However, due to the lack of a physical explanation of the stochastic findings, the subsequent predictions are limited to the near-term future. Deterministic analyses such as mathematical modelling and computer simulation of the physical phenomena provide a better understanding of the system under consideration. As a result, the information predicted from such analyses is applicable to both the near-term and long-term future. However, the validity of the deterministic predictions depends on the accuracy of the input parameters.

Therefore, a proper combination of these two (stochastic and deterministic) techniques would provide the best prediction regarding what will happen in future. It is recommended that a set of history matching procedures be developed so that analytical and field results can be combined in order to provide the best predictions.

Executable in IBM PC Compatible Microcomputers

The computer hardware and software requirements are considered. There are many reasons for developing computer models executable by IBM PC compatible microcomputers. Some of the advantages are as follows:

1. Due to their popularity, IBM PC compatible microcomputers are more readily available and accessible to industrial users.

2. Industrial users are generally more familiar with microcomputers than mainframe computers. Furthermore, it is easier and more convenient for beginners to learn how to operate microcomputers than mainframe computers.

3. Microcomputer-based programs can encourage users to explore and/or make extra simulation runs since users of microcomputers usually do not have to pay for computation time.

Fast Computational Speed

One potential difficulty exists in executing numerical simulation models using a microcomputer. The user may find that it takes the microcomputer too long to complete the task. There are a few effective approaches that can circumvent this kind of difficulty. One approach is the installation of a math-processor. A second approach is the use of a compiler-type language such as FORTRAN and C instead of the interpreter-type language such as BASIC. Consideration can be given to writing the time-consuming routines in assembly language. It should be noted that developing assembly language routines requires much more programming time than writing the routines in a high level language. This approach is, therefore, not recommended unless economic analysis can justify the use of the assembly language. The mathematical or numerical equations as well as the software can be written in a manner to reduce computational time. For example, numerical constants that will be used many times by the simulation program can be consolidated at the onset of the program and look-up tables can be used to reduce the number of computations. Consideration can be given to outputting the intermediate results for the user to interpret in order to keep the user occupied during the execution of the simulation program.

User Friendly

The human interface of the computer model should be user friendly in order to encourage the user to make extra simulation runs to better understand the effects of various parameters on methane emission. Two options for the user to choose the default input data are recommended. One option is the "hard" default which is a set of some fixed input values. A second option is the "soft" default which is the set of input values that the user used in the previous stimulation run. In addition, flexible conversion factors should be used in the computer program so that the user has the choice of submitting the input data in SI, British or other commonly used units.

Presenting the computer output results in graphical form has advantages and disadvantages. One historical disadvantage is the increased costs of the hardware requirements. A second disadvantage is the additional programming time required to develop the graphical output routines. These two disadvantages have been circumvented by recent advancements in the computer industry. The cost of computer peripherals with graphics capabilities has declined and many inexpensive computer software packages can be purchased to assist in outputting numerical values in graphical form. Many engineering firms have the hardware and software necessary to output numerical values in graphical form. It is, therefore, suggested that an option exists to output the simulation results in graphical form.

Ease of Future Improvements

As indicated in Table 4.1, the selected model parts may be implemented at two or three different stages. Therefore, the computer model should be programmed in a manner that allows future additions or improvements of model parts. This can be achieved by using modules or subroutines to represent the model parts. The design of the computer model should also be documented in a detailed manner.

# 5. PARAMETRIC STUDY OF A SELECTED MODEL

A series of simulation studies has been conducted to demonstrate the applicability of the PSU methane drainage model. In this analysis the methane content of the coal seam and direction of the mining activity were changed systematically in order to distinguish the role of these parameters on the methane emission rates. The simulation studies were conducted over a period of 230 days. During this time, mining of the coal section under consideration was completed. Table 5.1 summarizes the data used in describing the properties of the coal seam. Figure 5.1 represents the set of relative permeability curves assigned to the coal seam. In this parametric study, two numerical exercises were conducted with the objective of demonstrating the performance of the model. In the first exercise the methane emission rates into an active mine are studied. In the second exercise two horizontal boreholes are drilled into the coal from the roadways and methane production rates from these boreholes are calculated.

## Exercise 1

Figure 5.2 represents the coal seam which was under consideration. The dimensions of the seam, together with the dimensions of the roadways, are shown in the figure. In the simulation the development of roadways took 93.6 days, while the

**Table 5.1. INPUT DATA USED IN THE RUNS**

| | |
|---|---|
| Thickness, ft | 6.56 |
| Porosity, % | 2.0 |
| Absolute permeability in face cleat direction, md | 0.3 |
| Absolute permeability in butt cleat direction, md | 0.1 |
| Reservoir depth, ft | 2000.0 |
| Critical water saturation, fraction | 0.15 |
| Critical gas saturation, fraction | 0.0 |
| Relative permeability to gas at critical water saturation, fraction | 1.0 |
| Relative permeability to water at critical gas saturation, fraction | 1.0 |
| Initial gas saturation, fraction | 0.8 |
| Rock specific gravity, gm/cc | 1.36 |
| Langmuir pressure constant, atm | 10.2 |
| Sorption time constant, sec | $2.0 \times 10^6$ |
| Methane content, cc/gm | 9,12,15 |
| Radius of horizontal borehole, inch | 3.0 |
| Horizontal borehole length, ft | 205.0 |

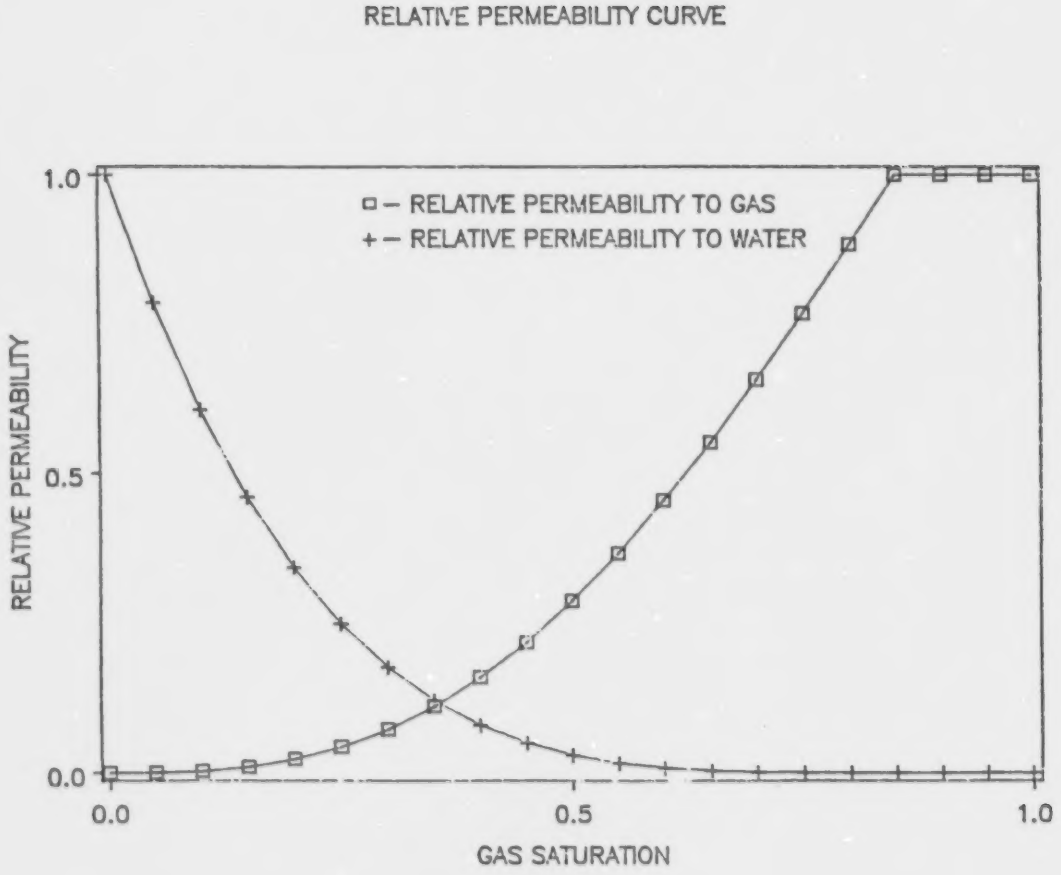


**Figure 5.1. RELATIVE PERMEABILITY CHARACTERISTICS IMPOSED ON THE COAL SEAM**

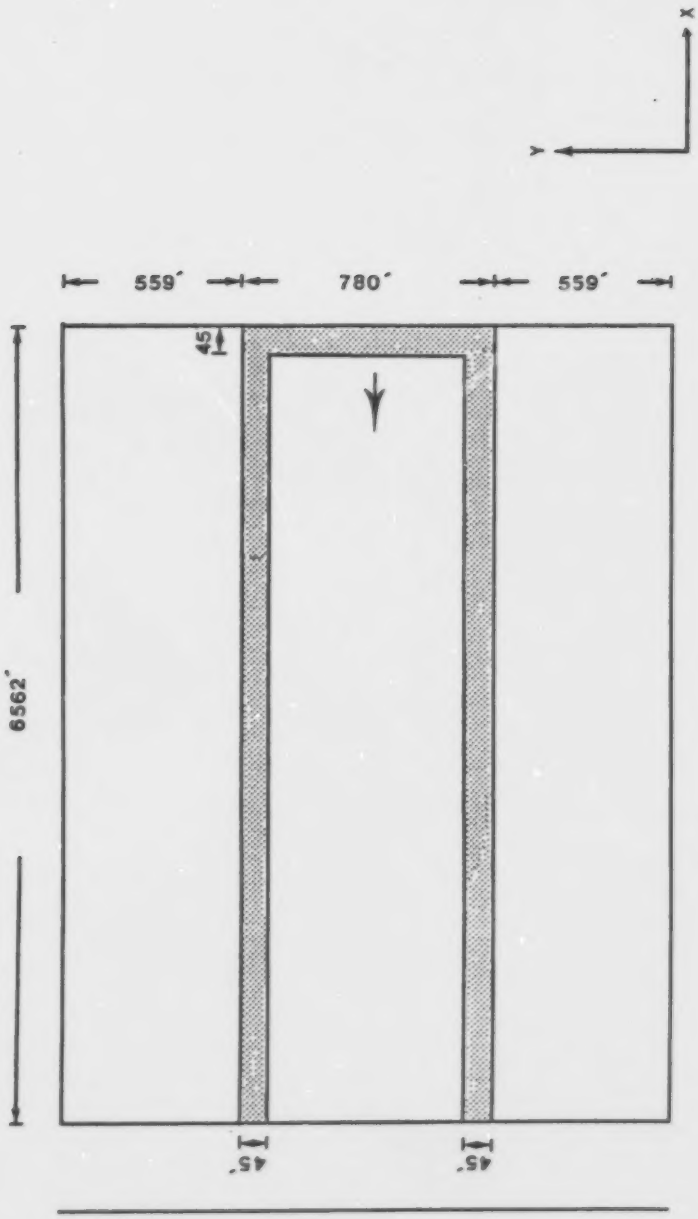


Figure 5.2. MINE LAYOUT AND RELEVANT DIMENSIONS

mining of the coal took 230 days. As shown in Figure 5.2, retreat direction is parallel to the specified x-direction. In order to understand the effect of the permeability anisotropicity on the methane emission rates, face cleat direction is first chosen to be parallel to the x-direction, then, it is chosen to coincide with the y-direction. Figure 5.3 shows the finite-difference grid which was used in the numerical computations.

In Figures 5.4 and 5.5 methane emission rates at the active mine face are plotted. As expected, as the original methane content of the coal seam is increased methane emission rate at the face increases. After an initial peak rate of 500 MSCF/D, emission rate stabilizes at around 100 MSCF/D. If the retreat direction is made perpendicular to the face cleat direction, these rates are drastically increased to 1000 MSCF/D and 280 MSCF/D, respectively. Table 5.2 gives a summary of total methane emission rates calculated for different parameters investigated. Methane emission volumes summarized in Table 5.2 represent the total volume of methane emitted from the active mine face and walls of the roadway. Substantially larger volumes of methane have been encountered when retreat direction is perpendicular to the face cleat direction. This is again expected because roadways are intersecting the more permeable face cleats orthogonally and this increases the emission of methane into the roadways via more the permeable face cleat system. For the coal seam with methane content of 9 $m^3$/tonne, the total amount of methane emitted at the active mine face during the mining

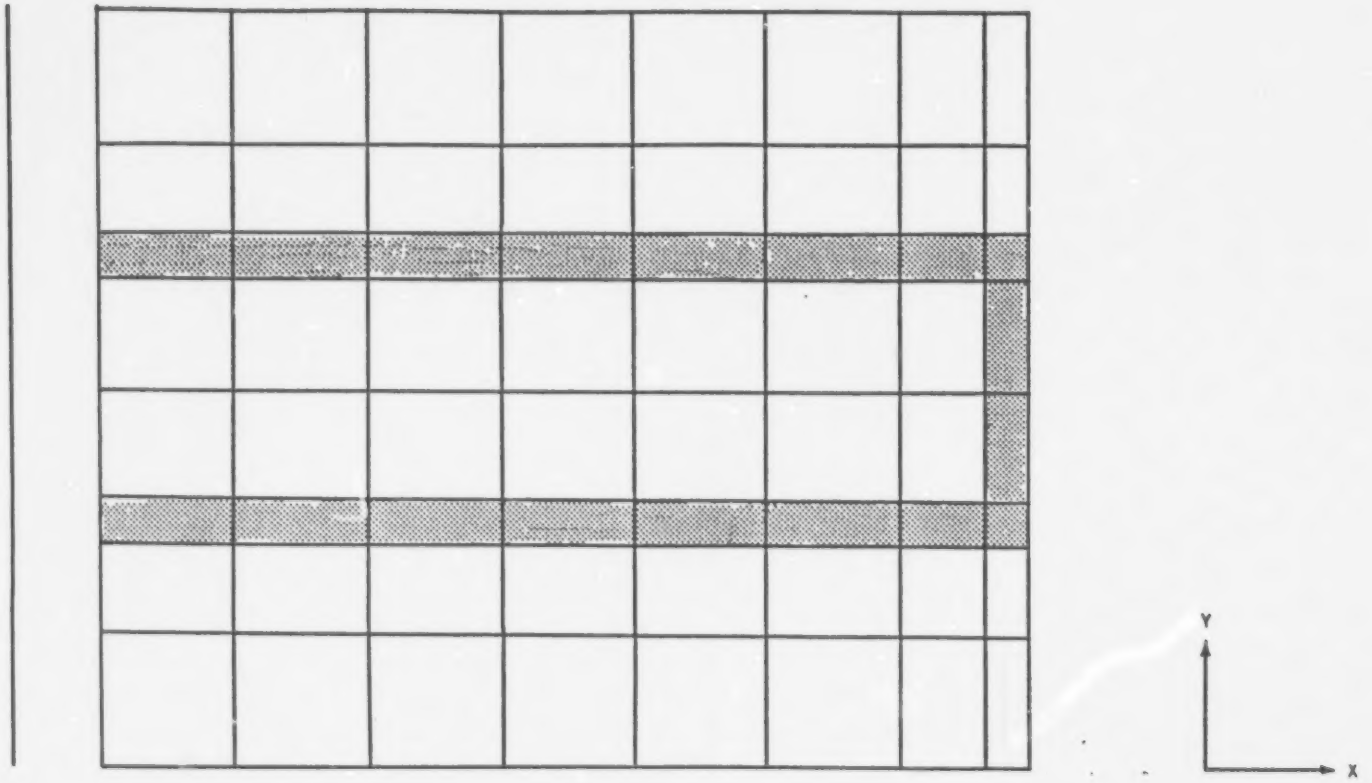




Figure 5.3. FINITE-DIFFERENCE GRID IMPOSED ON THE COAL SEAM

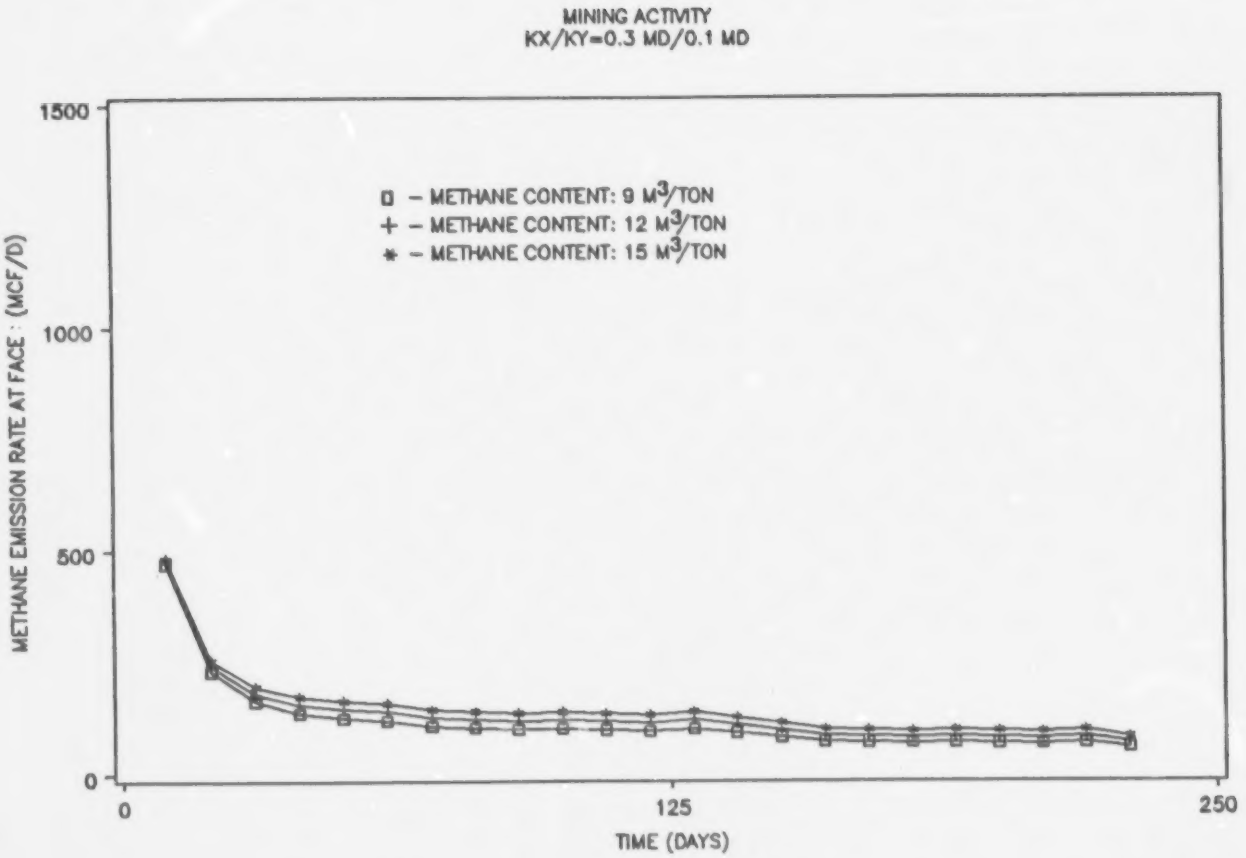


**Figure 5.4.** VARIATION OF METHANE EMISSION RATE AT THE ACTIVITY MINE FACE AS A FUNCTION OF TIME FOR THREE COALS OF DIFFERENT METHANE CONTENT RETREAT DIRECTION IS PARALLEL TO THE FACE CLEAT

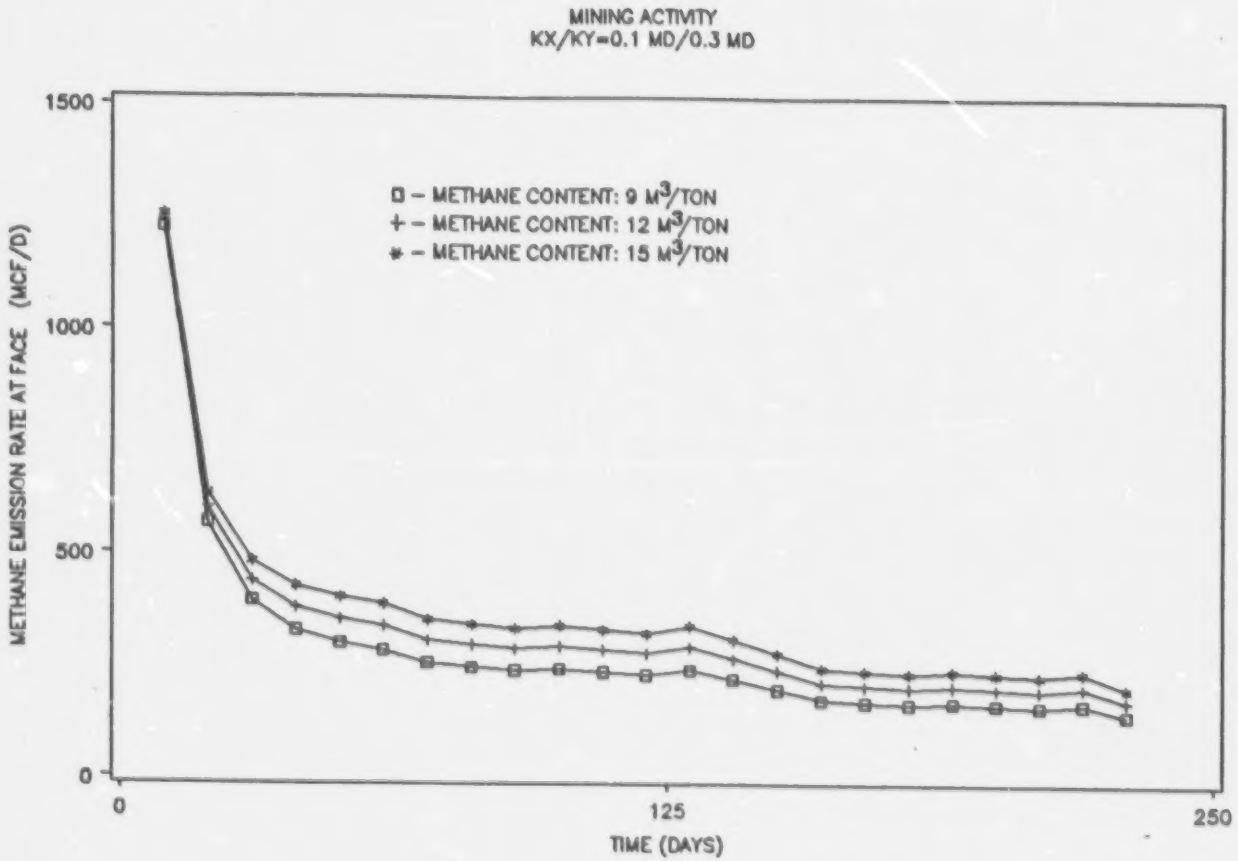


Figure 5.5. VARIATION OF METHANE EMISSION RATE AT THE ACTIVE MINE FACE AS A FUNCTION OF TIME FOR THREE COALS OF DIFFERENT METHANE CONTENT RETREAT DIRECTION IS PERPENDICULAR TO THE FACE CLEAT

**Table 5.2. SUMMARY OF RESULTS FOR EXERCISE 1**

| | $k_x$ = 0.3 md, $k_y$ = 0.1 md | | | $k_x$ = 0.1 md, $k_y$ = 0.3 md | | |
|---|---|---|---|---|---|---|
| Methane content (m3/ton) | 9 | 12 | 15 | 9 | 12 | 15 |
| Methane emission from all open coal surfaces (MMSCF) | 468.9 | 501.97 | 536.6 | 1136.54 | 1229.58 | 1310.63 |

operation is approximately 27.6 MMSCF/D. This corresponds to an average of 0.685 $m^3$/tonne of methane emission at the active mine face. For the same coal seam as indicated in Table 5.1, total methane emission from all open coal surfaces (active mine face and walls of the roadways) is 468.9 MMSCF/D, which translates to 11.65 $m^3$ of methane emission per tonne of coal mined.

Exercise 2

This exercise investigates the performance of the horizontal boreholes which are drilled into the coal from roadways. As shown in Figure 5.6 two horizontal boreholes with penetration lengths of 210 ft were drilled. During this exercise no mining activity was carried out and methane drainage rates via these boreholes were monitored for a period of 230 days. Figure 5.7 shows the finite-difference grid imposed on the system to conduct this exercise. Figures 5.8 and 5.9 give the instantaneous methane production rates when horizontal boreholes are drilled perpendicular to the face cleat direction. As expected, borehole #2, which is located away from the mine face, produces more than borehole #1. It should be recognized that some of the gas around borehole #1 will flow towards the mine face and will be emitted into the mine through the face. Figures 5.10 and 5.11 show similar trends when the orientation of the degasification holes with respect to face and butt cleat directions is changed orthogonally. Slightly smaller production rates are observed in Figures 5.10 and 5.11 for both of the boreholes. This is again

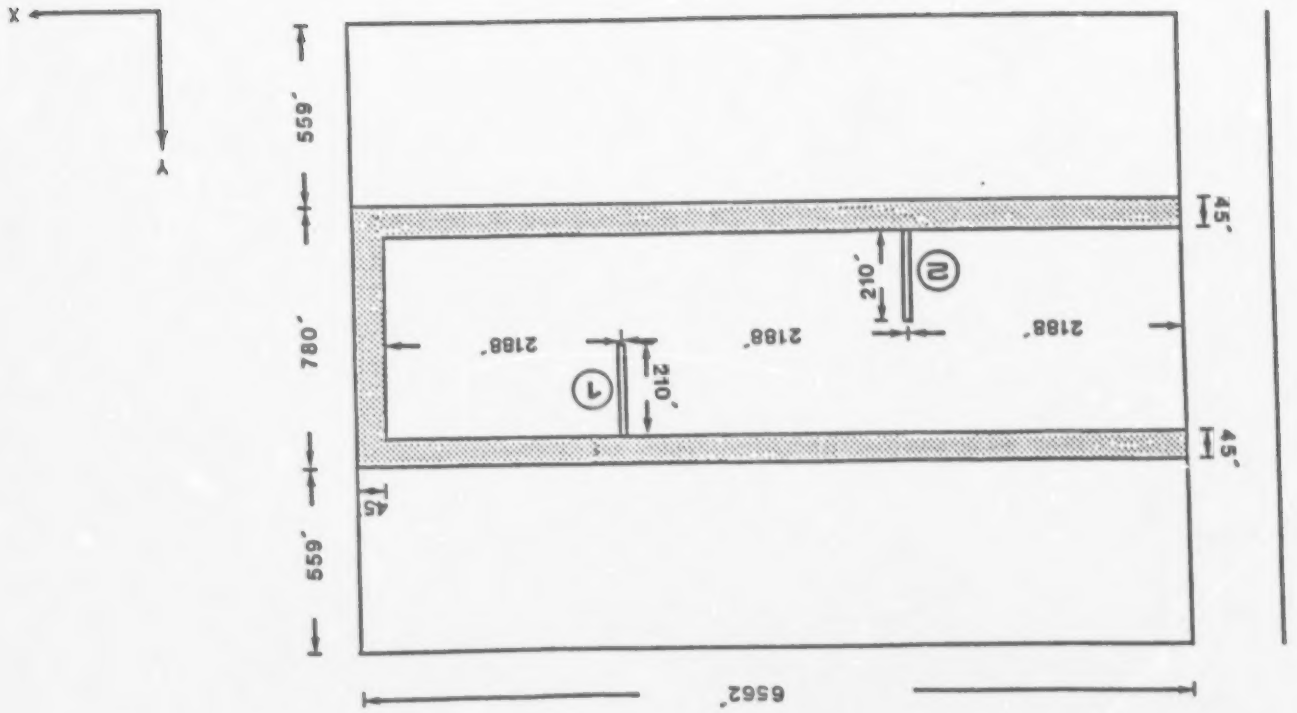


Figure 5.6. DEGASIFICATION OF METHANE WITH THE AID OF TWO BOREHOLES DRILLED FROM THE ROADWAYS

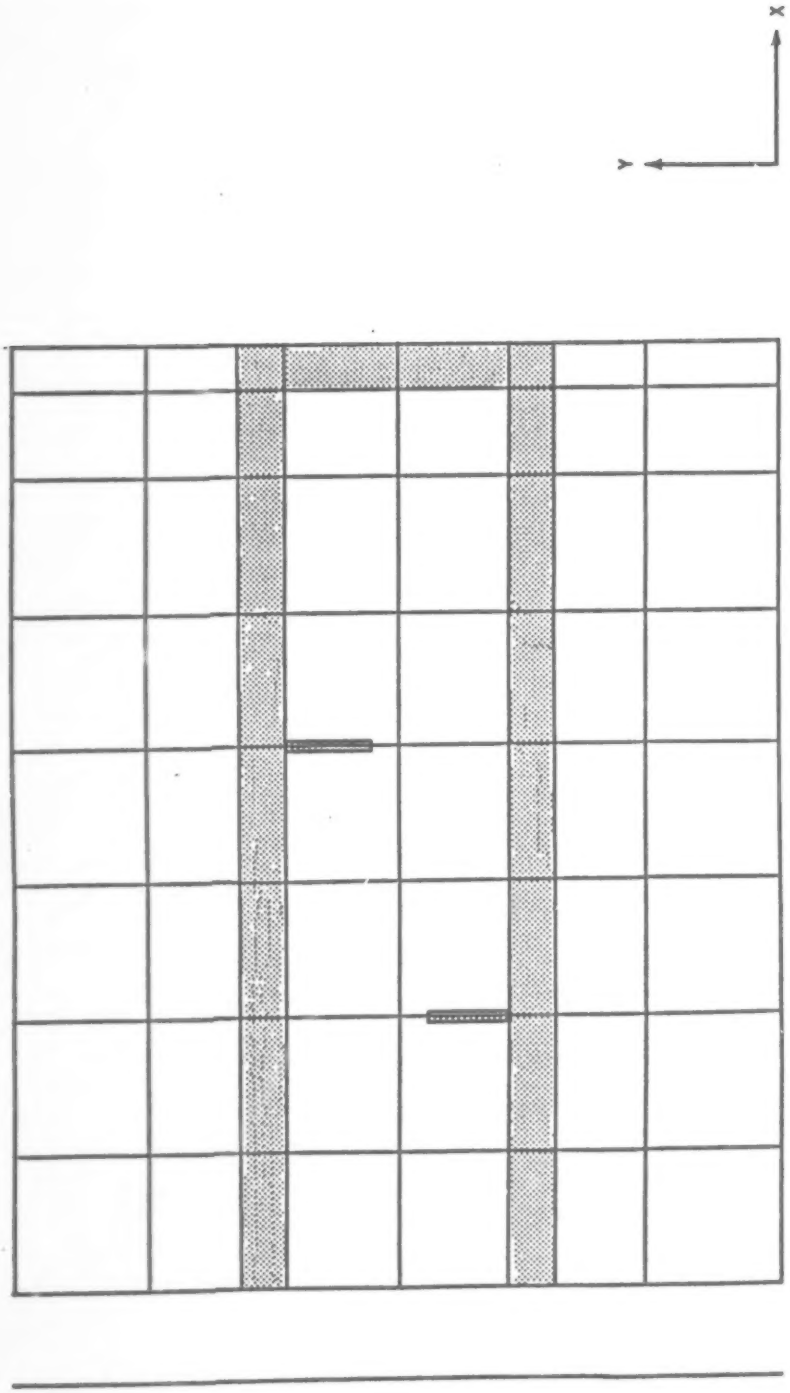


Figure 5.7. FINITE-DIFFERENCE GRID USED IN EXERCISE 2

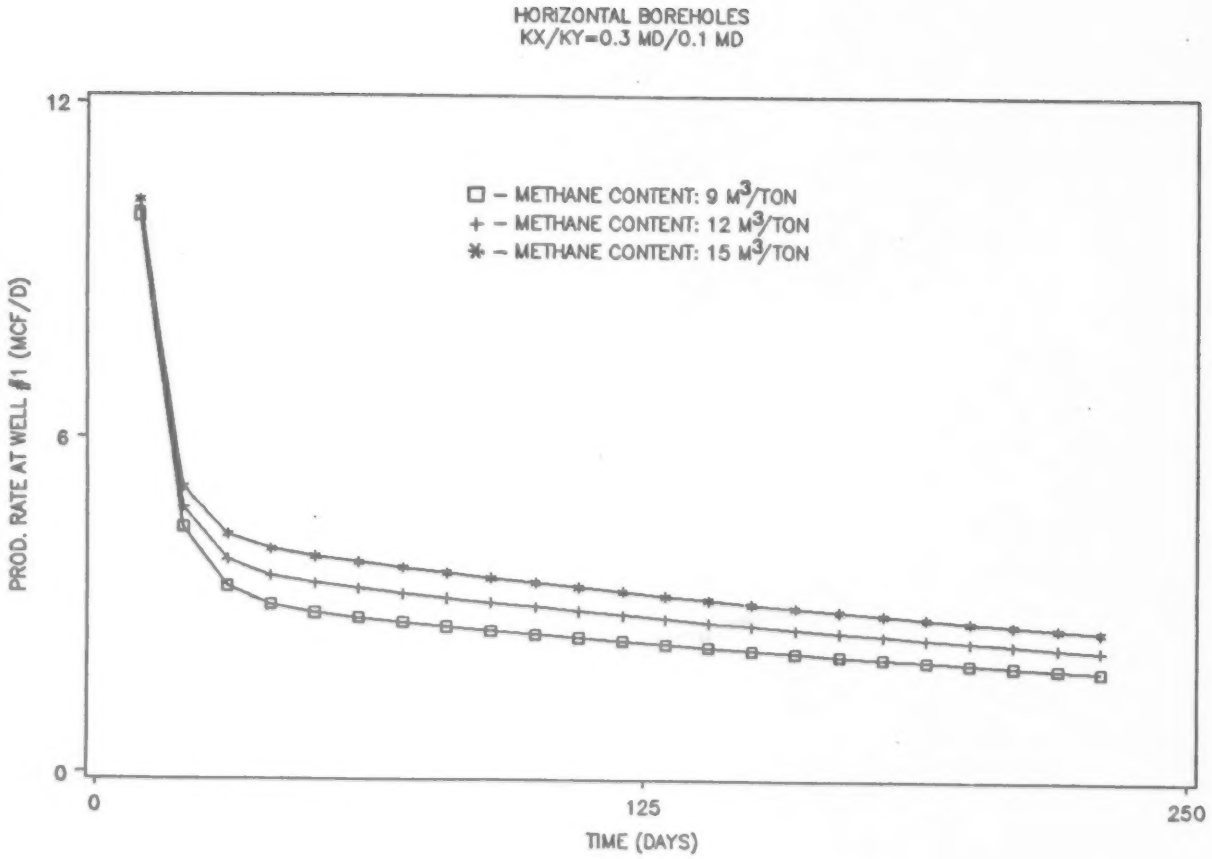


**Figure 5.8.** **PRODUCTION PERFORMANCE BEHAVIOUR OF HORIZONTAL BOREHOLE. BOREHOLE IS DRILLED PERPENDICULAR TO THE FACE CLEAT DIRECTION (WELL #1)**

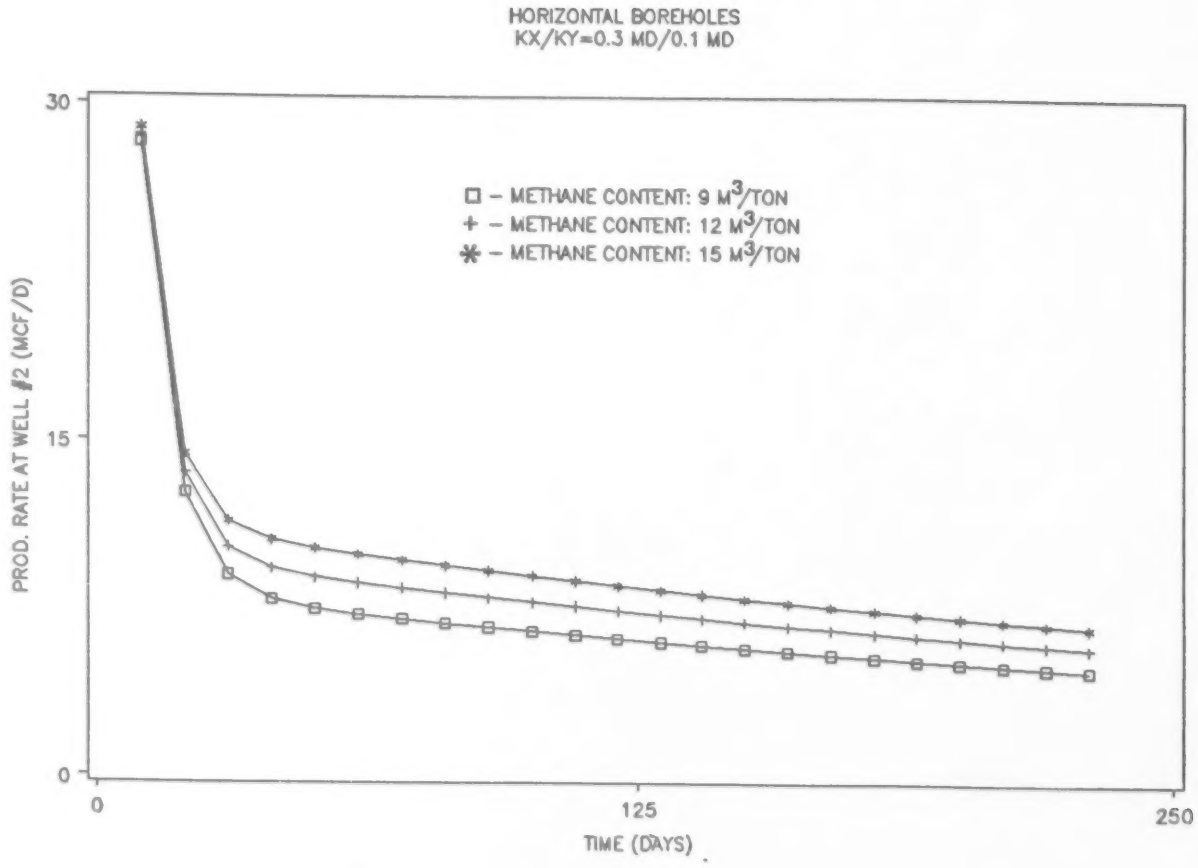


**Figure 5.9.** **PRODUCTION PERFORMANCE BEHAVIOUR OF HORIZONTAL BOREHOLE. BOREHOLE IS DRILLED PERPENDICULAR TO THE FACE CLEAT DIRECTION (WELL #2)**

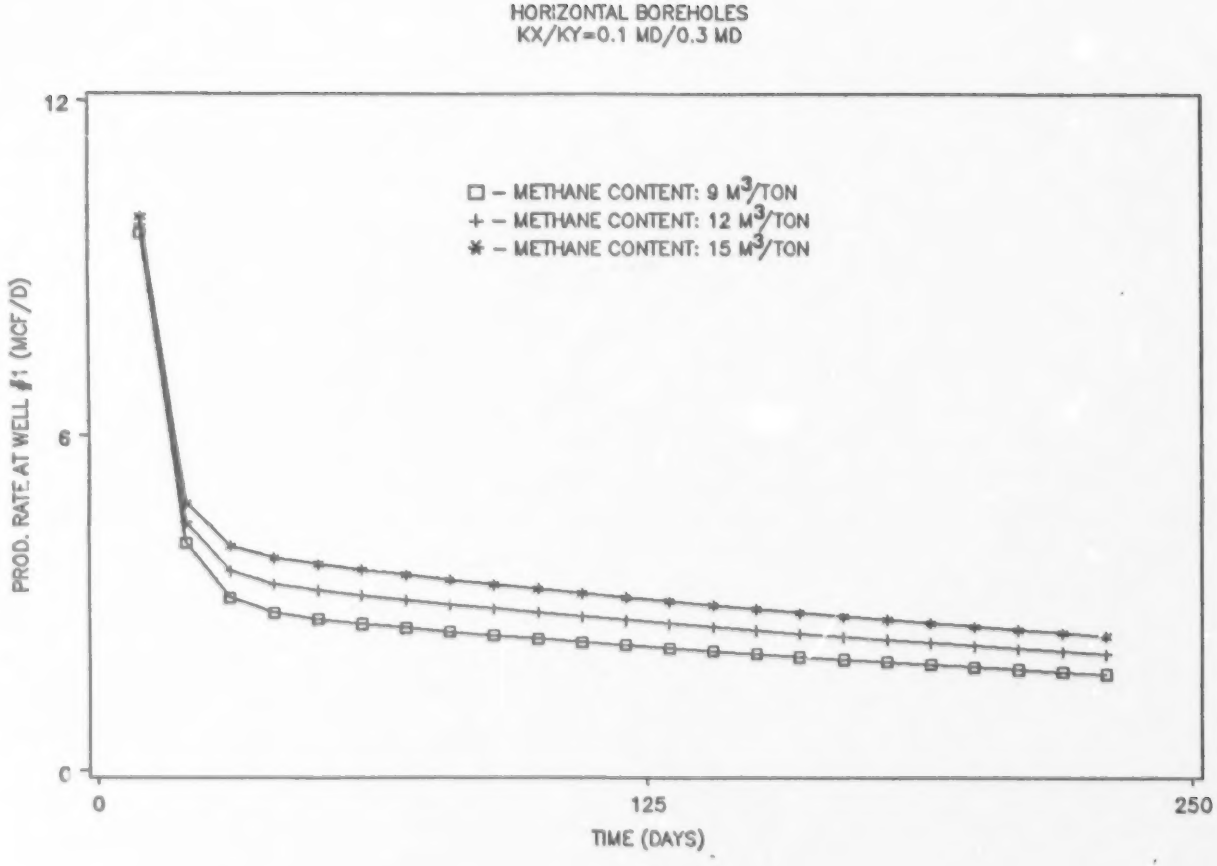


Figure 5.10. **PRODUCTION PERFORMANCE BEHAVIOUR OF HORIZONTAL BOREHOLE. BOREHOLE IS DRILLED PARALLEL TO THE FACE CLEAT DIRECTION (WELL #1)**

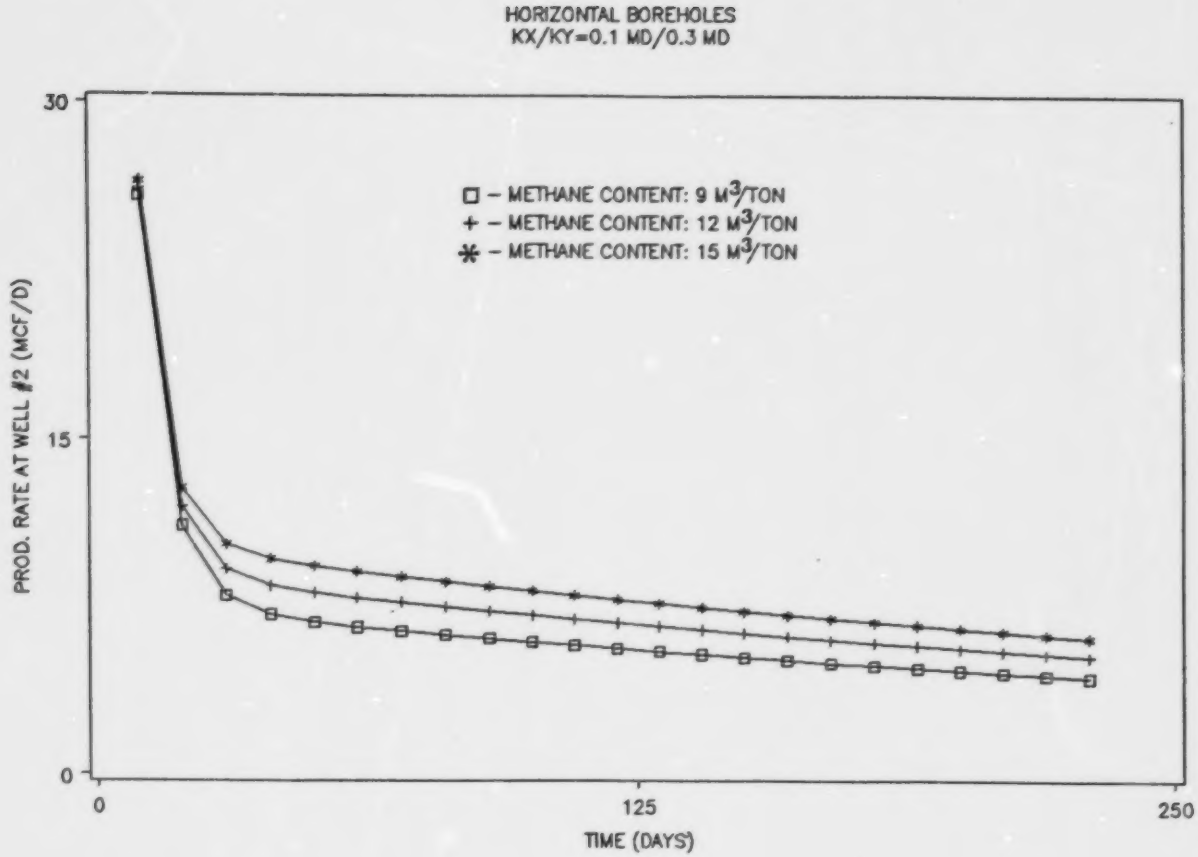


**Figure 5.11. PRODUCTION PERFORMANCE BEHAVIOUR OF HORIZONTAL BOREHOLE. BOREHOLE IS DRILLED PARALLEL TO THE FACE CLEAT DIRECTION (WELL #2)**

expected because the horizontal boreholes of Figures 5.8 and 5.9 are placed orthogonal to the more permeable face cleat direction and hence intersect more frequently with the more permeable flow channels. Table 5.3 gives a summary of the results of Exercise 2. From this table it is clear that two drainage holes together produce approximately 0.5% of the total methane emission. It is possible to increase the productivity of these drainage holes with the aid of a stimulation job around them.

**Table 5.3. SUMMARY OF RESULTS FOR EXERCISE 2**

| | $k_x$ = 0.3 md, $k_y$ = 0.1 md | | | $k_x$ = 0.1 md, $k_y$ = 0.3 md | | |
|---|---|---|---|---|---|---|
| Methane content (m3/ton) | 9 | 12 | 15 | 9 | 12 | 15 |
| Methane emission from all open coal surfaces (MMSCF) | 435 | 478 | 521 | 1030 | 1150 | 1260 |
| Methane drainage from boreholes (MMSCF) | 2.35 | 2.64 | 3.06 | 2.16 | 2.51 | 2.83 |

# 6. RESEARCH PLAN

This chapter presents an overview of the proposed research and development plan for the development of a computer-based numerical model for simulation of methane emission into longwall coal mine workings. The plan lists a number of research objectives required for the development of:

1. a computer-based, multi-seam methane flow model for predicting methane emission into longwall mines;

2. a series of application modules which would interpret the physical model in mine situations; and

3. a model verification program which would further enhance the accuracy and predictive capabilities of the model.

## Highlights of the Review

The review of the background of methane flow in coal seams (Chapter 2 & 3) has identified that modelling techniques for methane emission have progressed to a stage where most of the essential features required for modelling have been developed and tested. There are certain areas of modelling methane emission in coal mines that require further work. For example, modelling of the effect of stress on seam permeability. However, in most cases, the work on modelling techniques has far surpassed the

level of effort dedicated to the application of the developed methods.

The major limitation of the existing models concerns the application of the models for solving practical mine problems, and proper model verification and field testing. For application to Canadian coals, there are significant gaps in the capabilities of the reported models. For example, in most U.S. mines methane emission from the adjacent seams may not be as important as for longwall mines in Canada, therefore modelling of this problem is poorly developed. This and similar shortcomings in the existing models would have to be corrected before the models could be applied to Canadian mines.

Despite the above limitations, a number of model parts can be adapted from the existing computer models for use when modelling Canadian seams. Such a translation of the existing computer codes would require formulation of the existing programs into a modular form for implementation either on a mainframe or a microcomputer.

There is a minimum requirement for model complexity before it can be useful for simulating various practical mine situations (see Chapter 4). To achieve a state of model development satisfactory for mine applications, a minimum of additional programming and development work will be required for adaptation of the existing models. This work and the implementation of the model at the

Sydney Coal Research Laboratory would generate, however, benefits far in excess of the projected development cost. Development of the computer-based capabilities at Cape Breton mines is, therefore, significant for improving the mining environment, and for increased mining productivity and safety.

Objectives

The overall objective of the research plan is to develop, at the Sydney Coal Laboratory, a computer-based numerical model for simulation of the time-dependent release of methane gas into the longwall coal mine. The model should be capable of predicting major sources and rates of methane emission, the effect of methane drainage on methane emission in the face areas and other areas during mining, the effect of methane drainage or ventilation planning and mine productivity and safety.

There are additional specific objectives of the research plan. For example, the complete physical model and the application modules would be designed to be run by specialized technical and scientific personnel. At the mine working level, however, the model would have to be simplified and related to specific seam and longwall face workings. The reduction of the model and the required programming of the default values for the model parameters are important for the execution of the model in the mine environment.

The objectives for applications of the model should reflect the needs of mine operators and mine planners. The specific objectives of the model would include prediction of the methane flow at the face, methane drainage into the waste area, methane degasing prior to the mine working, and methane emission from the broken coal. It would also consider the worked seam and the adjacent seams, and the mining method.

Approach

A variety of conceptualizations exist as to what is a computer-based model. In our approach we will recognize three basic components of the computer model.

First, we will define a Physical Model which will include all equations describing the phenomena governing methane flow, all computer codes and subroutines that solve the equations, all numerical techniques and approximations used, and all computer subroutines that are required to run the program.

Second, we will define the Application Modules which will include the necessary codes that define the objectives of the calculations, input parameters and output parameters including the display and writing of the results of calculations of the Physical Model into a form that can be interpreted for a specific mine application.

Application Modules may address specific aspects of a comprehensive mine problem. For example, one module may calculate methane emission into the mine face, another module may calculate the emission of methane from the cut coal, etc. A more complex application module would perform a history matching by optimization of the input and output parameters, or would perform self-learning tasks by enabling new computational runs to draw on the results of the previous simulations.

The third component of the model includes the verification procedures. It would include, at minimum, comparison of the model predictions to the existing analytical or experimental results for simplified problems. It would involve history matching with the mine emission data collected over a longer period of mine working, etc.

The interrelation of the identified model components is depicted in Figure 6.1. More detailed descriptions of each model component and research plans pertaining to these components are given in the sections which follow.

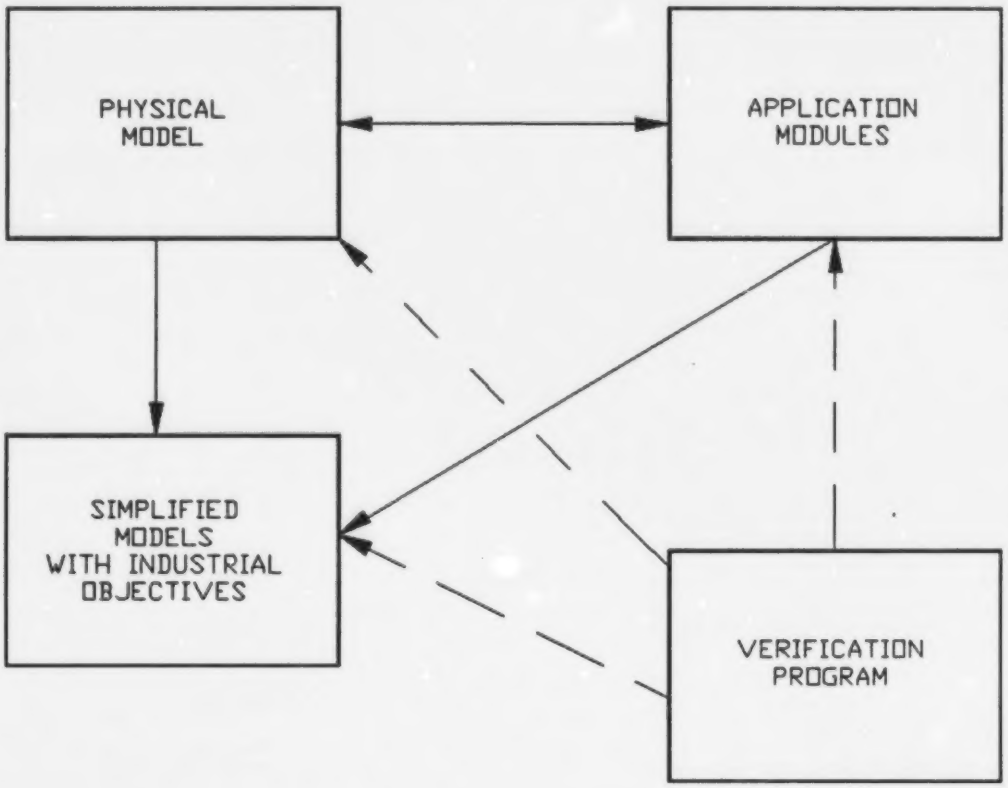


**Figure 6.1. SIMPLIFIED DIAGRAM OF THE MODEL COMPONENTS**

Work Plan

It is envisaged that the proposed research work be conducted in several phases over two to three years. In the first phase, we suggest the following work be completed:

1. Development of a numerical computer-based program which would entail the essential capabilities for modelling methane flow in longwall mines. It is expected that parts of the model may be based on the existing computer codes as discussed in detail in Chapter 4.

2. Implementation of the model on a mainframe or microcomputer at the CANMET Sydney laboratory and training of a core of scientists in the operation of the program.

3. Conducting a field validation program for the key simulation features of the model.

In Phase II of the program, we propose that the following work be completed:

1. Development of new computation and application improvements required by the model.

2. Development of specific applications routines for the transfer of simplified computer codes into the mine background.

3. Development and implementation of an extensive model validation program combining laboratory and field data on coal properties, measurements of methane concentration profile in mine working, etc.

4. Integration of the new computer program with other mine ventilation and productivity optimization programs.

Figure 6.2 depicts a stepwise implementation of the outlined R&D program including identification of the critical milestones and deliveries over a three year period. The proposed scheduling of the key tasks in Phase I is shown in Figure 6.3. A rationale for the execution of these tasks was given in more detail in Chapters 3 and 4. In the following section, only the major issues concerning the model components will be discussed.

Physical Model

A detailed description of the proposed development for the physical model is given in Chapter 4. The discussion of the model parts includes prioritization of the different model simulation features in relation to the relative importance of different capabilities to the user and the level of effort

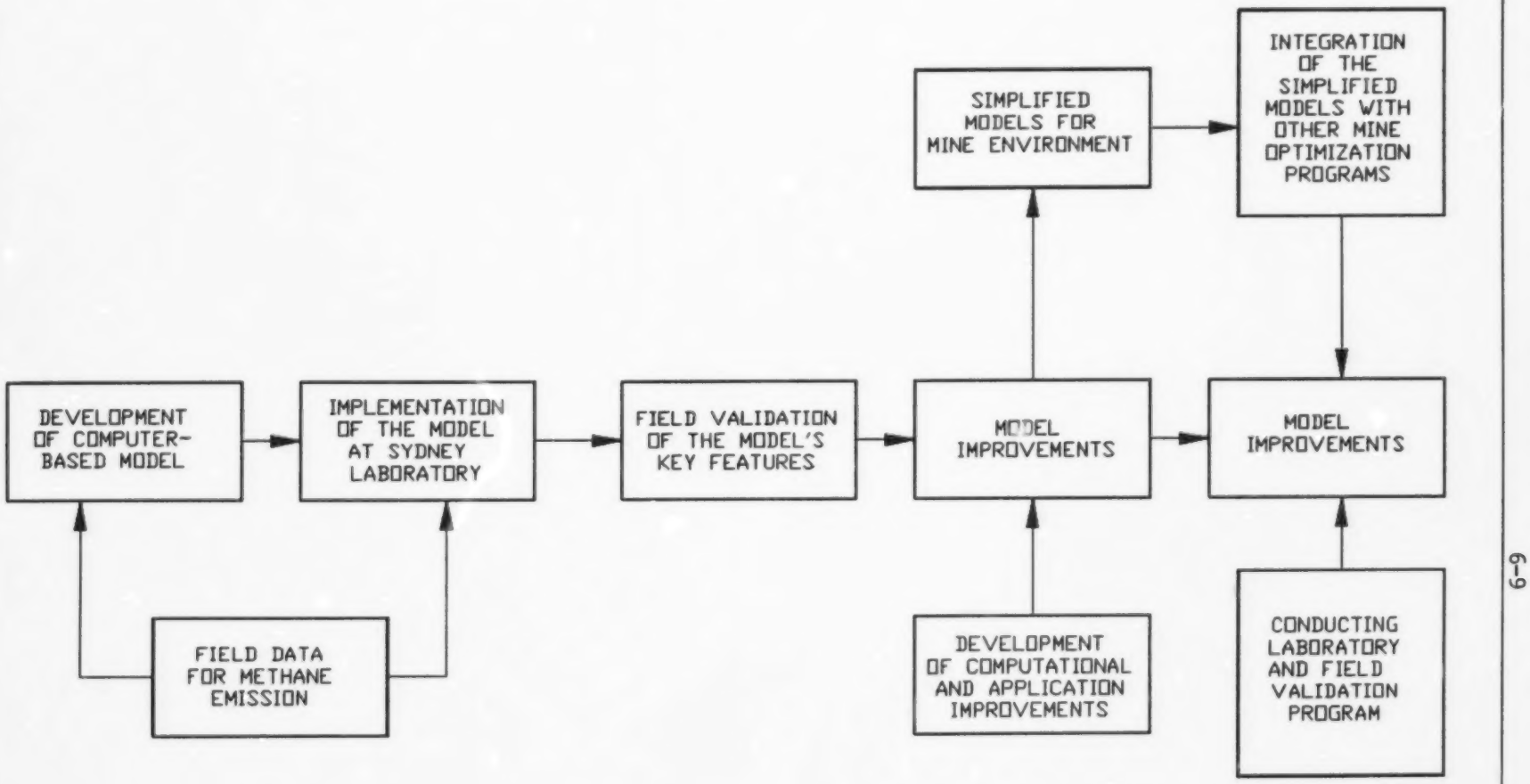
DEVELOPMENT OF COMPUTER-BASED MODEL
IMPLEMENTATION OF THE MODEL AT SYDNEY LABORATORY
FIELD VALIDATION OF THE MODEL'S KEY FEATURES
MODEL IMPROVEMENTS
SIMPLIFIED MODELS FOR MINE ENVIRONMENT
INTEGRATION OF THE SIMPLIFIED MODELS WITH OTHER MINE OPTIMIZATION PROGRAMS
MODEL IMPROVEMENTS
FIELD DATA FOR METHANE EMISSION
DEVELOPMENT OF COMPUTATIONAL AND APPLICATION IMPROVEMENTS
CONDUCTING LABORATORY AND FIELD VALIDATION PROGRAM

**Figure 6.2. METHANE FLOW MODEL RESEARCH AND DEVELOPMENT PROGRAM**

LOBBE TECHNOLOGIES LTD.

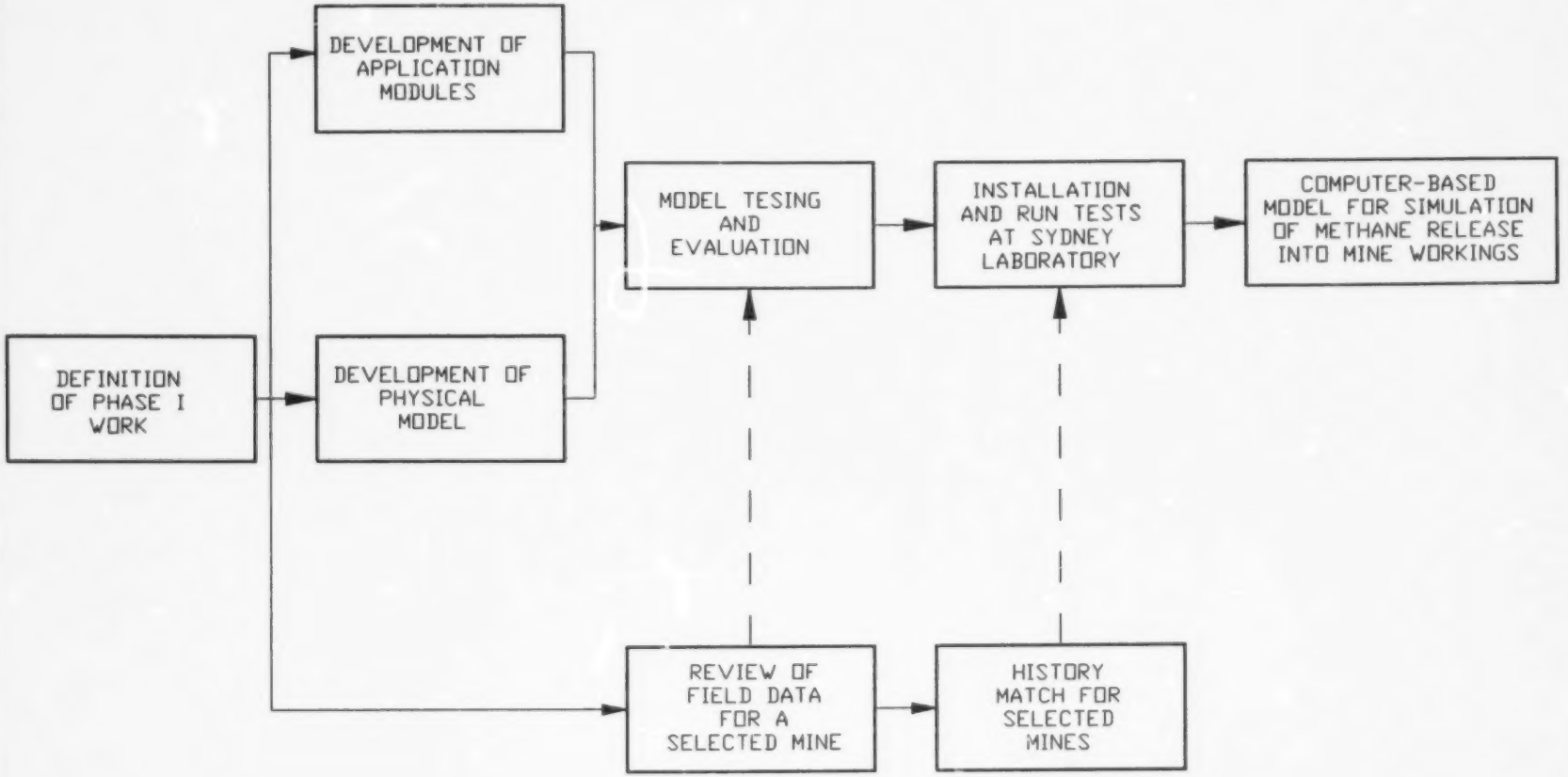
DEVELOPMENT OF APPLICATION MODULES
DEFINITION OF PHASE I WORK
DEVELOPMENT OF PHYSICAL MODEL
MODEL TESING AND EVALUATION
INSTALLATION AND RUN TESTS AT SYDNEY LABORATORY
COMPUTER-BASED MODEL FOR SIMULATION OF METHANE RELEASE INTO MINE WORKINGS
REVIEW OF FIELD DATA FOR A SELECTED MINE
HISTORY MATCH FOR SELECTED MINES

**Figure 6.3. METHANE FLOW MODEL RESEARCH AND DEVELOPMENT PROGRAM - PHASE I**

LOBBE TECHNOLOGIES LTD.

required for implementation of the R&D program. The recommended model capabilities are:

1. Essential Model Capabilities
   - dual-porosity
   - two-phase, three-dimensional flow
   - unsteady-state flow
   - Darcy's Law for water transport, and dual mechanism for gas flow
   - real gas law for the gas state
   - pseudo-steady-state sorption term
   - application module considering mine layout, interaction between multiple seams, emission from mine face and gob, coal advance rate, pressure in mine workings and some history matching

2. Important Model Capabilities
   - stress-dependent permeability
   - stress-dependent porosity
   - application modules for vertical, horizontal and slanted degasing boreholes
   - fast computational speed and user friendly

3. Useful Model Capabilities
   - effects of turbulence on water and gas transport
   - unsteady-state sorption term

Application Modules

Figure 6.4 depicts two application modules proposed for development in Phase I of the research. The modules would permit simulation of methane drainage during the preparation stage of the mine, as well as the prediction of total methane emission and emission at mine face during coal production.

These modules do not include optimization of the model input and output parameters with respect to history matching, nor do they include a capability to optimize mine and ventilation planning with the rate of the face advancement, or methane emission into the mine workings.

Model Verification Program

There is a need for a well planned and executed model verification program in order to ensure that model simulation results can be incorporated into the mine operations and planning process with sufficient confidence and certainty. Such a program would include experimental determination of laboratory and seam property data, collection of methane emission data at various mine locations over a range of mine working conditions, assembly of mine ventilation data for comparison, and history matching.

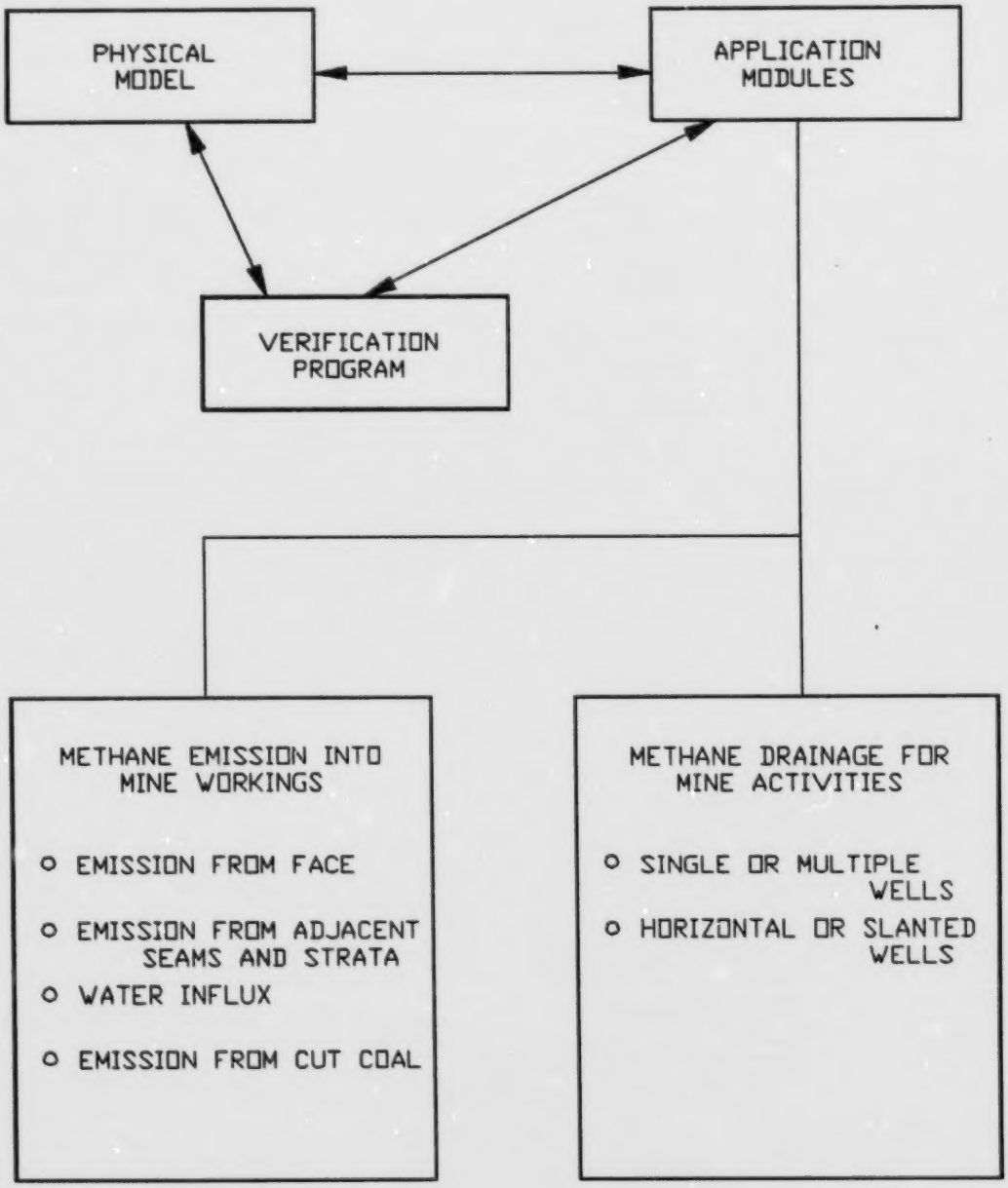
PHYSICAL MODEL
APPLICATION MODULES
VERIFICATION PROGRAM
METHANE EMISSION INTO MINE WORKINGS
o EMISSION FROM FACE
o EMISSION FROM ADJACENT SEAMS AND STRATA
o WATER INFLUX
o EMISSION FROM CUT COAL
METHANE DRAINAGE FOR MINE ACTIVITIES
o SINGLE OR MULTIPLE WELLS
o HORIZONTAL OR SLANTED WELLS

**Figure 6.4. METHANE FLOW MODEL SELECTED APPLICATION MODULES**

Figure 6.5 presents a schematic representation of elements of the proposed model verification program. It is envisaged that the program be carried out over two to three years. The program will include future R&D developments such as research on in-situ coal seam characterization techniques, optimization and error analysis of mine data, model simulation for history matching, use of the model for the design and planning of acquisition of mine emission data, etc.

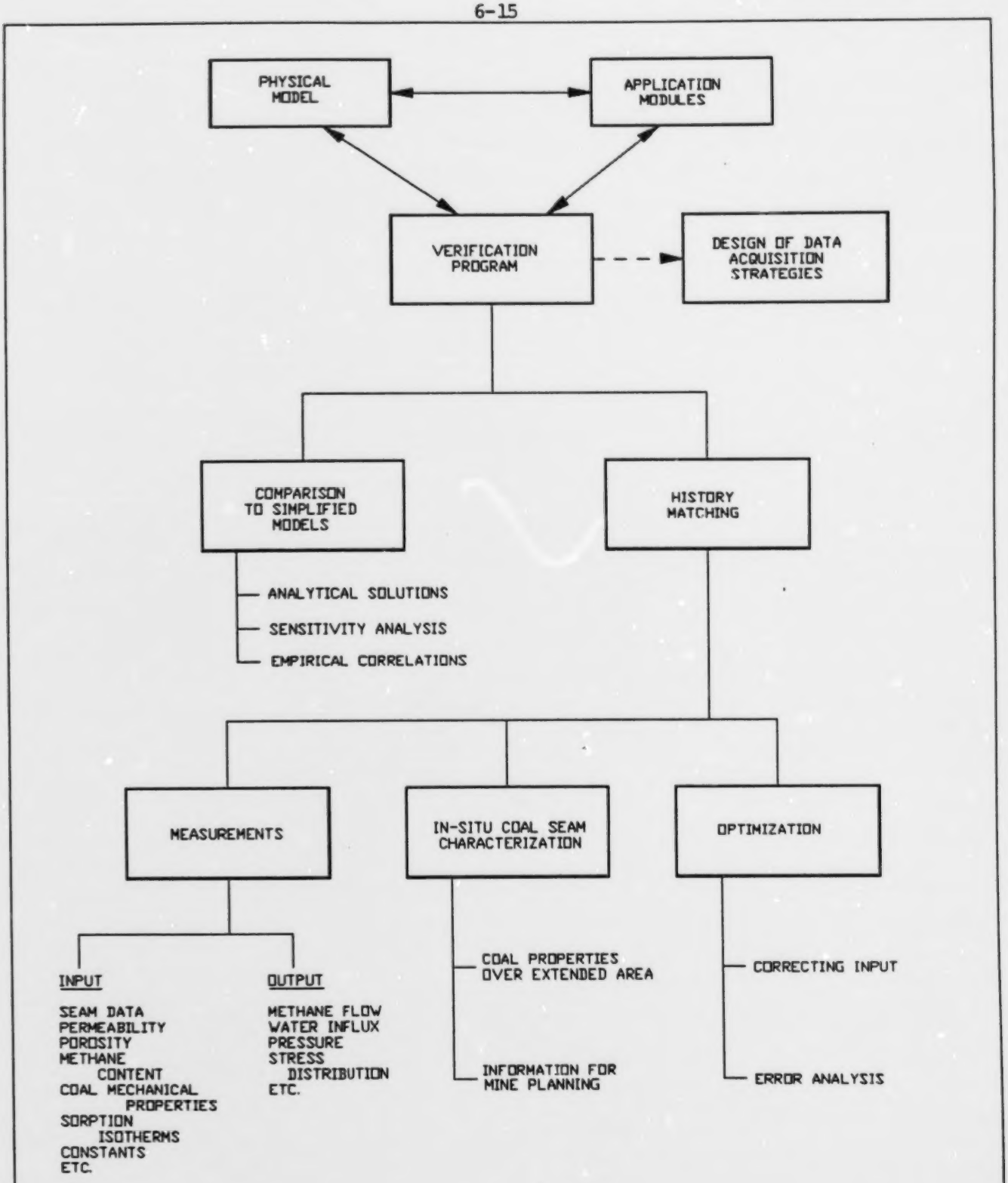


**Figure 6.5. METHANE FLOW MODEL VERIFICATION PROGRAM**

# 7. CONCLUSIONS AND RECOMMENDATIONS

The completed review of the background materials on methane flow in coal seams included information on topics such as porosity of coal, adsorption and desorption of gases, diffusion in coal, laminar and non-laminar flow and coal permeability. Other topics included were flow through a porous media, effects of stress on porosity, effects of water saturation on gas flow and a summary of approximate or numerical methods. The review provided state-of-the-art technical and scientific background on methane emission into coal mines.

The accuracy of predicting methane flow into coal mines by computer or empirical models depends on the detail in which the model describes the nature of coal, the flow of methane in the coal seam, and the mine activities that can affect the release of methane into mine workings. Based on the review of the background, it was concluded that a coal seam can be modelled as if it were a dual-porosity reservoir consisting of micropores (coal matrix) and macropores (coal fissures). In addition, methane stored in coal can be modelled as a free gas stored in the macropore system and a physically adsorbed gas in the micropores. The release of methane from micropores to the macropores can be modelled using concentration gradient or diffusion equations. The flow of methane through the macropore system to the mine workings can be modelled using a pressure gradient or Darcy's Law.

Five sets of computer models for predicting methane flow into coal mine workings were reviewed in depth including: 1) the Pennsylvania State University (PSU) model; 2) the METGEN model; 3) the University of Nottingham (UON) models; 4) the U.S. Bureau of Mines (BOM) models; and 5) the empirical (Airey's) models. In the review, special considerations were given to the primary and secondary objectives of the models and the assumptions imposed in describing the physical phenomena and the subsequent governing equations. Other issues addressed included numerical techniques and computer programs used to solve the model equations, methods applied to validate the computer model, and the merits and limitations of each model. A summary of the critical comments on each model is given below.

PSU Model

The latest PSU model incorporates, in extensive detail, the physical phenomena governing methane flow in coal seams. However, the model omits several phenomena which are important, i.e. it does not consider the flow effects due to variation in natural seam compaction, pressure distribution or methane content. The model also does not take into account interaction, and communication between multiple seams, and the effects of turbulence on gas flow. In addition, there is a need for several improvements in the PSU model such as elimination of the requirement that the directions of the principal permeabilities have to coincide with the model's geometric co-ordinate axis,

optimization of the computer programs to reduce the computational time and more extensive field testing of the model.

UON Model

The objective of the UON model was to explore possible computer-aided techniques for the prediction of methane flow through strata adjacent to a moving longwall coal face. The UON physical model does not have, however, sufficient complexity to describe the methane flow in coal. Many important features, such as the dual-porosity of coal, adsorption-desorption processes, two-phase flow conditions, gas slippage, etc., were not incorporated in the model. The uniqueness of the UON model is based on the application of the finite-element method for solving the model governing equations. Indeed, the calculus of variations on which the finite-element method is based can be applied to reduce the computational requirements of some of the governing equation, e.g., independent model parts such as stress analysis can be solved more efficiently using the finite-element method. For solution of all model governing equations, however, the use of the finite-element method as the main numerical technique is neither cost efficient nor time-effective.

BOM Model

The capabilities of the BOM are quite similar to the capabilities of the PSU model. The BOM model has additional features such as

stress-dependent porosity and permeability, and the turbulence effects incorporated in the water and gas flows. However, the PSU model has two significant advantages: 1) the PSU model is a three-dimensional model as compared to the two-dimensional BOM model; 2) the PSU computer model was written in FORTRAN versus USSTRAN computer language applied in the BOM model. A three-dimensional model is important to account for methane emission from multiple seams and FORTRAN is more machine transferable than USSTRAN.

Empirical Models

These models are based on empirical formulas incorporating the amount of methane adsorbed in the seam, and consideration of the mining parameters such as the height and depth of the emission zone, face length, extracted seam thickness, etc. These stochastic analyses or empirical formulas provide an insight into potential methane emissions. However, due to the lack of a physical model behind the stochastic findings, the empirical models are limited to extrapolation for similar mine and seam conditions and can not account for variations in the mining activities.

Airey's (1971) model, although based on empirical equations for predicting methane emission from cut coal, incorporates a phenomenological model for methane emission in the mine workings. The model was shown to successfully correlate a number of cases

for methane emission at the mine face for different face advancement rates. The model has, however, several limitations inherent to the model-governing equations. The model can not determine the amount of methane drainage from drainage holes. The model neglects that a pressure gradient may exist within coal grains, thus the calculated methane pressure is an average or equivalent pressure for a coal seam. The model assumes a known, uniform methane content of the coal seam, which for pre-drain seams poses some difficulties in accurately predicting methane flow at mine workings.

Based on the review of the existing models, the PSU computer model was selected for a parametric study of a methane emission in a longwall mine. In the study, two sets of permeability values and three different methane contents, which are characteristics of the Sydney mines, were applied including one simulation case for pre-drainage of the seam with two horizontal boreholes. The total methane emission was found in good agreement with field methane emission data reported by Konda et al. (1985). The emission from drainage holes was underpredicted for the seam input parameters studied, underlying the importance of the detailed evaluation of the seam permeability values.

Based on the reviewed models and background materials the following conclusions were drawn concerning the development of computer-based models for methane emission into mine workings:

1. Comprehensive computer programs are required for modelling methane flow into longwall mine workings including:

   (a) a computer-based, multi-seam methane flow model for predicting methane emission into longwall mines (Physical Model);

   (b) a series of Application Modules which would interpret the Physical Model in mine situations, and

   (c) a model verification program which would further enhance the accuracy and predictive capabilities of the model.

2. The twenty-nine Physical Model parts are important for the prediction of methane flow into mine workings (Table 4.1). Seventeen model parts must be implemented in order to provide an adequate prediction of methane flow into mine workings. Nine model parts can either improve the prediction accuracy or enhance the use of the computer simulation model. The remaining three are required to model special applications.

3. None of the existing computer models reviewed in Chapter 2 have all the seventeen essential model parts.

The identified shortcomings in the exiting model have been addressed in the proposed research and development plan for the development of computer-based modelling capabilities at the Sydney Coal Laboratory. It is recommended that the required research work be carried out in three phases over two to three years. Specifically, in Phase I, the following objectives are suggested:

1. Development of a numerical computer-based program which would entail the essential capabilities for modelling methane flow in longwall mines. It is expected that parts of the model may be based on the existing computer codes as discussed in detail in Chapter 3.

2. Implementation of the model on a mainframe or microcomputer at the CANMET Sydney laboratory and training of a core of scientists in the operation of the program.

3. Conducting a field validation program for the key simulation features of the model.

In Phase II of the program, the following objectives are recommended:

1. Development of new computation and application improvements required by the model.

2. Development of specific applications routines for the transfer of simplified computer codes into the mine background.

3. Development and implementation of an extensive model validation program combining laboratory and field data on coal properties, measurements of methane concentration profile in mine working, etc.

4. Integration of the new computer program with other mine ventilation and productivity optimization programs.

Phase III of the program will include future R&D developments such as research on in-situ coal seam characterization techniques, optimization and error analysis of mine data, model simulation for history matching, and use of the model for the design and planning the acquisition of mine emission data.

## 8. REFERENCES


Adzumi, H., "Studies on the Flow of Gaseous Mixtures Through Capillaries - II: The Molecular Flow of Gaseous Mixtures," Bull. Chem. Soc. Japan, Vol. 12, No. 6, 1937, pp. 285-291.

Airey, E.M., "Gas Emission from Broken Coal. An Experimental and Theoretical Investigation," International Journal of Rock Mechanics and Mechanics and Mining Sciences, Vol. 5, 1968, pp. 475-494.

Airey, E.M., A Theory of Gas Emission in Coal Mining Operations, Mining Research and Development Establishment, Report No. 21, 1971.

Airey, E.M., A Theory of Gas Emission in Coal Mining Operations, Part 2: Gas Emission from Seam Adjacent to Worked Seams, Mining Research and Development Establishment, Report No. 83, 1979.

Ancell, K.L., Lambert, S. and Johnson, F.S., "Analysis of the Coalbed Degasification Process at a Seventeen Well Pattern in the Warrior Basin of Alabama," Proceedings 1st Symposium on Unconventional Gas Recovery, Society of Petroleum Engineers, AIME, SPE Paper No. 8971, 1980, pp. 355-369.

Anderson, R.B., Bayer, J. and Hofer, L.J.E., Fuel, Vol. 44, 1965, pp. 443-452.

Aziz, K. and Flock, D.L., "Unsteady-State Gas Flow - Use of Drawdown Data in the Prediction of Gas Well Behavior," Journal of Canadian Petroleum Technology, Vol. 2, No. 1, 1963, pp. 9-15.

Barrett, E.P., Joyner, L.G. and Halenda, P.P., "Determination of Pore Volume and Area Distribution in Porous Substances. I. Computation From Nitrogen Isotherms," Journal of the American Chemical Society, Vol. 73, 1951, pp. 373-380.

Bear, J., Dynamics of Fluids in Porous Media, American Elsevier Publishing Company, New York, 1972, p. 129.

Bond, R.L. and Spencer, D.H.T., Conf. Ind. Carbon Graphite, Soc. Chem. Ind., London, 1957, pp. 231-251.

Boyer, C.M., Morrison, H.L., Pavone, A.M. and Schwerer, F.C., Methane Modelling - Predicting the Inflow of Methane Gas Into Coal Mines, Final Report under DOE Contract Number DE-ACC22-80PC30123, February 16, 1982.

Carman, P.C., Flow of Gases through Porous Media, Academic Press, New York, 1956.

Corey, A.T., "The Interrelation Between Gas and Oil Relative Permeabilities," Production Monthly, Vol. 19, 1954, pp. 34-41.

Crank, J., Mathematics of Diffusion, Clarendon Press, Oxford, 1956, p. 1.

Curl, S.J., Methane Prediction in Coal Mines, Report ICT IS/TR 14, IEA Coal Research, London, December 1978.

Currie, I.G., Fundamental Mechanics of Fluids, McGraw-Hill Inc., New York, 1974.

Dabbous, M.K., Reznik, A.A., Taber, J.J. and Fulton, P.F., "The Permeability of Coal to Gas and Water," Soc. Pet. *Eng. J., December, 1974, pp. 563-572.

Darcy, H., Les Fountains Publiques de la Ville de Dijon, Dalmont, Paris, 1865.

Deriguin, 1946

DeSwaan, A.O., "Analytic Solutions for Determining Naturally Fractured Reservoir Properties by Well Testing," SPEJ, June, 1976, pp. 117-122.

Durucan, S. and Edwards, J.S., "The Effects of Stress and Fracturing on Permeability of Coal", Mining Science and Technology, 3, 205-216, 1986.

Epstein, B.J., Franklin Inst., Vol. 244, 1947, pp. 471-477.

Ertekin, T., King, G.R. and Schwerer, F.C., "Dynamic Gas Slippage: A Unique Dual-Mechanism Approach to the Flow of Gas in Tight Formation," SPE Form. Eval., February, 1986, pp. 43-52.

Ertekin, T., King, G.R. and Schwerer, F.C., Development of Coal Gas Production Simulators and Mathematical Models for Well Test Strategies. Topical Report under GRI Contract Number 5081-321-0457, July, 1983.

Fick, A., Ann. Physik, Vol. 59, 1855, p. 170.

Firoozabadi, A. and Katz, D.L., "An Analysis of High-Velocity Gas Flow Through Porous Media," JPT, February, 1979, pp. 211-216.

Forchheimer, Ph., Zeits V. deutsch lng., Vol. 45, 1901, pp. 1782.

Fox, R.W. and McDonald, A.T., Introduction to Fluid Mechanics, John Wiley & Sons, Inc., New York, 1973.

Gan, H., Nandi, S.P. and Walker, P.L. Jr., "Nature of the Porosity in American Coals," Fuel, Vol. 51, 1972, pp. 272-277.

Gawuga, J.K., Flow of Gas Through Stressed Carboniferous Strata, Ph.D. Dissertation, The University of Nottingham, U.K. December, 1979.

Gorbachev, A.T., Alekeev, G.V. and Vorozhtosov, E.V., "Numerical Calculations in Three-Dimensional Cases of Degassing of Coal Seams," Fizikio-Tekhnicheskie Problemy Razrobotki Poleznykh Iskopaemykh, No. 2, March-April, 1973, pp. 83-92. Translated from Russian.

Gringarten, A.C., Ramey, H.J. and Raghavan, R., "Applied Pressure Analysis for Fractured Wells," Journal of Petroleum Technology, July 1975, pp. 887-892.

Gunn, R.D. and King, C.J., "Mass Transport in Porous Materials Under Combined Gradients of Composition and Pressure," AIChE Journal, Vol. 60, 1969, pp. 1548-1558.

Gunther, J., "Investigation of the Relationship between Coal and the Gas Contained In It," Int. Conf. of Dirs. of Safety of Mines, Min. of Power, Sheffield, *Eng., 1965, SMRE translation No. 5134.

Hantush, M.S., "Hydraulics of Wells," Advances in Hydroscience, Academic Press, New York, Vol. 1, 1964, pp. 281-432.

Hyman, D.M. and Stahl, P.A., "A Computer Implemented Coalbed Methane Model," Proceedings of Second Conference on the Use of Computer in the Coal Industry, Society of Mining Engineers, AIME, 1985.

Jacob, C.E. and Lohman, S.W., "Nonsteady Flow to a Well of Constant Drawdown in an Extensive Aquifer," Transactions AGU, August 1952, pp. 559-569.

Jones, A.H., Ahmed, U., Abou-Sayed, Mahyera, A. and Sakashita, B., Fractured Vertical Wells Versus Horizontal Boreholes for Methane Drainage in Advance of Mining U.S. Coals. Paper presented at the Symposium on Gas Drainage with Particular Reference to the Working Seam, University of Wollongong, Australia, May 11-14, 1982.

Jones, F.O. Jr., "A Laboratory Study of the Effects of Confining Pressure on Fracture Flow and Storage Capacity in Carbonate Rocks," Soc. Pet. Eng., Preprint 4559, October, 1973.

Jones, F.O. Jr., "A Laboratory Study of the Effects of Confining Pressure on Fracture Flow and Storage Capacity in Carbonate Rocks," J. Petrol. Technol., January, 1975, pp. 21-27.

Karagodin, L.N. and Krigman, R.K., "The Use of Hydraulic Modelling to Determine the Natural Gas Permeability of Coal Seam," Fizikio-Tekhnicheskie Problemy Razrobotki Poleznykh Iskopaemykh, No. 4, July-August, 1974, pp. 118-121. Translated from Russian.

Katz, D.L. et al., Handbook of Natural Gas Engineering, McGraw-Hill Book Company, New York, 1959, p. 46.

Keen, T.F., The Simulation of Methane Flow in Carboniferous Strata, Ph.D. Thesis, Nottingham University, 1977.

Kim, A.G., Estimating Methane Content of Bituminous Coalbeds from Adsorption Data, RI 8245, U.S. Bureau of Mines, 1977.

Kim, A.G., Experimental Studies on the Origin and Accumulation of Coalbed Gas, RI 8317, U.S. Bureau of Mines, 1978.

King, G.R., Numerical Simulation of the Simultaneous Flow of Methane and Water Through Dual-Porosity Coal Seams During the Degasification Process, Ph.D. Dissertation, The Pennsylvania State University, May 1985.

King, G.R., Ertekin, T. and Schwerer, F.C., "Numerical Simulation of the Transient Behavior of Coal Seam Degasification Wells," SPE Form. Eval., April, 1986, pp. 165-183.

Klinkenberg, L.J., "The Permeability of Porous Media to Liquids and Gases," API Drilling and Production Practices, 1941, pp. 200-213.

Kolesar, J.E. and Ertekin, T., "The Unsteady-State Nature of Sorption and Diffusion Phenomena in the Micropore Structure of Coal." Paper SPE 15233 presented at the Unconventional Gas Technology Symposium, Louisville, KY, May, 1986.

Konda, B.W. and Kochhar, J., Methane Emission and Control at Lingan Colliery, CANMET Report ERP/CRL 85-73 (OP,J).

Kovalev, Y.M. and Kuznetsov, S.V., "Filtration of Gas in a Coal Seam Being Worked in the Presence of Diffusion Desorption," Fizikio-Tekhnicheskie Problemy Razrobotki Poleznykh Iskopaemykh, No. 6, November-December, 1974, pp. 74-77. Translated from Russian.

Kucuk, F., Transient Flow in Elliptical Systems, Ph.D. Dissertation, Stanford University, May 1978.

Kundt, A. and Warburg, E., "Ueber Reibung and Waermeleitung Verduennter Gase," Ann. Physik, Poggendorf, 1875.

Mahajan, O.P. and Walker, P.L., Jr., "Porosity of Coals and Coal Products," Analytical Methods for Coal and Coal Products, edited by Karr, C., Jr., Academic Press, New York, Vol. 1, 1978, pp. 125-162.

Marsh, H. and Siemieniewska, T., "The Surface Area of Coals as Estimated From the Adsorption Isotherms of Carbon Dioxide Using the Dubinin-Polanyi Equation," Fuel, Vol. 44, 1965, pp. 355-367.

Maxwell, 1860

McKee, C.R., Bomb, A.C. and Koenig, R.A., "Stress Dependent Permeability and Porosity of Coal," Proceedings of the 1987 Coalbed Methane Symposium, Tuscaloosa, Alabama, November 16-19, 1987, pp. 183-194.

McPherson, M.J., "The Occurrence of Methane in Mine Workings," Journal of the Mine Ventilation Society of South Africa, Vol. 28, No. 8, August 1975.

Methane Modelling - Predicting the Inflow of Methane Gas into Coal Mines, Final Report Prepared by the United States Steel Corporation for the Bureau of Mines, United States Department of the Interior, December 1984.

Mordecai, M. and Morris, L.H., "The Effects of Stress on the Flow of Gas through Coal Measure Strata," The Mining Engineer, Vol. 133, No. 164, July, 1974, pp. 435-443.

O'Shaughnessy, S.M., The Computer Simulation of Methane Flow Through Strata Adjacent to a Working Longwall Coalface, Ph.D. Dissertation, The University of Nottingham, U.K., May, 1980.

Ostensen, R.W., "The Effect of Stress-Dependent Permeability on Gas Production and Well Testing," Proceedings of 57th Technical Conference, Society of Petroleum Engineers, AIME, SPE Paper No. 11220, 1982.

Ostensen, R.W., "Microcrack Permeability in Tight Gas Sandstone," Society of Petroleum Engineers Journal, 1983, pp. 919-927.

Owili-Eger, S.C., Simulation of Quantity and Quality Control in Mine Ventilation, M.S. Thesis, The Pennsylvania State University, March, 1973.

Patching, T.H., "The Retention and Release of Gas in Coal - A Review," CIM Trans., Vol. 73, 1970a, pp. 328-334.

Patching, T.H., "The Retention and Release of Gas in Coal - A Review," The Canadian Mining and Metallurgical Bulletin, Vol. 63, No. 703, November, 1970b, pp. 1302-1308.

Patching, T.H., "Variations in Permeability of Coal," Proc. Rock Mech. Symp., TN 292-59C, Toronto, 1965.

Pavone, A.M. and Schwerer, F.C., Development of Coal Gas Production Simulators and Mathematical Models for Well Test Strategies. Final Report under GRI Contract Number 5081-321-0457, April, 1984.

Pearson, C.E., Numerical Methods in Engineering and Science, Van Nostrand Reinhold Company Inc., New York, 1986.

Price, H.S. and Abdalla, A.A., Mathematical Model Simulating Flow of Methane and Water in Coal Mine Systems. Final Report under U.S. Bureau of Mines Contract Number S0110752, 1972.

Price, H.S. and Ancell, K.L., "The Feasibility of Methane from Coal," Methane Gas from Coalbeds - Development, Production, and Utilization, MERC/SP-78/1, January 18, 1978, pp. 37-73.

Price, H.S., McCulloch, R.C., Edwards, J.C. and Kissell, F.N., "A Computer Model Study of Methane Migration in Coal Beds," The Canadian Mining and Metallurgical Bulletin, Vol. 66, No. 737, September, 1973, pp. 103-112.

Reddy, J.N., An Introduction to the Finite-Element Method, McGraw-Hill Inc., New York, 1984.

Remner, D.J., Ertekin, T., Sung, W. and King, G.R., "A Parametric Efficiency," SPE Res. *Eng., November 1986, pp. 633-646.

Richards, M.J., "Longwall Front Abutment Stress Effects on Firedamp Release", Mining Science and Technology, 1, 215-229, 1984.

Rose, W.D., "Permeability and Gas-Slippage Phenomenon," Drill. and Prod. Prac., API, 1941, pp. 200-213.

Schlichting, H., Boundary-Layer Theory, McGraw-Hill Inc., New York, 1979.

Sevenster, P.G., "Diffusion of Gases Through Coal", Fuel, Vol. 38, 1959, p. 403.

Smith, D.M. and Williams, F.L., Diffusional Effects in the Recovery of Methane from Coalbeds. Paper SPE/DOE 10821 presented at the SPE/DOE Symposium on Unconventional Gas Recovery, Pittsburgh, PA, May 16-18, 1982.

Somerton, W.H., Soylemezoglu, L.M. and Dudley, R.C., "Effect of Stress on Permeability of Coal," J. Rock Mech. Min. Sci. & Geomech., Vol. 12, 1975, pp. 129-145.

Sung, W., Ertekin, T. and Schwerer, F.C., The Development, Testing and Application of a Comprehensive Coal Seam Degasification Model. Paper SPE 15247 presented at the Unconventional Gas Technology Symposium, Louisville, KY, May 1986.

Tek, M.R., Coats, K.H. and Katz, D.L., "The Effect of Turbulence on Flow of Natural Gas through Porous Reservoirs," JPT, July 1962, pp. 799-806.

Terzaghi, K., Theoretical Soil Mechanics, John Wiley and Sons, New York, 1943.

Thimons, E.P. and Kissell, F.N., "Diffusion of Methane through Coal," Fuel, 1973, pp. 274-280.

Todd, M.R., O'Dell, P.M. and Hirasaki, G.J., "Methods for Increased Accuracy in Numerical Reservoir Simulations," Society of Petroleum Engineers Journal, December 1972, pp. 515-530.

TRW Energy Systems Group, Economic Analysis of Vertical Wells for Coalbed Methane Recovery. Final Report under DOE Contract Number DE-AC21-78MC08089, April, 1981.

Van Krevelen, D.W. and Schayer, J., Coal Science, Elsevier Scientific Publishing Co., Amsterdam, 1967.

Vorozhtosov, E.V., Gorbachev, A.T. and Fedorov, A.V., "The Calculation of the Motions of Gas in a Coal Seam with a Quasilinear Law of Filtration," Fizikio-Tekhnicheskie Problemy Razrobotki Poleznykh Iskopaemykh, No. 4, July-August, 1975, pp. 83-91. Translated from Russian.

Vylegzhanin, V.N., "An Algorithm for Predicting Gas Emission in a Development Working," Fizikio-Tekhnicheskie Problemy Razrobotki Poleznykh Iskopaemykh, No. 5, September-October, 1974, pp. 80-84. Translated from Russian.

Walker, P.L., Jr. and Patel, R.L., "Surface Areas of Coals From Carbon Dioxide Adsorption at 298°K," Fuel, Vol. 49, 1970, pp. 91-94.

Walsh, J.B., "Effect of Pore Pressure and Confining Pressure on Fracture Permeability," Int. J. Rock Mech. Min. Sci. & Geomech. Abstr., Vol. 18, 1981, pp. 429-435.

Wang, Y.J. and Saperstein, L.W., "Computer-Aided Solution of Complex Ventilation Networks," SME Trans., Vol. 247, No. 1, 1963, pp. 9-15.

Warren, J.E. and Root, P.J., "The Behavior of Naturally Fractured Reservoirs," SPEJ, September, 1963, pp. 245-255.

Washburn, E.W., Proc. Nat. Acad. Sci. U.S., Vol. 7, 1921, pp.115-116.

Wattenbarger, R.A. and Ramey, H.J., "Gas Well Testing with Turbulence, Damage and Wellbore Storage," JPT, August, 1968, pp. 877-887.

Wylie, C.R. and Barrent, L.C., Advanced Engineering Mathematics, McGraw-Hill Inc., New York, 1982.

Zwietering, P., Overeem, J. and Van Krevelen, D.W., Fuel, Vol. 35, 1956, pp. 66-70.